Modelling water-borne infections: the impact of hygiene, metapopulation movements and the biological control of cholera

by
Hatson John Boscoh Njagarah

Thesis presented in partial fulfilment of the
academic requirements for the degree of
Doctor of Philosophy (Mathematics)
at the University of Stellenbosch

Advisor: Prof. Farai Nyabadza
(University of Stellenbosch)

Declaration

By submitting this thesis/dissertation electronically, I declare that the entirety of the work contained therein is my own, original work, that I am the sole author thereof (save to the extent explicitly otherwise stated), that reproduction and publication thereof by Stellenbosch University will not infringe any third party rights and that I have not previously in its entirety or in part submitted it for obtaining any qualification.

November 25, 2014

Hatson John Boscoh Njagarah

Date

Abstract

Water-borne infections have been a menace in many countries around the globe, claiming millions of lives. Cholera in particular has spread to all continents and now on its seventh epidemic. Although control measures have been continually developed through sanitation, vaccination and rehydration, the infection still devastates populations whenever there is an outbreak. In this research work, mathematical models for cholera transmission dynamics with focus on the impact of sanitation and hygiene, metapopulation spread, optimal control and biological control using a bacteriophage specific for pathogenic *Vibrio cholerae* are constructed and analysed. Vital analyses for the models are precisely given as well as numerical results depicting long term behaviour and the evolution of populations over time. The results of our analysis indicate that; improved sanitation and hand-hygiene are vital in reducing cholera infections; the spread of disease across metapopulations characterised by exchange of individuals and no cross community infection is associated with synchronous fluctuation of populations in both adjacent communities; during control of cholera, the control measures/efforts ought to be optimal especially at the beginning of the epidemic where the outbreak is often explosive in nature; and biological control if well implemented would avert many potential infections by lowering the concentration of pathogenic vibrios in the aquatic environment to values lower than the infectious dose.

Opsomming

Water-infeksies is 'n bedreiging in baie lande regoor die wêreld en eis miljoene lewens. Cholera in die besonder, het op sy sewende epidemie na alle kontinente versprei. Hoewel beheermaatreëls voortdurend ontwikkel word deur middel van higiëne, inentings en rehidrasie, vernietig die infeksie steeds bevolkings wanneer daar 'n uitbraak voorkom. In hierdie navorsingswerk, word wiskundige modelle vir cholera-oordrag dinamika met die fokus op die impak van higiëne, metabevolking verspreiding, optimale beheer en biologiese beheer met behulp van 'n bakteriofaag spesifiek vir patogene *Vibrio cholerae* gebou en ontleed. Noodsaaklike ontledings vir die modelle is gegee sowel as numeriese resultate wat die langtermyn gedrag uitbeeld en die ontwikkeling van die bevolking oor tyd. Die resultate van ons ontleding dui daarop dat; verbeterde higiëne is noodsaaklik in die vermindering van cholera infeksies; die verspreiding van die siekte oor metapopulaties gekenmerk deur die uitruil van individue en geen kruis gemeenskap infeksie wat verband hou met sinchrone skommeling van bevolkings in beide aangrensende gemeenskappe; tydens die beheer van cholera,behoort die beheermaatreëls/pogings optimaal te wees veral aan die begin van die epidemie waar die uitbreking dikwels plofbaar in die natuur is; en biologiese beheer, indien dit goed geïmplementeer word, kan baie potensiële infeksies voorkom deur 'n vermindering in die konsentrasie van patogene vibrio in die water tot waardes laer as die aansteeklike dosis.

Dedications

To my beloved mum, Redemptor Byaruhanga and my siblings Yuda Tadeo Mutebi, Mary Kyalisiima, Margaret Kobusingye, Damascius Kyakuwa and Pauline Kemugisha.

Acknowledgements

Since this work was not done in vacuum, this is enough to indicate that a great people supported me, encouraged me and guided me through the entire process.

The almighty our creator, Father and provider, has generously granted me the gift of life and the ability to wake up every single day of my life to add to this project. All I can say is "Ad Majorem Dei Gloriam".

My supervisor Prof. Farai Nyabadza, you have not only been my supervisor, but a friend, a guide, advisor in both academic and non academic works as well as professional development. You have always been instrument in sourcing funds for my progress and living. How can I ever repay you honestly? May you continue with that selfless heart and acts of kindness, guiding learners all over the African Continent. You are a true pan African. May God's grace, favour and will always be bestowed upon you and your family.

To the department of Mathematical Sciences, Stellenbosch University; Prof. Ingrid Rewisky, you were instrumental in acquiring funds for me in various ways; Prof. Florian Breuer for all the opportunities given to me to serve and develop professionally; Prof. Z. Janelidze, Prof. S. Mouton, Prof. A Fransman, Prof. L. van Wyk, Ms L. K. Wessels, I have worked with you as a demi and facilitator in some of the courses you were teaching and during the organisation of the SAMS 2012, hosted at Stellenbosch among others. Mrs W. Isaacs, Mr I. Jacobs, I'm grateful for all your support, interactions and discussions. Mrs L. Adams and Mrs O. Marias you took your valuable time to make work easy, you have friendly and approachable. May you continue with your kind spirit.

To my family and friends: my Mum and my siblings to whom I dedicate this work, you have been a great inspiration to me, prayed for me unceasingly and you put your faith and hope in me. I will try my best to always be by your side and the best days are yet to come. May you all be blessed abundantly. To my friends Nagla Numan and Alex Bamunoba, you are true and great friends. And to Alex, I can not forget the "sleepless nights". You have been more like a brother.

Contents

List of Figures

List of Tables

Chapter 1

Introduction

Water-borne infections have been and continue to be a problem in many developing countries. The World Health Organisation (WHO) estimates that water related diseases are the leading causes of the death around the world with an estimated annual death toll of about 3.4 million people [2]. WHO characterises water-related diseases in a relatively broad sense to include; diseases due to chemicals and micro-organisms in water which people drink, infections due to organisms that have their life cycle in water such as schistomiasis, diseases such as malaria whose vectors breed in water, diseases such as cholera whose aetiologic agent's natural habitat is the aquatic environment, other water-related injuries due to water sports recreation and some drownings, legionnaires' disease (Legionellosis) whose causing micro-organisms are carried in aerosols [3], cryptosporiosis and shigella among others. The severity of water-related infections is mainly attributed to poor sanitation and hygiene, This includes lack of access to clean drinking water as well as poor handling of foodstuffs. According to Berman [2], the human death toll attributed to lack of clean and safe drinking water is greater than the combined death toll attributed to terrorism and weapons of mass destruction.

The vast nature of the problems related to water-borne infections span many infections, some of which are common while the others may be rare or considered neglected diseases. The severity of the problem often varies from community to community and this is often related to the level of sanitation and hand-hygiene which are partly related to the social economic status. The biggest scale water related infections is localised in impoverished countries. However, the dynamics of the infections within the affected countries tend to differ from community to community as well as with respect to specific transmission dynamics of the infection under consideration. There are many water-borne infections some of which com-

mon and others rare. A major daunting task would be that of considering all these infections, in an all inclusive modelling framework. For the purpose of our study therefore, we limit our study cholera. Emphasis in our study is put on understanding the epidemic in general and in the South African context owing to the 2000-2002 epidemic that greatly affected almost the whole country. In some cases however, general information regarding to the disease is considered with literature cutting across other studies from published literature. In this respect, we also give a brief highlight of the problem on the global scale from antiquity, the scale on the African continent before localising it to our anticipated specific transmission dynamics within a South African community setting.

1.1 Research objectives

The general objectives of this research work are largely centred around developing and using mathematical models to understand specific aspects of the transmission dynamics of cholera. The specific objectives are based on the work presented in the various chapters and are summarised as follows

(i) to briefly describe the epidemiology and aetiology of cholera as a major water-borne infection, and give an overview of the infection on the global scale as well as in the South African Perspective.

(ii) to investigate the effect of sanitation on cholera transmission dynamics and give some conditions necessary for containing the epidemic.

(iii) to ascertain the effect of migration on cholera transmission dynamics and the possible severity that may be associated with the movement patterns as well as fluctuations in the population related to migration patterns and exchange of individuals between adjacent communities.

(iv) to investigate the potential effect of improved hand hygiene, access to clean water and vaccination on the duration of the disease in the community in comparison to disease self-limitation.

(v) to study the potential control of cholera through use a biological agent (bacteriophage specific for virulent vibrios) that can reduce the concentration of vibrios in the aquatic environment.

All control measures that reduce the likelihood of immunologically naive individuals coming in contact with the parasite, are vital in deducing the severity of the epidemic.

1.2 Significance of the Study

In the current era mulled by significant number of water-borne infections, understanding the transmission dynamics and potential control measures is vital if such diseases are to be contained. Our study is therefore, important in the following aspects:

(i) It adds onto the platform for research in mathematical modelling of water-borne infections and gives an insight into possible predictions of the course of the epidemic given different transmission patterns.

(ii) It gives an insight into shaping policy making processes related to control of cholera and the plausibility of restricting movement to and fro cholera endemic areas.

(iii) The mathematical framework presented adds to the elaborate bank of knowledge and procedure for carrying out analyses related to mathematical models for cholera transmission and mathematical epidemiology in general.

Due to the fact that no effort towards containing diseases is insignificant, a critical look at the aspects presented in this thesis not fully considered previously may be valuable. Disease transmission, manifestation and global spread follows a chain of events some of which are related to human movement, lifestyle, social economic status and policies made in communities. Therefore, the aspects which include sanitation, human movement, control strategies for the disease are worth investigating. We note here that if credible data is available on the various critical aspects of the disease, projection of future trends can be done. However, in the absence of such data, mathematical models do not necessarily serve as substitutes but as guiding tools to understanding vital dynamics.

1.3 Pathology, life cycle *Vibrio cholerae* and cholera vaccines

When *Vibrio cholerae* enters the digestive system, it embeds itself in the villi of the absorptive intestinal cells and releases cholera toxin. The cholera toxin (CT) is an enterotoxin made up of five B-subunits that form a spore that fits one A- subunit [4]. The pathogenesis of cholera infection includes a number of factors including transmission of the *Vibrio cholerae*,

colonization of the intestines, production of enterotoxins and persistence of the disease in the environment.

Physiological responses and symptoms that follow release of cholera toxin include stimulation of mucosal lining of the intestine to secrete fluids. The symptoms include, profuse watery diarrhoea that has a "rice water" quality, vomiting, rapid (severe) dehydration which result in urine suppression , fall in blood pressure, cramps in legs and abdomen, subnormal temperatures and complete collapse [5]. The consequences of excessive dehydration can be fatal. If uncontrolled through prompt medical intervention, death can occur within 24 hours of onset. In general if not treated, death does occur 50-70% of the time [6].

Cholera not only affects the population with regard to morbidity, mortality and Disability adjusted life years (DALYs), it also imposes serious social and economic setbacks. It can cost the government of South Africa billions of rand to eradicate and working time is lost due to absenteeism of employees who would be affected or attending to patients. The lost working time affects production in the industry and consequently tax revenue and a drop in export potential in the long run [7, 8, 9]. In acute cases, cholera can result in mortality related to acute myocardial infarction, acute cerebral infarction as well as acute intestinal gangrene [10]. Cholera can be prevented through proper disposal of human excreta through building and using proper sanitation systems, proper and safe preparation and handling of food. Although proper sanitation systems are vital in containing the epidemic, this alone may not be effective if no effective primary health care education is emphasised.

1.3.1 *Vibrio cholerae*

Pathogenic *V. cholerae* is a "comma" shaped gram-negative with a single flagellum for movement [11]. They are non-sporulating, non-capsulated, facultative anaerobes, catalase-positive and motile by means of a single polar flagellum [11]. In liquid media all vibrios show vigorous darting motility. Most species are oxidase-positive and reduce nitrates to nitrites [12]. There are several strains of *V. cholerae*, some of which are pathogenic and some are non pathogenic. *V. cholerae* was initially divided into two main strains, namely O1 and non-O1 strains. This classification of the serogroups of vibrios was mainly based on the group and the antigen. Prior to 1992, the only known pathogenic *V. cholerae* was the serogroup O1, that is of antigen O and group 1. This serotype is classified into two biotypes, Classical and El Tor [13]. Each of the two biotypes (Classical and El Tor) are classified into three serotypes depending on the type-specific antigen. The three serotypes include, Ogawa, Inaba, and Hikojima. All the serotypes have a common antigen **A** and the type-specific antigens, **B**

(Ogawa), **C** (Inaba) and **B, C** (Hikojima)[13]. In Figure 1.1, we give a brief summary of the classification of one of the virulent strains of *V. cholerae*, *V. cholerae* O1.

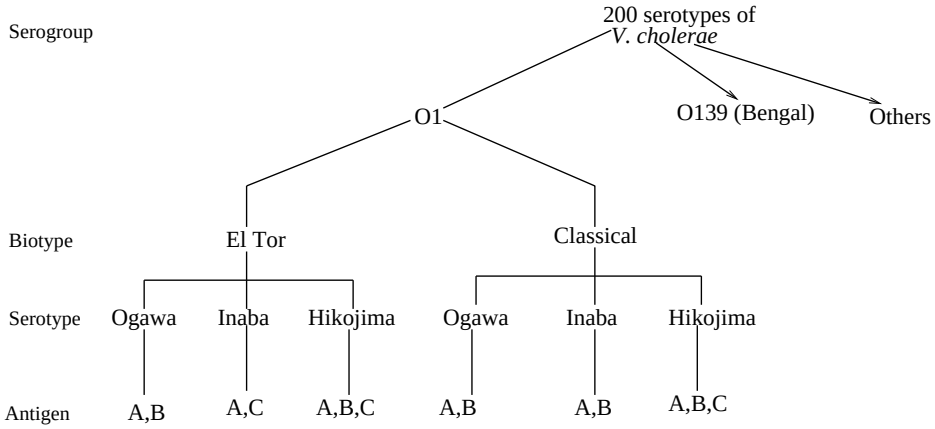

Figure 1.1: Source [13]: Classification of the strains of *V. cholerae*

Of all the three serotypes, Hikojima is the rarest and is predominantly found in Japan. The most widely distributed pathogenic strain is the *V. cholerae* serotype O1 El Tor N 16961 strain that causes the pandemic disease cholera [13]. The latest pathogenic serotype O139 was discovered in 1992. The El Tor strain was active in the seventh and the most recent pandemic of cholera from 1960s to 1970s as well as the early 1990s along with serotype 0139, both displaying resistance to multiple drugs.

In the ecological niche, pathogenic vibrios prefer a highly saline environment with relatively high temperatures [14]. They are however, easily killed by chlorine and exposure to sunlight. The organism can survive adverse decrease in temperature or salinity by transforming into a spore-like dormant state yet still infectious [15] and the references therein. In this state, the vibrios are non-culturable [16] but still infectious [17].

A single plankton copepod can carry upto 10^4 *V. cholerae* organisms and this is about 10 times the infectious dose determined in studies. *V. cholerae* is a non invasive organism. Therefore, infection with cholera does not result in fever. Pathogenic *V. cholerae* is an acid sensitive micro-organism. Therefore, hydrochloric acid or the use of gastric acid suppressing medication increases susceptibility to infection with cholera.

1.3.2 Life cycle and viability of pathogenic *Vibrio cholerae*

Cholera is an infectious diseases caused by the bacteria species *Vibrio cholerae*. The main portal or entry of the pathogen into the human body is through oral ingestion. The infec-

tion is mainly spread by drinking contaminated water or eating food contaminated with the pathogenic bacteria. Therefore, cholera can be classified as a water-borne/food borne disease. The bacteria present in the faecal matter of an infected person is the main source of infection. Once one is infected, the main site affected in the human body is the gastrointestinal tract. When *Vibrio cholerae* enters the gastrointestinal tract, it embeds itself in the villi of the absorptive intestinal cells and releases cholera toxin. The cholera toxin (CT) is an enterotoxin (a protein exotoxin often produced by micro organisms and it targets the intestines) made up of five B-subunits that form a spore that fits one A-subunit [4].

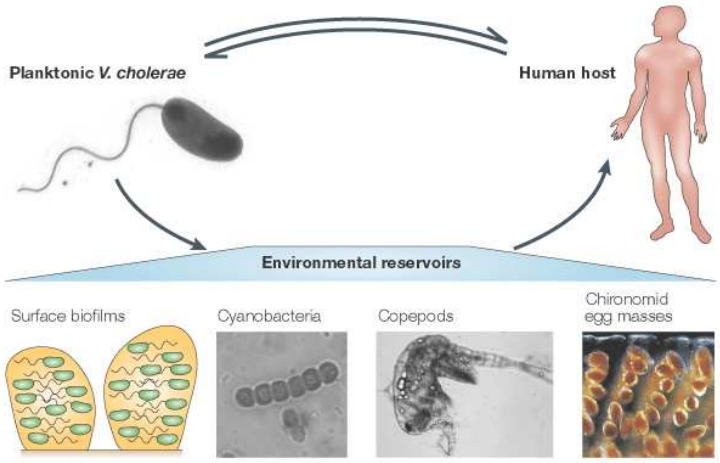

Figure 1.2: Source [18]: The life cycle of pathogenic *Vibrio cholerae*.

Individuals who are protected from cholera via access to clean water can still acquire the disease through consumption of contaminated foods. In this case therefore, vaccination maybe be a plausible and reasonably effective solution to containing the infection. The justification for this observation can be traced from studies conducted in Haiti where clean water was distributed to a small subset of the population in one study and vaccination of an identical number of individuals in another [19]. Vaccination was observed to produce a much bigger impact on the case counts as opposed to sole supply of clean water. The main reason is that whereas individuals who receive clean water still remain susceptible to infection, vaccinated individuals may not easily contract the pathogen and pass it on.

The persistence and seasonality of the epidemic can be attributed to health carriers of the pathogen[20], climate and migration and movement patterns of individuals [16]. We examine each of these factors to ascertain how they affect the cholera epidemic [21]. The healthy carriers of the pathogen *V. cholerae* asymptomatic individuals who intermittently excrete the pathogen at relatively short durations of 6 to 15 days with the maximum period being be-

tween 30 to 40 days [22] and the references therein. However, there are also chronic convalescent carriers and these have been observed to excrete the pathogen intermittently for periods of 4 to 15 months [22].

V. cholerae are capable of normal growth and development in surface water for a period ranging between 1 hour to 13 days [22] and the references there in. Its survival is entirely centred around the chemical, biological and physical characteristics of the given stream of estuarine water. Although the viability of *V. cholerae* may be short in polluted aquatic environment, faecal contamination from victims of the epidemics and healthy carriers of the pathogen continue to reinforce their population in water.

1.3.3 Cholera Vaccines

The world health organisation recommends use of oral cholera vaccines (OCV) in endemic, pandemic and emergency situations [23]. However, it is still emphasized that OCVs be administered while still effecting the other control measures such as use of Oral rehydration salts (to those infected to restore the ion balance), and supplying clean disinfected water to the general population.

Cholera vaccines given by injection can help prevent cholera but only reduce the risk by $25-50\%$ [24]. In addition, injectable vaccines are associated with unpleasant side effects which include fever, pain at the site of injection, headache and malaise [25]. Given the low efficacy and the associated side effects, WHO abandoned the use injectable cholera vaccines [25] in all public health programs since the 1970s. More emphasis has since been put on oral vaccines. This is a plausible gesture since it is now clear that both adults and children in most societies prefer oral vaccines to those administered via a parenteral injection [26]. In the recent study on Cholera in Haiti, Mukandavire et al [27] suggest that vaccines with efficacy of 50% would result in Cholera control in all the departments under study except in Artibonite. It was however observed that cholera in Artibonite would be controlled with the use of a vaccine of 65% efficacy which is similar to most new-generation vaccines [27] and the references therein. Since the current vaccines have a relatively low efficacy, it is important that although one may have received the vaccine, they must take precaution to avoid being in cholera infected areas, ensure consumption of uncontaminated food, water and maintain proper hygiene. For travellers who anticipate going to cholera endemic regions, it is recommended that they complete the scheduled vaccine dosage before travel and get booster dozes every six months. There are however growing concerns about the efficacy of the vaccines with respect to preventing cholera carriers state or geographical spread of the disease [28].

According to WHO [23], investigation of the role of mass vaccination in prevention of cholera is under way. The major issues of interest to be addressed in the investigation include logistics, cost effectiveness of mass vaccination, timing, the capacity of producing the vaccine and the criteria that may be followed during mass vaccination to contain outbreaks. Some examples of cholera vaccines include [29];

(i) Cholera vaccine USP: This vaccine is prepared as a suspension V. cholerae serotypes Ogawa and Inaba[5]. During preparation, the vaccine is composed of 8 units of equal parts of the serotypes Ogawa and Inaba per millimetre [5]. The vaccine is administered in an injection with a sodium chloride buffer. The administration of the injection may be intra-cutaneous (applied to layers between the skin), subcutaneous (an injection below to the skin directly below the dermis or epidermis) or intramuscular but not intravenous. When applying the vaccine medical personnel are compelled to adhere to standard procedures of using a separate sterilised syringe and needle per individual, in order to prevent the spread of infections.

(ii) Vaccine Dokoral (WC-rBS) [29] is a monovalent vaccine based on formalin and heat killed whole cells (WC) of *V. cholerae* 01 (classical and El Tor, Inaba and Ogawa) plus recombinant cholera toxin B subunit. Thus, Dukoral is a B-subunit killed whole cell vaccine [30]. The vaccine is given with a bicarbonate buffer which helps protect the B subunits from being destroyed by gastric acid. Once prepared from the 3 ml single dose vials together with the bicarbonate buffer [31], the vaccine is orally administered. This vaccine can have upto three years on shelf life time depending on the storage temperature, i.e if stored at a temperature from 2 to 8°C, and when stored at 37°C, it remains stable for upto one month [32]. For effective working of the vaccine, it is recommended that ingestion of food or drinks should be avoided at least one hour prior and after taking the vaccine and then boosters should be given every after 6 months [29]. The vaccine has been rendered safe during pregnancy and in immuno-compromised individuals such as HIV-infected individuals [29]. It is licensed for persons 2 years of age and older [30]. It has been applied in a number of countries including Indonesia, Uganda, and Sudan (before South Sudan had separated from Sudan) and it is now licensed for use in many countries around the world. The vaccine has an average protective efficacy of 50% sustained over a period of 3 year. The protective efficacy varies from a high of 85% in the first 4 months to about 57% in the second year with negligible protection thereafter [25].

(iii) The vaccine Shanchol^{TM}, is an oral vaccine produced by Shantha Biotechnics of Hy-

derabad India. The vaccine is made of killed whole cells from a mixture of cholera pathogenic strains *V. cholerae* 01 and 0139 [31]. This vaccine meets the international Good Manufacturing Practice (GMP) standards and is produced under WHO guidelines. It has been tried and shown to be safe and immunogenic in both adults and children. Therefore, it can be used in children aged 1 and older as well as adults. During administration of the vaccine, it is applied in two doses with a period of one to six weeks apart. This vaccine offers protection between 65- 67% for a period of upto two years [25, 31] in a place highly endemic with cholera.

Of the two currently used oral vaccines Dukoral and Shanchol, Shanchol has been observed to have the following advantages over Dukoral [31];

- Schanchol requires no administration buffer. This greatly simplifies its application in field conditions such as post-crisis situations and in refuge camps.
- Shanchol is available at relatively affordable prices which makes it accessible to many cholera affected countries especially in Asia and Africa.
- The vaccine has got higher efficacy and lasts longer than Dukoral in children aged 1 to 5 years. This an age group characterised with high child mortality

According to WHO [23], there is no parenteral vaccine recommended at the moment. This is due to the low protective efficacy and high occurrence of severe adverse reactions. The currently recommended vaccine for use including in emergency situations is the Oral Cholera Vaccine (OCV). This vaccine has been used recently in Haiti during the cholera outbreak that hit Haiti after the 2010-2011 Earthquake [33].

1.4 Historic perspective of cholera spread

Up to seven pandemics have been recorded so far with effects felt globally. These pandemics started in the subcontinent of India [7] and then spread to other parts of the world. The first six epidemics were mainly caused by *V. cholerae* 01 classical biotype. The most recent pandemic is was however different from the first six pandemics associated with the origin and the disease causing *V. cholerae* serotype. The seventh pandemic originated in Indonesia and was caused by *V. cholerae* serotype El Tol. Although it is vital to understanding the attributes of these pandemics, our emphasis will be on the seventh epidemics. It is during the spring of the seventh epidemic that the pandemic reached the African continent including South Africa [28].

Pandemic	Year	Length
1	1817-1823	6 years
2	1826-1838	12 year
3	1938-1855	16 years
4	1863-1874	11 years
5	1881-1896	15 years
6	1899-1923	24 years
7	1961-1975	14 years

Table 1.1: Source [13]: The first seven cholera pandemics

In the Figure 1.3, we give a summary of the cholera cases, deaths and reporting countries that we recorded by the World Health Organisation between 1970 – 2004. These were typically recorded during the seventh epidemic. We note that for the duration over which data

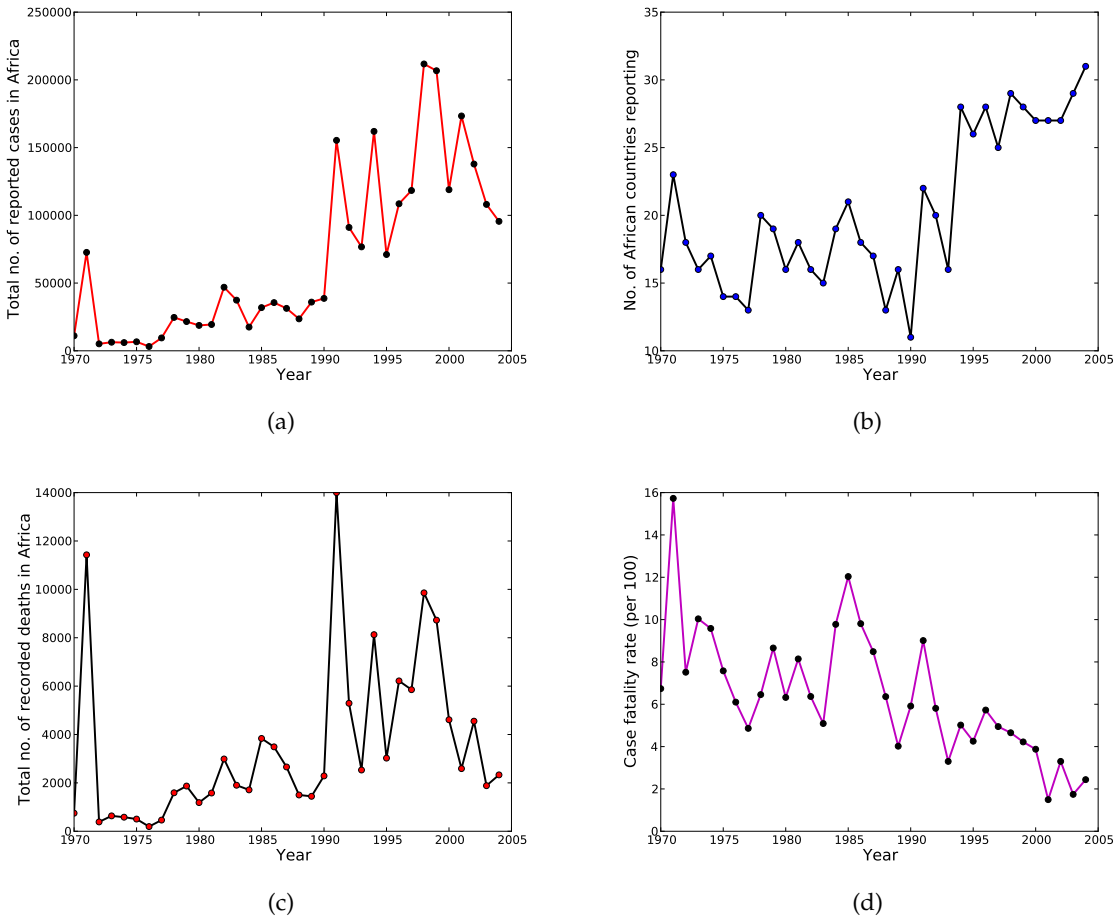

Figure 1.3: Source [1]: Cholera cases, deaths, case fatality rates and the number of countries in Africa that reported cholera from 1970 to 2004

was recorded, cholera spread to more African countries over the years with the number of affected countries increasing from 16 in 1970 to 31 in 2004 (see Figure 1.3(b)). The number of cases were also in-tandem with the number of reporting countries. The lowest reported cases being 3180 from 14 countries and the highest being 211748 cases from 29 reporting countries (see Figures 1.3(a) and 1.3(b) for comparison). Although there is an observed increase in the recorded deaths (see Figure 1.3(c)), the case fatality rate (CFR) indicates a relatively opposite trend (see Figure 1.3(d)). In our view the CFR is a better measure of how cholera cases were managed. The reduction in the CFR over the years could be attributed to improvement in the ways cholera cases are managed, sanitation and the general health care system.

1.4.1 A survey of the cholera epidemic in South Africa

Some of the first cases of cholera in South Africa were detected around 1973 in the gold mines [28]. The introduction of cholera was attributed to migrant labourers from the then cholera endemic countries such as Malawi, Mozambique and Angola who had come to work in the gold mines. From that time on cholera cases have been reported in various parts of the country sometimes in small and pronounced amounts. The major challenge with properly studying cholera in most communities is due to lack of well documented information and data on the transmission process, the cholera cases and deaths. This challenge is not unheard of in many communities in South Africa. Although cholera in South Africa was first detected in 1973 [28], many cases might have not been properly documented given the country's political history. Some of the documented information from health statistics South Africa and the Kwazulu Natal health department (*http://www.kznhealth.gov.za/*) from the link (*http://indicators.hst.org.za/healthstats/179/data*) indicating the scope of the disease is given in Table 1.2.

The data indicates the cholera cases reported from the 9 provinces of South Africa and the country case fatality rate (CFR)[1]. As it can be observed in the table the most recent epidemic that greatly affected the country started in the year 2000 and only subsided in 2002/2003 after spreading to all but one of the provinces in the country.

By around July 2001, the cholera epidemic had spread to seven of the nine provinces of South Africa. The major affected areas were the North and Southern parts of KwaZulu Natal where the outbreak had occurred as early as August 2000. The affected area of KwaZulu Natal had 99% of all the 106224 case reported nationally. Currently, KwaZulu Natal, North-

[1]The case fatality rate in this case is defined as *"The number of deaths divided by the number of case expressed as a percentage"*

Rep. Cases	**EC**	**FS**	**GP**	**KZN**	**LP**	**MP**	**NC**	**NW**	**WC**	**ZA**	CFR
1994	0	0	2	3	0	0	0	0	0	5	-
1995	0	0	1	1	0	0	0	0	0	2	-
1997	0	0	0	0	0	1	0	0	0	1	-
1998	1	0	3	6	0	20	0	2	0	32	-
1999	0	0	0	3	0	1	0	0	0	4	-
2000	0	1	0	10161	0	0	0	4	0	10166	0.8
2000/01 season	9	1	65	105389	792	125	0	6	1	106389	0.2
2001	9	1	65	97059	793	125	0	6	1	98059	0.2
2001/02 season	2335	0	24	15062	465	4	0	12	0	17902	0.7
2002	2352	0	24	13536	465	4	0	12	1	16394	0.7
2003	3142	2	4	560	0	159	0	0	1	3866	1.1
2004	-	-	-	-	-	-	-	-	-	2780	1.3
2005	-	-	-	-	-	-	-	-	-	0	-
2008	-	-	-	-	-	-	-	-	-	4343	-
2009	2	0	47	0	618	6855	0	28	4	7554	-
2009 NICD LCC	-	-	37	0	449	61	-	19	4	570	-
2010 NICD LCC	-	-	1	-	-	-	-	-	-	1	-
2011 NICD LCC	-	-	-	-	1	-	-	-	-	1	-

Table 1.2: Cholera cases reported from different provinces of South Africa. **EC**: Eastern Cape **FS**: Free State **GP**: Gauteng **KZN**: KwaZulu-Natal **LP**: Limpopo **MP**: Mpumalanga **NC**: Northern Cape **NW**: North West **WC**: Western Cape **ZA**: South Africa, **CFR**: Case Fatality rate, **NICD**: National institute for communicable diseases, **LCC** laboratory confirmed case

ern province, Eastern cape, Mpumalanga and Gauteng are some of the severely affected provinces with water-borne infections including cholera. Of all the provinces KwaZulu Natal is still the most affected province. The characteristic areas in the provinces that were mainly affected include townships and informal settlements where there is rapid urbanisation yet no adequate access to clean drinking water, poor hygiene, over crowding with respect to living conditions, unsafe preparation of food, handling and storage, famine and flooding. The transmission of the mode of the infection was observed to be through consumption of water and food contaminated with *Vibrio cholerae* pathogen. In recent studies however, on the cholera infection indicate that the disease can be spread through person-to-person contact and consumption of contaminated food and water. In the outbreak in Zimbabwe in from November 2008 to July 2009 which had 98, 585 reported cases and caused 4, 287 deaths [34] the major transmission was attributed to person-to-person contact. A similar argument is plausible for the case of South Africa's $2000 - 2002$ epidemic which spread to various provinces yet affected provinces are not all connected by common river networks.

1.5 Climate and water-borne infections

The intensity of infectious disease outbreaks usually depends on and is driven by climatic influence and the level of immunity of the host population [35]. Climatic variability is one of the vital factors that often affect the patterns of vector-borne diseases such as cholera, malaria, trypanosomiasis, schistosomiasis and West Nile virus among others. The major climatic influencing factors are mainly temperature and rainfall patterns and amount received in the area. Temperature usually affects the development of mosquito eggs and larvae, the pupal stage of trypanosomes and miracidia in the life cycle of schistosomes. The effect on these species affects their survival, multiplication and virulence. Low temperatures are often characterised by inactivity of the organisms due to inhibition of enzymatic activity within the organism. High temperatures on the other hand may denature the enzymes causing inactivity or killing the micro-organism. All organisms have specific temperatures ranges for optimal functionality and it varies from one organism to another. Temperature also affects the growth of copepods, phytoplankton and zoo-plankton which often are food nutrients for some vectors or shelter for others. Climate not only affects the micro-organisms but also the host human population. Rainfall patterns often lead to variation in the levels of water in rivers and lakes. These are often recreational areas where humans often come into contact with water-borne pathogens such as schistosomes, *V. cholerae* and cryptosporidiasis among others. In areas with poor sanitation and poor disposal of faecal matter and excreta, run-off during the wet seasons washes the pathogen into the aquatic reservoir. The aquatic reservoirs are conducive environments for the multiplication of the pathogen. Note that although the environmental temperature ranges may be big, the water temperature ranges tend to be narrow. The narrow temperature range tends to be conducive for micro- organisms, zooplanktons , copepods (zooplanktons which are widely dispersed), phytoplankton as well as bacteriophage which may prey on some pathogenic vibrios.

Climatic conditions affect the dilution, ionic concentration, salinity and organic nutrients of the aquatic reservoirs. Dilution is associated with the concentration of pathogen species per unit volume and the molar concentration of ions. This is vital with regard to the quantity of species an individual must consume in order to develop the infection as well as their ionic nutrients. For example, in the case of cholera this is referred to as ID_{50} [36], i.e the amount of vibrios which when consumed result in fifty percent probability of contracting the infection. Extreme weather conditions not only affect the virulence and concentration of the pathogen but also the mobility of humans. For instance, during high rainfall seasons, extreme wintry conditions and very high temperatures, the movement of humans is greatly

hampered reducing spatial spread of individuals. On the other hand, after a wet season increased mobility can enhance spatial spread of the disease.

The transmission pattern of the infection may be confounded by the immunity of the population resulting from outbreaks that could have occurred previously, or low number of susceptible individuals. Quite often, the transmission of the pathogen in the population is a result of non-linear interaction between the susceptible and infectious individuals or the susceptible individuals consuming the pathogen from an aquatic reservoir.

Date	Cases	Deaths	Date	Cases	Deaths
Oct 13, 2000	2175	22	Dec 29, 2000	11183	51
Oct 18, 2000	3271	26	Jan 7, 2001	15983	60
Oct 19, 2000	3279	27	Jan 25, 2001	27431	72
Oct 26, 2000	3806	31*	Feb 4, 2001	37204	85
Nov 2, 2000	4270	32	Feb 14, 2001	48647	108
Nov 10, 2000	4580	33	Feb 23, 2001	56092	120
Nov 11, 2000	5385	35	Mar 3, 2001	62607	131
Nov 27, 2000	5876	35	Mar 14, 2001	69761	139
Dec 5, 2000	6548	41	Mar 27, 2001	78140	163
Dec 18, 2000	8137	41	April 16, 2001	86107	181

Table 1.3: Cases and deaths due to cholera reported to WHO during the 2000/2001, cholera outbreak in KwaZulu Natal. The number highlighted with an asterisk was originally recorded as 33 and later corrected by WHO as 31

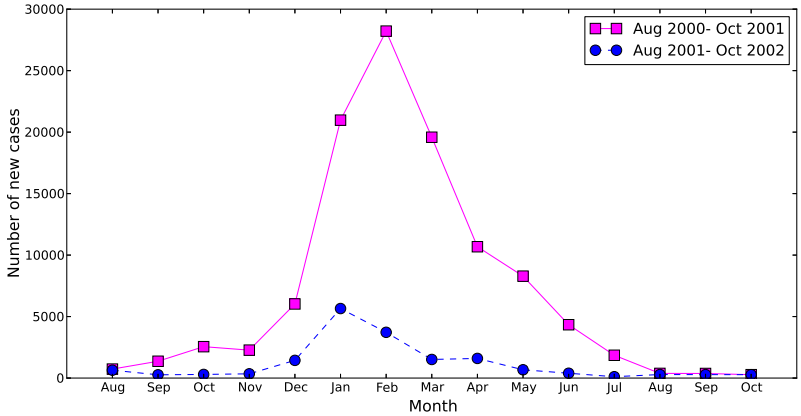

Figure 1.4: Comparison between the 2000/01 and 2001/02 cholera epidemics in KwaZulu-Natal

The cholera cases peaked during the hottest months (mid summer) of the year for the two subsequent years when the disease greatly affected the country.

1.6 Outline of this work

In Chapter 2 we give a brief review of the modelling work done on transmission dynamics of cholera. The review includes highlights on the general transmission routes (i.e the primary as well as the secondary route), classification of infective individuals, some control measures incorporated in some mathematical models (e.g biological control with a bacteriophage) as well as some mathematical treatise applied to the mathematical models.

In Chapter 3, we study the effect of sanitation on the severity of cholera with the main aim or examining the level necessary to contain the infection. Mathematical analysis of the model is done, sensitivity analysis of the model to some key parameters performed using the Latin hypercube sampling scheme and numerical simulations to ascertain the long term dynamics of the sub-populations.

In Chapter 4, a two community model is formulated with the link between communities accounted for by movements across communities. In the model it is assumed that no cross community infection occurs and that the infection is transmitted through both the primary and secondary routes. Mathematical analyses of the model is done. Sensitivity analysis is also performed on the model parameters and it indicates that movement across communities could spur the epidemic even in the less prone community.

In Chapter 5, optimal control of cholera between linked communities is studied. The permissible control are assumed to be non linear and that implementation of controls may contain the infection in about half the time it would take the infection under self-limitation.

In Chapter 6, biological control of cholera as a result of predatory relationships between bacteriophage and *V cholerae* is studied. In the model used, Holling type II response function is used contrary to previous work in [37, 38], logistic growth for the *V cholerae* is assumed in tandem with [38] but contrary to Malthusian growth used in [37].

1.7 Publications

This thesis was built around the following papers and work presented at conferences as follows

Chapter 3

- "Modelling the impact of hygiene on the dynamics of cholera", J.B.H. Njagarah and F. Nyabadza, (**in review**).

  The results in this paper were presented at the 55nd annual South African Mathematical Society (SAMS) conference hosted at Stellenbosch University, South Africa, October 30,-November 02, 2012

Chapter 4

- J.B.H. Njagarah and F. Nyabadza, "A metapopulation model for cholera transmission dynamics between communities linked by migration", *Applied Mathematics and Computation*, **241**:317-331: 2014. [39].

  The results of this paper were presented at the Southern Africa Mathematical Sciences Association (SAMSA) conference, November 25-29, 2013, Jointly hosted by the Stellenbosch University, UCT, UWC and CPUT.

Chapter 5

- "Modelling optimal control of cholera in communities linked by migration", J.B.H. Njagarah and F. Nyabadza, (**in review**)

Chapter 6

- "Modelling the control of *V cholarae* with a pathogen specific bacteriophage", J.B.H. Njagarah and F. Nyabadza, *in preparation*.

Chapter 2

Literature review

Cholera being an ancient disease, it could not escape the treatment of mathematical models to understand its dynamics. The models developed and the subsequent modifications made to the existing models, are motivated by the continued understanding of the dynamics of the disease. Special treatment in some developed models is devoted to the specific places that could be under study. This is on the belief that even though the aetiological agent of cholera is the same, the transmission and dynamics of the disease may vary from place to place. This may require explicit determination of parameter values related to the complex transmission dynamics of the disease in the area in question. It is as-well plausible to believe that, with the progressive trends of research on the infection, more factors that drive the epidemic are identified. Some of the identified factors may be feasible to incorporate in the transmission dynamics of the models developed.

Some of the major challenges that have existed in modelling cholera dynamics have been consideration of all the possible transmission pathways, which include human- to-human transmission and the indirect environment-to human transmission [40], at the same time incorporating the population classifications (into symptomatic and asymptomatic) as well as the influence from other biological agents such as vibrio specific bacteriophage in an all inclusive model. We therefore, review some of the previous work done on modelling of cholera and highlight the key results from the selected models.

2.1 Mathematical models of cholera dynamics

In an attempt to study the complex transmission pathways, epidemiological models that describe the human-environment interaction have been developed. One of the earliest math-

ematical model for the transmission dynamics of cholera was proposed by Capasso and Paveri-Fontana [41] when studying the cholera epidemic in the Bali 1973. This model was published in 1979, a period when mathematical modelling of cholera was in its infancy. The model consist of two coupled differential equations given in system (2.1) as

$$\begin{aligned} \frac{dx_1}{dt} &= -a_{11}x_1 + a_{12}x_2, \\ \frac{dx_2}{dt} &= g(x_1) - a_{22}x_2. \end{aligned} \tag{2.1}$$

The two compartments (state variables) in this model include x_1 which describes the concentration of the pathogen in the aquatic environment, and x_2 the population of infected people. In the model all the constants a_{ij} are constant. The function $g(x_1)$ accounts for the incidence of cholera infection. The model presented in system of equations (2.1) describes the dynamics of the population infected with cholera and the pathogen freely living in the environment. In the model construction, time delay was neglected and focus was put on the sewage system simply carrying faecal cholera bacteria into the sea.

In Codeço's 2001 paper [36], the model by Capasso and Paveri-Fontana [41] was extended. In the extended model, the author considered the role played by the aquatic reservoir in the dynamics of cholera. In addition to the concentration of the pathogen in the aquatic environment and population of infected individuals, Codeço considered the population of susceptible individuals in a three compartmental model. The resulting model is given by the system of equations (2.2),

$$\begin{aligned} \frac{dS}{dt} &= n(H - S) - a\lambda(B)S, \\ \frac{dI}{dt} &= a\lambda(B)S - rI, \\ \frac{dB}{dt} &= eI - (mb - nb)B, \end{aligned} \tag{2.2}$$

where $\lambda(B) = \frac{B}{K+B}$. In the model, the terms S, I, B and H represent the susceptible population, the infected individuals, the concentration of the pathogen (*V. cholerae*) in the aquatic environment and the total human population respectively. n represents the human natural natality/mortality rates (day^{-1}). $\lambda(B)$ is the probability that an individual who has contact or consumes untreated water catches cholera and a the rate of contact with untreated water. The combination of the two terms yields a saturation function $a\lambda(B)$, which describes the rate at which susceptible individuals become infected. We note that the argument that the function $\lambda \in [0, 1]$ was also used in [41] where it is indicated that λ is approximately equal to vibrio concentration for at small concentrations of the pathogen and approximately equal

to one at very high vbrio concentrations. Therefore, the continuous function $\lambda(B)$ of the vibrio concentration satisfies the saturation requirement for agreement between mathematical modelling and cholera data. This similar argument has been always implied in ensuing mathematical models of cholera transmission dynamics.

Hartley *et al.* [42] extended the model presented by Codeço [36] in which the pathogen was not classified in accordance to its infective states. The model in [42] incorporated the hyperinfective (HI) and non hyperinfective (LI) states in the transmission dynamics of the cholera pathogen. The model equations of [42] is indicated in the system of equations (2.3).

$$\begin{aligned}
\frac{dS}{dt} &= bN - \beta_L S\frac{B_L}{k_L + B_L} - \beta_H S\frac{B_H}{k_H + B_H} - bS,\\
\frac{dI}{dt} &= \beta_L S\frac{B_L}{k_L + B_L} + \beta_H S\frac{B_H}{k_H + B_H} - (\gamma + b)I,\\
\frac{dR}{dt} &= \gamma I - bR,\\
\frac{dB_H}{dt} &= \xi I - \chi B_H,\\
\frac{dB_L}{dt} &= \chi B_H - \delta_L B_L.
\end{aligned} \tag{2.3}$$

In this model, B_H and B_L are the concentrations of HI and LI per ml, I are the infectious individuals and S the susceptible population. β_L and β_H is the rate of drinking LI and HI *V. cholerae* respectively. The rest of the parameters are well explained in [42]. In the numerical simulations, it is indicated that transmission due to HI produces majority of the new infections with a peak ratio of 1.6 between the HI and non-HI. In the same way, it was shown that the non-HI is responsible for the slow dynamics where as HI for the fast dynamics. The reproduction number for the model was calculated and indicated to be 18.2 when $\beta_H \sim \beta_L$. It however, reduces as β_L becomes smaller that β_H until it approaches a value of 3.2 when there is no contact with HI *V. cholerae* ($\beta_H = 0$). The major observation was that, the freshly excreted pathogen was more infectious than the recently excreted pathogen. It would also dominate the epidemic in case poor hygiene, continued and poor access to clean water. On the other hand, if good hygiene is maintained and proper disposal of sewage, the older non-hyperinfective organisms would dominate the epidemic. The model in [42] therefore suggests that irrespective of the time when an immunologically naive individual gets into contact with the pathogen there is always a possibility of contracting the disease. The major difference is only observed in the hyperinfectivity of the pathogenic vibrios one gets into contact with.

Mukandavire *et al.* [34] proposed a model that considers both human-to-human and environment-

to human transmission pathways. The model was used to study the dynamics of the cholera outbreak in Zimbabwe in 2008-2009. The model was used to estimate the basic reproduction numbers as well as partial reproduction numbers of the 10 provinces that were affected by the cholera epidemic. The model is presented in by the system of equations (2.4).

$$\begin{aligned}
\frac{dS}{dt} &= \mu N - \beta_e S\frac{B}{k+B} - \beta_h SI - \mu S,\\
\frac{dI}{dt} &= \beta_e S\frac{B}{K+B} + \beta_h SI - (\gamma+\mu)I,\\
\frac{dR}{dt} &= \gamma I - \mu R,\\
\frac{dB}{dt} &= \xi I - \delta B.
\end{aligned} \tag{2.4}$$

In the obtained results, the authors observed high heterogeneities in the variation of the both basic reproduction numbers as well as partial reproduction numbers across provinces. This could be due to the different transmission processes involved in the different provinces as well as the differences in living conditions. One intriguing observation was that human-to-human transmission was significant and accounted for about $41-95\%$ of all the transmission. This observation strongly supports the view that cholera may be contagious which dates back to Filippo Pacini's 1865 discoveries [43].

Jensen *et al.* [38] model which involved deterministic control of *V. cholerae* by the lytic bacteriophage specific for *V. cholerae* is presented below

$$\begin{aligned}
\frac{dS}{dt} &= -\pi\left(\frac{V}{C(a)k+V}\right)^a S - \delta S + \delta N,\\
\frac{dI_-}{dt} &= \pi\left(\frac{l}{l+P}\right)\left(\frac{V}{C(a)k+V}\right)^a S - (\mu_- + \delta)I_-,\\
\frac{dI_+}{dt} &= \pi\left(\frac{P}{l+P}\right)\left(\frac{V}{C(a)k+V}\right)^a S - (\mu_+ + \delta)I_+,\\
\frac{dR}{dt} &= \mu_- I_- + \mu_+ I_+ - \delta R,\\
\frac{dV}{dt} &= \left[m\left(1-\frac{V}{k_v}\right) - \gamma P\right]V + c(I_- + I+),\\
\frac{dP}{dt} &= (\beta\gamma V - \omega)P + \alpha c I_+.
\end{aligned} \tag{2.5}$$

The description of the state variables and the parameters is given in [38]. The bacteriophage in the model was considered to be antagonistic to the vibrio concentration. In this respect the phage concentration can have an influence on the bacterial bloom that initiates the infection and the severity of the infection.

In 2012, Wang and Liao [44] published a generalised cholera model where they did epidemic-endemic analysis. In the model, the authors utilised a generalised incidence function $f(I,B)$ which includes multiple transmission pathways. Although no explicit incidence function was given, the authors stated possible examples of such function as those used in the aforementioned models [34, 36, 38, 42]. In their generalised model, the authors also accounted for the pathogen growth function, $h(I,B)$, stating that it depends on both the ecology of the pathogen in the aquatic environment as well as the climatic conditions. Their generalised model is presented below.

$$\begin{aligned}\frac{dS}{dt} &= bN - Sf(I,B) - bS,\\ \frac{dI}{dt} &= Sf(I,B) - (\gamma + b)I,\\ \frac{dR}{dt} &= \gamma I - bR,\\ \frac{dB}{dt} &= h(I,B).\end{aligned} \tag{2.6}$$

In the model both the natural natality and mortality rates are equal and the total human population under consideration is constant.

Other models on cholera include; the model "On space-time evolution of cholera epidemic" which focuses on cholera spread along a river network [45]. The model which incorporates intervention strategies as well as the classification of infected individuals into those symptomatic and asymptomatic [20], the model incorporating the climatic changes and their influence on cholera indicating double peaks per year [9] among others.

Some questions to answer, observations from aforementioned models and possible modifications that can be made are highlighted below

(i) In the aforementioned models, no account is given of disease induced mortality and for that matter the general population mostly considered to be constant. If the disease induced mortality is considered, then the population will not be constant and the models would give generally different and more realistic dynamics.

(ii) The aforementioned transmission models do not put into consideration that in the wake of the epidemic or outbreak, individuals also change behaviour. For example they start to practice proper hygiene, boil drinking water, avoid consumption of potentially *Vibrio* contaminated food, properly dispose faecal matter the general decrease in movement to and from cholera endemic areas. These factors if accounted for can give a plausible basis for proper control of the infection.

(iii) With respect to the model with bacteriophage in the control process, the interactions is purely deterministic and presupposes that the aquatic medium is purely homogeneous. It is currently clear that more *V. cholerae* will be concentrated in areas where there is high effluent disposal (warm and nutrient rich) and also have a strong dynamics with both zooplankton (especially copepods) and phytoplankton. In addition, other factors such as temperature, salinity and PH make the aquatic environment heterogeneous and with ambient conditions of such factors, multiplication of vibrios in the environment is enhanced.

(iv) In the cholera dynamics, the person to person transmission root is not given much weight in most of the aforementioned models. This leaves a key question of whether this transmission root is really negligible, after the observing the spread of the infection during the 2000-2002 epidemic that devastated all but one province in South Africa, and the 2008 epidemic in Zimbabwe. In addition, there are concerns on the control of the epidemics and the efforts needed to contain any cholera outbreak.

Chapter 3

Role of hygiene driven contact in cholera transmission dynamics

3.1 Introduction

Cholera is one of the most notorious water borne infections affecting people world wide. It is mainly a problem in areas where people have no access to clean water, where there is poor hygiene, handling and storage of food. There have been numerous studies on the infection since John Snows work in England in 1811 during the outbreak in England. He pointed to the sewage contaminated water source to contain the pathogen that caused the disease. The pathogen (etiologic agent *Vibrio cholerae*) was discovered by an Italian microbiologist Filippo Pacini (1812-1883) in 1854 [43, 46] during the epidemic in Florence-Italy. However, he had not been recognised for this discovery not until 1956, 83 years after his death. All the credit had gone to a German Microbiologist Robert Koch who also discovered the same pathogen in his separate studies without knowledge of Pacini's work. During Pacini's work on cholera, he steadfastly reiterated that the disease is contagious [43, 47]. Since 1811, upto seven epidemics of cholera have swept many parts of the world with the most affected areas being India, Bangladesh and Indonesia. The first cases of cholera on the African continent were in 1971 during the seventh epidemic.

The first cases in South Africa were mainly concentrated in mines [28]. Once the person is infected with the pathogen, it attacks the gastric lining causing sever diarrhoea. Although it can be contained through oral rehydration and restoration of the electrolyte imbalance in the body, the infections still result in some disease induced mortality. Indeed the mortality and cases observed in the recent outbreaks can not be ignored. Here we cite the example of the recent outbreak in Haiti where upto 217 000 people were infected. The epidemic

had also claimed about 4 000 lives by January 2011 since its beginning in October 2010 [19]. Such mortality is not negligible and ought to be given some consideration in studies aimed at understanding the cholera transmission dynamics and severity. Although the last major outbreak of cholera epidemic was in 2000-2001, in KwaZulu Natal, there have been sporadic cases of the disease in the Northern Cape, Limpopo, Eastern cape and still in KwaZulu Natal provinces.

3.2 Model development and analysis

A number of mathematical models have been developed to study the dynamics of cholera infection. The very first model was Capasso and Paveri-Fontana [41] where they studied the 1973 cholera epidemic in Bali, Italy. The model consisted of system of two differential equations describing the population of infected individuals and the concentration of the pathogen in the aquatic reservoir. The model was later extended by Codeço [36] who included an equation of the susceptible population in order to study the long term dynamics of the population. In addition she explicitly considered the role played by the pathogen in the aquatic reservoir. Here she used a maximum saturation function $\lambda(B) = \frac{B}{K+B}$, where B is the concentration of the pathogen in the aquatic environment and K the concentration of the pathogen that can cause 50% chance of getting infected if consumed. This same function has been used in the recent models of cholera dynamics, see for instance [34, 38, 42] among others. The saturation function of the form of $\lambda(B)$ indicates that the increase in rate of incidence of the disease more gradual than linear in B and S. In addition, this ensures that the contact rate is bounded.

We use a mathematical model (which is a modification from the aforementioned models in Chapter 2) to analyse the transmission dynamics of cholera. In this model we assume that in the wake of the epidemic, the population changes behaviour with respect to devoting to proper sanitary practices, good handling and storage of food, reduction in person-to person contact. We represent the expression for behaviour change with an exponential function that decreases as a result of improvement in hygiene. In the aforementioned models, the natality and mortality rates are assumed to be the same with no infection aggravated mortality. In our view, even though, the mortality due to cholera might have reduced recently due to presence of proper medical care, rehydration and restoration of electrolyte imbalance, the mortality cases are still significant.

In our model we assume that once the infection breaks out, the population may change be-

haviour by starting to boil drinking water and properly dispose faecal material, and as a result of awareness and provision of clean water and bleach to clean the water, the tread of the epidemic will decrease. We compartmentalise the population basing on different levels of infection. The recruitment into the susceptible population is at a constant rate. The recruitment is due to natural natality as well as immigration. The population infected with *V. cholerae* is not all symptomatic. We have a group of healthy carriers of the pathogen. These remain asymptomatic yet in case of improper disposal of waste material shed the pathogen in the environment and water sources and this contributes to the spread of the infection.

3.2.1 Hygiene related contact function

The spread of cholera and the concentration of both the hyperinfective pathogen (newly shed into the environment) and the non hyperinfective *V. cholerae* is influenced by the level Hygiene of the affected community. Hygiene may involve proper preparation and handling food, boiling or filtering drinking water as well as ensuring proper disposal of faecal material. In the model we assume that the effective person to person contact is influenced by the level of hygiene. Therefore, we propose a functional relationship $f(H)$, between person to person contact and level of hygiene. We denote the hygiene level by the variable H, which is related to the total population. H measures the proportion of the population that practising proper hygiene. The function $f(H)$ describes the contact rate which is dependent on the level of hygiene. It is plausible to believe that the effective contact rate will reduce with increased levels of hygiene.

$$f(H) = \begin{cases} \beta_c, & \text{(3.1a)} \\ \beta_{\max} - \eta_1 H, & \text{(3.1b)} \\ \beta_{\max} e^{-\eta_2 H}, & \text{(3.1c)} \\ \dfrac{\beta_{\max}}{1 + e^{\eta_3 (H - H_{50})}}. & \text{(3.1d)} \end{cases}$$

The constant contact rate has been used previously in modelling person-to-person contact in cholera transmission dynamics by Mukandavire *et al.* [34]. The equations (3.1b)-(3.1d) have been suggested by [48] as potential candidates for the functional relationship between effective contact rate and hygiene in the model for hepatitis A. Equation (3.1b) predicts that the effective person-to-person contact rate is reduced linearly proportionally to the improvement in the level of hygiene. Such a linear reduction would only be viable if the transmission

mode is through contact with members of the same house-hold [48]. The equation (3.1c) is feasible if all individuals share a common source of the pathogen. On the other hand, equation (3.1d) is most useful in the situation where; if the level of hygiene is low, there is a small effect on the transmission dynamics of the pathogen but the effect increases at higher hygiene levels [48].

We propose a contact rate function that is dependent on the proportion of the population that practices proper hygiene.

$$f(H) = \frac{\beta_h^{\max}}{1 + Ae^{\eta H}} \tag{3.2}$$

The constant A is the scale parameter and η the shape parameter. The parameter A is such that $0 < A \ll 1$. This implies that if the level of hygiene is very poor, the rate of spread of the pathogen through person-to-person contact will be approximately $\beta_h^{\max}$. This could be of a devastating impact in case of an outbreak. The parameter η determines how fast the impact of improved hygiene can be felt in case of an outbreak. It is important to note that if $H = 1$, $f(H) \to 0$ when $\eta \to \infty$. Therefore, the parameter η must be chosen such that $f(H) \to 0$ as $H \to 1$. A typical example of hygiene driven change in person-to-person contact rate is showed in Figure 3.1.

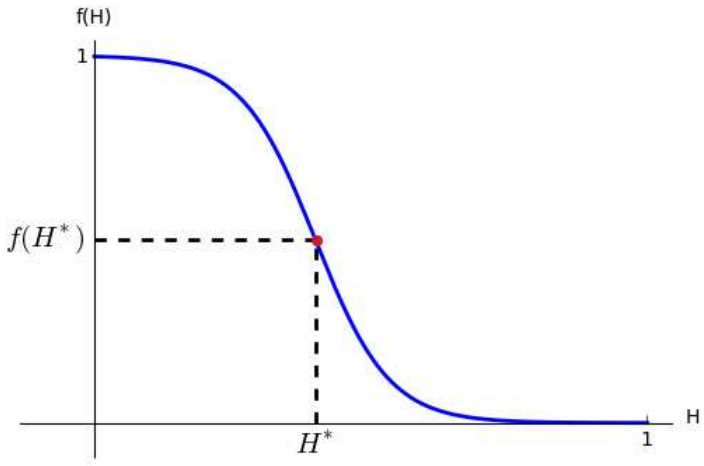

Figure 3.1: Contact rate as a function of the level of hygiene in the community.

We note that for $H < \frac{\ln(A)}{\eta}$, $f(H)$ is concave down indicating an increasing negative change of contact with the level of hygiene. On the other hand at $H > \frac{\ln(A)}{\eta}$, $f(H)$ is concave up showing a decreasing negative contact with the level of hygiene. We also propose that the rate at which symptomatic and asymptomatic individuals shed the pathogen into the environment differs. Although, this shedding rate may depend on the level of hygiene, quan-

tifying it with a functional response is a daunting task. The symptomatic individuals are believed to shed the pathogen into the environment in greater quantities but for a slightly short time. On the other hand, asymptomatic individuals shed the lower concentrations into the aquatic environment compared to symptomatic individuals. However, the shedding time is much longer for the asymptomatically infected individuals. The flow diagram, Figure 3.2, shows the dynamics of the population in different compartments as well as the interaction with the aquatic environment. The typical Susceptible-Infected-Recovered (SIR) model describes the vital dynamics which are typical of the cholera epidemics. The infectious population is classified into symptomatic and asymptomatic individuals. The major routes of infection include consumption of vibrio contaminated water and well as through person-to-person contact characterised by consumption of unhygienic food stuffs.

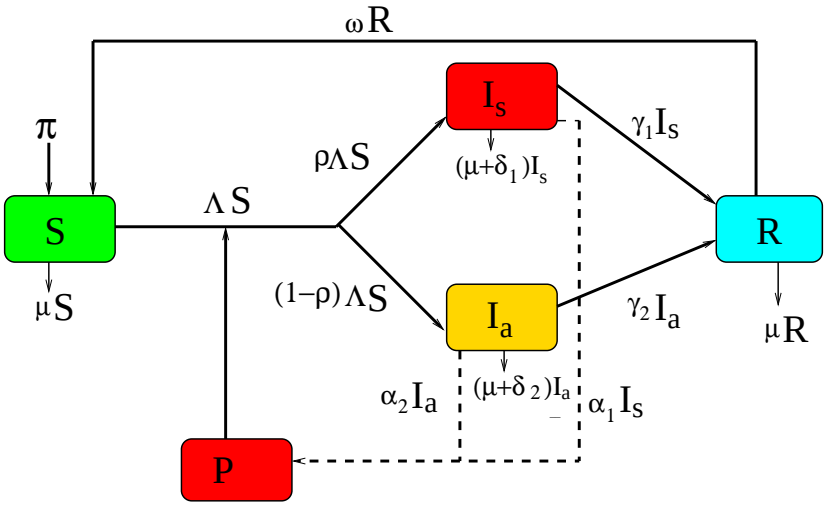

Figure 3.2: Flow diagram of dynamics of the populations involved in the dynamics of cholera.

State	Description
S	Population of susceptible individuals
I_s	Infected individuals who are symptomatic
I_a	Infected individuals who are asymptomatic
R	Recovered individuals
P	Concentration of *vibrios* in the aquatic environment

Table 3.1: Description of the model phase state variables

3.2.2 Model

The proposed system of differential equations is

$$\frac{dS}{dt} = \pi + wR - \beta\frac{P}{K+P}S - f(H)IS - \mu S, \tag{3.3a}$$

$$\frac{dI_s}{dt} = \rho\left(\beta\frac{P}{K+P}S + f(H)IS\right) - (\mu + \delta_1 + \gamma_1)I_s, \tag{3.3b}$$

$$\frac{dI_a}{dt} = (1-\rho)\left(\beta\frac{P}{K+P}S + f(H)IS\right) - (\mu + \delta_2 + \gamma_2)I_a, \tag{3.3c}$$

$$\frac{dR}{dt} = \gamma_1 I_s + \gamma_2 I_a - (\mu + w)R, \tag{3.3d}$$

$$\frac{dP}{dt} = \alpha_1(H)I_s + \alpha_2(H)I_a - \mu_p P + rP\left(1 - \frac{P}{K_p}\right). \tag{3.3e}$$

The description of model parameters as summarised in the Table 3.2

Parameter	Description
π	Rate of recruitment of individuals into the susceptible class
w	Rate at which immunity acquired due to cholera waves
β	Rate at which susceptible individuals contact with the aquatic reservoir
K	Concentration of *Vibrios* that can cause a 50% chance of infection
μ	Natural morality rate of the general population
δ_1	Mortality rate of I_s individuals due to cholera
δ_2	Mortality rate of I_a individuals due to cholera
γ_1	Rate of recovery of symptomatically infected individuals
γ_2	Rate of recovery of asymptomatically infected individuals
K_p	Carrying capacity of the aquatic reservoir for the pathogen
α_1	Rate at I_s individuals shed the pathogen in the environment
α_1	Rate at I_a individuals shed the pathogen in the environment
r	Growth rate of the pathogen
μ_p	Decay rate of the pathogen
ρ	Proportion of infected individuals who are symptomatic

Table 3.2: Description of the model parameters

3.2.3 Model analysis

Given that person-to-person contact is based on the level of hygiene, the improvement is hygiene should be such an effort to reduce the infections or even to prevent the infection completely. We observe that the number of infected individuals will decrease if the model parameters are such that $\frac{dI}{dt} < 0$, where $I = I_a + I_s$. From (3.3), the change in the number of those infected with cholera is given by

$$\frac{dI}{dt} = \beta\frac{P}{K+P}S + f(H)IS - (\mu + \delta + \gamma)\,T. \tag{3.4}$$

The infection will be contained if the person to person contact which is dependent on level of hygiene is such that

$$f(H) < \frac{QI(K+P) - \beta PS}{(K+P)IS}, \text{ where } Q = (\mu + \delta + \gamma). \tag{3.5}$$

This expression for hygiene dependent person-to-person contact (3.2) substituted into the inequality (3.5) gives the threshold hygiene level as

$$H = \frac{1}{\eta} \ln \left[\frac{1}{A} \left(\frac{C_{\max}(K+P)IS}{QI(K+P) - \beta PS} - 1 \right) \right]. \tag{3.6}$$

Note from the expression (3.6) that the level of hygiene is influenced by contact with water supplies as well interaction between individuals. If the aquatic environment is assumed to play the major role, then the expression becomes

$$H = \frac{1}{\eta} \ln \left[\frac{1}{A} \left(\frac{C_{\max} S}{Q} - 1 \right) \right],$$

which involves only the direct transmission route.

Positivity of solutions

We show that if the system starts with non-negative initial conditions $(S_0, I_{s0}, I_{a0}, R_0, P_0)$, the solutions/trajectories of (3.3) will remain non-negative for all $t \in [0, \infty)$. This is an ideal condition to check since the model monitors human population and the pathogen concentration in the aquatic environment. We thus have the following theorem

Theorem 3.2.1. *Given that the initial conditions of the system* (3.3) $(S_0 > 0, I_{s0} > 0, I_{a0} > 0, R_0 > 0, P_0 > 0)$, *the resulting solutions* $(S(t), I_s(t), I_a(t), R(t), P(t))$ *are all non-negative for all* $t \in [0, \infty)$.

Proof. To show positivity of solution, it is enough to show that each of the trajectories of system (3.3) is non negative for all $t > 0$. From equation (3.3a), the differential inequality describing the evolution of the susceptible population over time is given by

$$\frac{dS}{dt} \geq -\left(\frac{\beta P(t)}{K + P(t)} + f(H)I(t) + \mu \right) S. \tag{3.7}$$

The resulting differential inequality can be solved by separation of variables. Since at $t = 0$, $S(0) = S_0$, then the complete solution to the differential inequality for the susceptible population is given by

$$S(t) \geq S_0 \exp\left\{ -\left(\mu t + \int_0^t \left(\frac{\beta P(\tau)}{K + P(\tau)} + f(H)I(\tau) \right) d\tau \right) \right\}. \tag{3.8}$$

From (3.8) it can be shown that

$$\liminf_{t\to\infty} S(t) \geq 0. \tag{3.9}$$

Using the same principle, the rest of the phase space variables t approaches infinity can be shown to satisfy

$$I_s(t) \geq I_{s0}e^{-Q_1 t}, \;\; I_a(t) \geq I_{a0}e^{-Q_2 t}, \;\; R(t) \geq R_0 e^{-(\mu+\omega)t}, \tag{3.10}$$

from which the limit inf of the corresponding state variables can be shown to be non-negative. Using the equation describing the evolution of the pathogen concentration, we have a differential inequality given by

$$\frac{dP}{dt} + (\mu_P - r)P \geq -\frac{rP^2}{K_P}. \tag{3.11}$$

Equation (3.11) is a Bernoulli type of equation. It is solved by substitution, i.e $P = y^{-1}$ to obtain

$$P \geq \frac{1}{CK_P(\mu_P - r)e^{(\mu_P - r)t} - r} \geq \frac{e^{-(\mu_P - r)t}}{CK_P(\mu_P - r)}. \tag{3.12}$$

□

Boundedness of solutions

The model can be separated into two parts which include, the human population $\mathcal{W}_H$ and the concentration of the pathogen in the aquatic environment $\mathcal{W}_P$ such that

$$\mathcal{W}_H = \{(S, I_a, I_s, R) : S + I_a + I_s + R = N\} \in \mathbb{R}^4_+ \tag{3.13}$$

and

$$\mathcal{W}_P = \{P\} \in \mathbb{R}^1_+, \tag{3.14}$$

respectively. From equation (3.3a) the differential inequality of the susceptible population is given by

$$\frac{dS}{dt} + \mu S \leq \pi + \omega R. \tag{3.15}$$

Using a suitable integrating factor, I.f $= \mathrm{e}^{\mu t}$, the differential inequality (3.15) can be solved to obtain

$$S \leq \frac{\pi}{\mu} + e^{-\mu t}\int_0^t \omega R(\tau)e^{\mu\tau}d\tau. \tag{3.16}$$

Following the theorem of differential inequality by Birkhoff and Rota [49] we obtain

$$\limsup_{t\to\infty} S(t) \leq \frac{\pi}{\mu}. \tag{3.17}$$

Therefore, the state variables describing the evolution of the susceptible population is less or equal to the ratio of the recruitment rate and the natural mortality rate.

We note also that the total population is given as $N = S + I_s + I_a + R$. If we take the time derivative of N i.e $\frac{dN}{dt}$ and substitute the equations (3.3a) -(3.3d) into the resulting expression we obtain

$$\frac{dN}{dt} = \pi - \mu N - (\delta_1 + \gamma_1) I_s - (\delta_2 + \gamma_2) I_a. \tag{3.18}$$

The solution (3.18) can be obtained by separating variables and integrating both sides with respect to the corresponding variable. This results into

$$\ln|\pi - \mu N| \geq -\mu t + c, \tag{3.19}$$

where c is a constant of integration. If we exponentiate both sides and assume that the initial total population is N_0, the solution becomes

$$N \leq \frac{\pi}{\mu} - \left(\frac{\pi}{\mu} - N_0\right) e^{-\mu t}. \tag{3.20}$$

Therefore,

$$\limsup_{t\to\infty} N = \frac{\pi}{\mu}. \tag{3.21}$$

Since N is the sum of all state space variables, then each of the individual state variables is less or equal to $\frac{\pi}{\mu}$.

Using equation (3.3e), we assume that the growth rate of the pathogen in linear at a constant rate r. We therefore obtain a differential inequality

$$\frac{dP}{dt} \leq \alpha_1 I_s + \alpha_2 I_a - \mu_P P + rP. \tag{3.22}$$

Since each of I_s and I_a is less or equal to $\frac{\pi}{\mu}$, the equation (3.22) becomes

$$\frac{dP}{dt} \leq (\alpha_1 + \alpha_2) \frac{\pi}{\mu} - \mu_P P + rP. \tag{3.23}$$

The solution to this equation can be obtained by using a suitable integrating factor to obtain

$$P \leq \frac{(\alpha_1 + \alpha_2)\pi}{\mu(\mu_P - r)} + Ae^{-(\mu_P - r)t}. \tag{3.24}$$

Therefore,

$$\limsup_{t\to\infty} P(t) \leq \frac{(\alpha_1 + \alpha_2)\pi}{\mu(\mu_P - r)}. \tag{3.25}$$

The domain of biological significance of the system (3.3) is

$$\Omega := \left\{ S, I_s, I_a, R, P \geq 0 : S + I_s + I_a + R \leq \frac{\pi}{\mu}, P(t) \leq \frac{(\alpha_1 + \alpha_2)\pi}{\mu(\mu_P - r)} \right\} \tag{3.26}$$

The domain Ω is positively invariant under the flow induced by the system (3.3). Therefore, the system (3.3) is biologically meaningful and it is feasible to analyse the model in the domain Ω.

3.2.4 Disease free equilibrium and its stability

Supposing that the community has not experienced cholera infection for very a long time, say for generations, no individual will be expected to be immune. This is because, immunity to cholera infection is often acquired because of passed infection or exposure and or immunisation. This implies that the entire community will be rendered susceptible to the infection. In this respect, there will be no symptomatic or asymptomatic infectious individuals. In addition, the aquatic reservoirs with which the general population has contact are free of virulent or toxigenic *vibrios* [36]. Therefore, the community is free the infection and the disease free equilibrium is given by

$$\mathbb{E}_0 = (S^*, I_s^*, I_a^*, R^*, P^*) = \left(\frac{\pi}{\mu}, 0, 0, 0, 0 \right). \tag{3.27}$$

Therefore, if initially neither the infective nor the pathogen exists in the environment, the community is expected to remain free of the disease. On the other hand, in the treatment of the initial conditions, if either $I_{a0} > 0$ or $I_{s0} > 0$ and $P_0 = 0$, the infection will originate from the infected people in the community. On the contrary, if $I_{a0} = 0$ and $I_{s0} = 0$ but $P_0 > 0$, the infection would be triggered by freely leaving vibrios in the environment.

Basic reproduction number

In this model new infections are generated in three ways, namely; by consumption of the pathogen from the aquatic environment, contact with symptomatically or asymptomatically infected individuals. We therefore define the basic reproduction number $(\mathcal{R}_0)$ as "the average number of new infections generated by a single (asymptomatic or symptomatic) infected individual in a completely susceptible population [50] or through contact with the pathogen infested aquatic reservoir". We also emphasize that the reproduction number computed should reflect all the routes contributing to new infections. We use the next-generation matrix method by van den Driessche and Watmough [51], such that the matrices of new infec-

tions and transitions are given by

$$\mathcal{F} = \begin{pmatrix} \rho\left(\frac{\beta PS}{K+P} + IS\right) \\ (1-\rho)\left(\frac{\beta PS}{K+P} + CIS\right) \\ 0 \end{pmatrix}, \qquad \mathcal{V} = \begin{pmatrix} Q_1 I_s \\ Q_2 I_a \\ -\alpha_1 I_s - \alpha_2 I_a + Q_4 P \end{pmatrix}, \tag{3.28}$$

where $Q_1 = (\mu + \delta_1 + \gamma_1)$, $Q_2 = (\mu + \delta_2 + \gamma_2)$, $Q_4 = (\mu_P - r)$ and $C = C_{\max}\beta_h$. In this case the C is the effective person-to-person contact rate. It is the product of the maximum possible contacts, $C_{\max}$ and the probability β_h, that a contact results into cholera infection. The derivatives of the resulting matrix expressions for the new infections and transition states evaluated at the disease free equilibrium are given by

$$F = \begin{pmatrix} \frac{\rho C\pi}{\mu} & \frac{\rho C\pi}{\mu} & \frac{\rho\beta\pi}{\mu K} \\ \frac{(1-\rho)C\pi}{\mu} & \frac{(1-\rho)C\pi}{\mu} & \frac{(1-\rho)\beta\pi}{\mu K} \\ 0 & 0 & 0 \end{pmatrix}, \qquad V = \begin{pmatrix} Q_1 & 0 & 0 \\ 0 & Q_2 & 0 \\ -\alpha_1 & -\alpha_2 & Q_4 \end{pmatrix}. \tag{3.29}$$

The entry (i, j) of the matrix V^{-1} is defined as the average life expectancy if an individual in compartment i and entry (i, j) of F the rate at which an infected individual in compartment j produces new infections in compartment i [51]. The reproduction number $\mathcal{R}_0$ is given as the spectral radius of matrix FV^{-1} which is classified as the next generation matrix.

$$\begin{aligned} \mathcal{R}_0 &= \rho\left(FV^{-1}\right), \\ &= \frac{\rho\pi}{\mu Q_1 Q_4}\left(\frac{\beta\alpha_1}{K} + CQ_4\right) + \frac{(1-\rho)\pi}{\mu Q_2 Q_4}\left(\frac{\beta\alpha_2}{K} + CQ_4\right). \end{aligned} \tag{3.30}$$

The terms $1/Q_1$ and $1/Q_2$ indicate the maximum time an individual is expected to stay in compartments I_s and I_a respectively. The reproduction number consists of four terms which characterise the contribution from the different pathways to new infections with cholera. The terms $R_{01} = \frac{\rho\pi\beta\alpha_1}{\mu Q_1 Q_4 K}$ and $R_{02} = \frac{(1-\rho)\pi\beta\alpha_2}{\mu Q_2 Q_4}$ represent the new infections of symptomatic and asymptomatic individuals respectively that result from consumption of the pathogen from the aquatic environment. On the other hand the terms $R_{03} = \frac{\rho\pi C}{\mu Q_1}$ and $R_{04} = \frac{(1-\rho)\pi C}{\mu Q_2}$ show new infections of symptomatic and asymptomatic individuals respectively due to person-to-person contact.

Local stability of the disease free equilibrium (DFE)

Theorem 3.2.2. *The cholera free equilibrium of locally asymptotically stable whenever $\mathcal{R}_0 < 1$ and unstable otherwise.*

The result of Theorem 3.2.2 follows directly from the next generation matrix. An alternative proof can be given by linearising the system of equation (3.3) at the disease free equilibrium. In this case, the a constant value for the hygiene driven person-to-person transmission is assumed and the alternative proof is given as follows.

Proof. To prove local stability of the model, we linearise the system (3.3) and evaluate the Jacobian at the disease free equilibrium $\mathbb{E}_0$. In this proof the person to person transmission rate $f(H)$ is assumed to be some constant value f_h. The Jacobian is therefore given by

$$J(\mathbb{E}_0) = \begin{pmatrix} -\mu & \frac{\rho f_h \pi}{\mu} & \frac{\rho f_h \pi}{\mu} & \omega & \frac{\rho\beta\pi}{\mu K} \\ 0 & \frac{\rho f_h \pi}{\mu} - Q_1 & \frac{\rho f_h \pi}{\mu} & 0 & \frac{\rho\beta\pi}{\mu} \\ 0 & \frac{(1-\rho) f_h \pi}{\mu} & \frac{(1-\rho) f_h \pi}{\mu} - Q_2 & 0 & \frac{(1-\rho)\beta\pi}{\mu K} \\ 0 & \gamma_1 & \gamma_2 & -Q_3 & 0 \\ 0 & \alpha_1 & \alpha_2 & 0 & -Q_4 \end{pmatrix} \tag{3.31}$$

The matrix (3.31) has two negative eigenvalues $\lambda_1 = -\mu$ and $\lambda_2 = -Q_3$. The rest of the eigenvalues are the roots of the polynomial

$$P(\lambda) = \lambda^3 + a_2\lambda^2 + a_1\lambda + a_0, \tag{3.32}$$

where the constants are such that

$$\begin{cases} a_1 = Q_1Q_4[1 - (R_{01} + R_{02})] + Q_2Q_4[1 - (R_{03} + R_{04})] + Q_1Q_2[1 - (R_{02} + R_{04})], \\ a_2 = Q_1(1 - R_{02}) + Q_2(1 - R_{04}) + Q_4, \\ a_0 = Q_1Q_2Q_4(1 - \mathcal{R}_0). \end{cases}$$

We note that when $R_0 \leq 1$, the coefficients a_0 and a_1 will be positive. We now use Routh-Hurwitz condition for a third order polynomial [52]. We note that if all the coefficients a_0, a_1 and a_2 are positive, then the roots of the polynomial (3.32) will all be either negative or with negative real parts if $a_1a_2 > a_0$. Thus, using the coefficients of the polynomial (3.32), we have

$$\begin{aligned} a_1a_2 - a_0 = {} & Q_1Q_4\left(Q_1 + Q_4 - \frac{f_h\pi}{\mu}\right)(1 - R_{01} - R_{02}) \\ & + Q_2Q_4\left(Q_2 + Q_4 - \frac{f_h\pi}{\mu}\right)(1 - R_{03} - R_{04}) \\ & + Q_1Q_2\left(Q_1 + Q_2 + Q_4 - \frac{f_h\pi}{\mu}\right)(1 - R_{02} - R_{04}) + Q_1Q_2Q_4 > 0. \end{aligned} \tag{3.33}$$

Therefore, the disease free equilibrium $\mathbb{E}_0 \in \Omega$ is locally asymptotically stable when $\mathcal{R}_0 < 1$ and unstable elsewhere. This completes the proof. □

It is necessary to clarify what exactly happens when the basic reproduction number is less or greater than unity, with respect to progression of the disease or containment of the disease

burden. When $\mathcal{R}_0 \leq 1$, in presence of a small number of infectives introduced in the community, the resulting number of subsequent infective individuals will be lower than that of their predecessors. As a result the change in the number of those infected with time will be negative an therefore, the infection cannot progress in the population. On the other hand, if $\mathcal{R}_0 > 1$, the subsequent generation of infective individuals will be greater than their predecessors. As a result the infection will spread and become endemic in the population until the susceptible population reaches such a level that the probability of infective individuals transmitting the disease to new individuals is very low due to depletion of the susceptible pool. This implies that given all the parameter values of the model, we can find the critical value of susceptibles below which the infection can not spread. To obtain this critical value for the model, we use the approach outlined in [50] based on the disease threshold. Given the reproduction number (3.30), make use of the susceptible population at the disease free steady state. If we set $\mathcal{R}_0 = 1$ and that $S_0^* = \frac{\pi}{\mu}$, then we have the critical value of the susceptible population given by

$$S_c = \frac{Q_1 Q_2 Q_4 K}{\beta(\rho\alpha_1 Q_2 + (1-\rho)Q_1\alpha_2) + f_h K Q_4(\rho Q_2 + (1-\rho)Q_1)}. \tag{3.34}$$

We note here that if the population of infectious individuals is not classified into those symptomatic and asymptomatic, which would imply that $Q_1 = Q_2 = Q$ and $\alpha_1 = \alpha_2 = \alpha$, the critical value of the susceptible population reduces to a value similar to that obtained in [50]. We note that the threshold susceptible population S_c changes with key parameters as indicated below:

1. it is inversely proportional to the effective person-to-person contact rate. Since this rate is proportional to the level of hygiene, then with improved hygiene, a large population of susceptible individuals will be required for onset of the epidemic.

2. It is directly proportional to the concentration of vibrios which when ingested cause 50% chance of infection with cholera.

This concentration K is also referred to as infection barrier [36]. If the model incorporates no person-to-person contact, this proportionality of S_c to K would be typically linear if other parameters are kept constant.

Global stability of the disease free equilibrium

The equilibrium point of a dynamical system (3.3) is said to be stable if solutions of such a system starting close to the equilibrium point within the invariant region approach the equilibrium point. On the contrary, if the equilibrium point is unstable, then all solutions starting sufficiently close to that particular equilibrium point will move away from the equilibrium point.

Theorem 3.2.3. *The disease free equilibrium $\mathbb{E}_0$ of the model system (3.3) is globally asymptotically stable in the invariant region Ω whenever $\mathcal{R}_0 < 1$ and unstable otherwise.*

Proof. To prove Theorem 3.2.3, we chose a suitable Lyapunov function given by

$$V(t) = a_1 I_s(t) + a_2 I_a(t) + a_3 P(t), \tag{3.35}$$

which involves individuals who directly contribute to escalation of the infection together with the pathogen. The constants a_1, a_2, a_3 are all non negative and we ought to find them. We note that Lyapunov function, $V(t)$ is a C^1 and a positive definite function for all $x \notin \mathbb{E}_0$. The time derivative of the Lyapunov function (3.35) is given by

$$\begin{aligned}\frac{dV}{dt} &= a_1\frac{dI_s}{dt} + a_2\frac{dI_a}{dt} + a_3\frac{P}{dt},\\ &= a_1\left[\rho\left(\beta\frac{P}{K+P}S + f_h IS\right) - Q_1 I_s\right] + a_2\left[(1-\rho)\left(\beta\frac{P}{K+P}S + f_h IS\right) - Q_2 I_a\right]\\ &\quad + a_3\left[\alpha_1 I_s + \alpha_2 I_a - Q_4 P\right].\end{aligned}$$

We note that $S \leq \frac{\pi}{\mu}$ and assume that near the disease free equilibrium, $K \gg P$ (the concentration of the pathogen is negligible compared to the carrying capacity) such that $K + P \approx K$. Therefore, the time derivative of the Lyapunov function satisfies the following inequality

$$\begin{aligned}\frac{dV}{dt} \leq &\left[a_1\frac{\rho\pi\beta}{\mu K} + a_1\frac{(1-\rho)\pi\beta}{\mu K} - a_3 Q_4\right] P\\ &+ \left[a_1\frac{\rho\pi f_h}{\mu} - a_1 Q_1 + a_2\frac{(1-\rho)\pi f_h}{\mu} + a_3\alpha_1\right] I_s\\ &+ \left[a_1\frac{\rho\pi f_h}{\mu} + a_2\frac{(1-\rho)\pi f_h}{\mu} - a_2 Q_2 + a_3\alpha_2\right] I_a.\end{aligned} \tag{3.36}$$

We equate the coefficients of the components I_a and P to zero and solve for the coefficients of the Lyapunov function obtaining

$$a_1 = Q_2 - \frac{\pi(1-\rho)}{\mu}\left(\frac{\beta\alpha_2}{Q_4 K} + f_h\right),\ a_2 = \frac{\pi\rho}{\mu}\left(\frac{\beta\alpha_2}{Q_4 K} + f_h\right),\ a_3 = \frac{\pi\beta\rho Q_2}{\mu Q_4 K}. \tag{3.37}$$

Substituting the constants a_1, a_2 and a_3 into the inequality (3.36), we obtain

$$\frac{dV}{dt} \leq -Q_1 Q_2\left[1 - \mathcal{R}_0\right] I_s. \tag{3.38}$$

When $\mathcal{R}_0 \leq 1$, $\frac{dV}{dt}$ is negative semidefinite, with equality at $\mathcal{R}_0 = 1$ and, or $I_s \in \mathbb{E}_0$. Therefore, the largest compact invariant set in Ω such that $\frac{dV}{dt} = 0$ when $\mathcal{R}_0 \leq 1$ is the singleton $\mathbb{E}_0$. Therefore, by the LaSalle Invariance Principle [53], the disease free equilibrium $\mathbb{E}_0$ is globally asymptotically stable in Ω if $\mathcal{R}_0 \leq 1$ and unstable otherwise. □

Epidemiologically, the implication of Theorem 3.2.3 is that when $\mathcal{R}_0$ is less than one, a small influx of cholera infected individuals into the community, will not generate an outbreak. The subsequent numbers of those infected will be less than that of their predecessors and eventually the disease will be annihilated. We note also that a number of parameters are necessary in reducing the disease threshold to a value $0 < \mathcal{R}_0 < 1$. Some of these parameter are related to consumption of contaminated water and foods. Control of hygiene related processes may involve chlorination of drinking water and those related to human behaviour may entail alteration of traditional community historical habits which may be challenging. From a mathematical modelling perspective, consideration of controls may require treatment of the modelling work as an optimal control problem. A model with controls is presented in Chapter 5 with focus on the metapopulation spread of the infection.

3.2.5 The endemic equilibrium

Let the endemic equilibrium be represented by the phase space

$$\mathbf{E_1} = (S^*, I_a^*, I_b^*, R^*, P^*) \in \mathbb{R}_+^5$$

. At the endemic equilibrium, each of the population phase space variable is constant, such that the rate of change of each of the components is zero. We note that the endemic equilibrium may be exhibited at some point related the concentration of the pathogen. Either when the concentration of the pathogen is low such that $P \ll K_p$ or when $P \simeq K_p$. However, the latter case implies that the entire aquatic environment would be contaminated which is less likely since vibrios may not sustain their concentration in the environment without constant shedding [41]. The first case scenario implies that the term $P/K_p \simeq 0$, the evolution of pathogen in the environment in absence of shedding from infected persons will be Malthusian where it may be increasing or decreasing depending on the difference between decay and growth rates. Malthusian growth is a plausible assumption at low concentration of the pathogen also supported by the rapid growth of the innoculum of vibrios observed in [54] (more details to this are indicated in Chapter 6). Assuming that $P \ll K_p$ at the endemic

equilibrium, from (3.3) We obtain

$$0 = \pi + wR^* - \beta\frac{P^*}{K+P^*}S^* - f(H)I^*S^* - \mu S^*, \tag{3.39a}$$

$$0 = \rho\left(\beta\frac{P^*}{K+P^*}S^* + f(H)I^*S^*\right) - Q_1 I_s^*, \tag{3.39b}$$

$$0 = (1-\rho)\left(\beta\frac{P^*}{K+P^*}S + f(H)I^*S^*\right) - Q_2 I_a^*, \tag{3.39c}$$

$$0 = \gamma_1 I_s^* + \gamma_2 I_a^* - Q_3 R^*, \tag{3.39d}$$

$$0 = \alpha_1 I_s^* + \alpha_2 I_a^* - Q_4 P^* \tag{3.39e}$$

From equations (3.39b) and (3.39c), we obtain the expression of all new infections in terms I_s^* as follows

$$\frac{Q_1 I_s^*}{\rho} = \left(\beta\frac{P^*}{K+P^*}S^* + f(H)I^*S^*\right), \tag{3.40}$$

$$\frac{Q_2 I_a^*}{1-\rho} = \left(\beta\frac{P^*}{K+P^*}S + f(H)I^*S^*\right). \tag{3.41}$$

Equating the left hand sides of equations (3.40) and (3.41), we obtain the expression of asymptomatically infected individuals as a function of those symptomatically infected as

$$I_a^* = \frac{(1-\rho)Q_1 I_s^*}{\rho Q_2}. \tag{3.42}$$

Using this relation we have,

$$I^* = I_a^* + I_s^* = \Phi_3 I_s^*, \text{ where } \Phi_3 = \frac{(1-\rho)Q_1 + \rho Q_2}{\rho Q_2}. \tag{3.43}$$

From equation (3.39d) the endemic equilibrium population of individuals who have recovered can be given respectively as

$$\begin{aligned} R^* &= \frac{\gamma_1 I_s + \gamma_2 I_a}{Q_3} \\ &= \Phi_2 I_s, \text{ where } \Phi_2 = \frac{\rho\gamma_1 Q_2 + (1-\rho)\gamma_2 Q_1}{\rho Q_2 Q_3}. \end{aligned} \tag{3.44}$$

Similarly, from equation (3.39e) the equilibrium concentration of the pathogen is given by

$$\begin{aligned} P^* &= \frac{\alpha_1 I_s^* + \alpha_2 I_a^*}{\mu_p}, \\ &= \Phi_1 I_s^* \text{ where } \Phi_1 = \frac{\rho\alpha_1 Q_2 + (1-\rho)\alpha_2 Q_1}{\rho Q_2 Q_4} \end{aligned} \tag{3.45}$$

If we substitute equation (3.39b) into equation (3.39c), we obtain, the expression for the sus-

ceptible population as

$$\begin{aligned} S^* &= \frac{\pi}{\mu} + \frac{\omega R^*}{\mu} - \frac{Q_1 I_s^*}{\rho}, \\ &= \frac{\pi}{\mu} + \frac{\omega \Phi_2 I_s}{\mu} - \frac{Q_1 I_s^*}{\rho} \\ &= \frac{\pi}{\mu} - \Phi_4 I_s^* \text{ where } \Phi_4 = \frac{Q_1}{\mu\rho}\left[1 - \omega\left(\frac{\gamma_1\rho}{Q_1Q_2} + \frac{(1-\rho)\gamma_2}{Q_2Q_3}\right)\right]. \end{aligned} \tag{3.46}$$

Since the solution of the system (3.3) is only feasible in the invariant region Ω, the expression (3.46) is only feasible when $\Phi_4 \geq 0$, with equality at the disease free equilibrium. Similarly, if we substitute for P^* and I_a^* in equation (3.39b), we obtain

$$\left[\frac{\beta\Phi_1}{K + \Phi_1 I_s^*} + f_h\Phi_3\right] I_s^* S^* = \frac{Q_1 I_s^*}{\rho}. \tag{3.47}$$

This implies that one of the roots of the equation is $I_s^* = 0$, which corresponds to the disease free equilibrium $\mathbb{E}_0$ (see expression (3.27)). At this equilibrium point, the expression of S^* is equal to S_c (see expression (3.34)). If $I_s^* \neq 0$, we then obtain the expression of S^* from eq. (3.47) as

$$S^* = \frac{Q_1(K + \Phi_1 I_s^*)}{\beta\Phi_1\rho + \rho(K + \Phi_1 I_s^*) f_h \Phi_3}. \tag{3.48}$$

If we equate the equations (3.46) and (3.48), we obtain a quadratic equation of the form

$$a_2 I_s^{*2} + a_1 I_s^* + a_0 = 0, \tag{3.49}$$

where the constants are given as

$$\begin{aligned} a_0 &= Q_1 K(1 - R_0), \\ a_1 &= Q_1\Phi_1\left[1 - (R_{03} + R_{04})\right] + \rho\Phi_4\left(\Phi_1\beta + K f_h \Phi_3\right), \\ a_2 &= \frac{\Phi_1\Phi_2 Q_1 f_h}{\mu}\left[1 - \omega\left(\frac{\gamma_1\rho}{Q_1Q_2} + \frac{\gamma_2(1-\rho)}{Q_2Q_3}\right)\right] > 0. \end{aligned} \tag{3.50}$$

When $\mathcal{R}_0$ is greater than unity, the equation (3.49) has only one positive root. In addition, if $\mathcal{R}_0 \leq 1$, the equation (3.49) has no positive root. This result leads to the following lemma

Lemma 3.2.1. *The dynamical system (3.3), has a unique endemic equilibrium whenever $\mathcal{R}_0 > 1$ and disease free equilibrium whenever $\mathcal{R}_0 < 1$.*

3.3 Numerical results

3.3.1 Parameter estimation

Although not often communicated, there is a lot of uncertainty in the choice of parameter values for the model. Some of the data from which parameters for models are chosen may be from experiments, case control studies, clinical trials or surveys among others. All these methods are not completely error proof much as efforts may be made to minimise possible errors. It is therefore important to carefully study the disease dynamics, put into consideration individual differences, location, social economic status while selecting parameter values. In this section therefore, we estimate some of the parameters values from existing literature in order to parametrize the model. Although some parameters are chosen from a wide range of studies, most of the parameters chosen are with greater focus to Southern Africa and more so to South Africa.

The life expectancy of South Africa has been varying over the years and from province to province [55]. In our estimation of the demographic parameters, we capitalise on KwaZulu Natal province owing to the fact that it is one of the provinces severely affected by cholera and most recently the 2000-2002 outbreak. In the research paper by Bertuzzo *et al.* [45] the life expectancy of KZN region was taken to be 60 years . However, according to Statistics South Africa, the general country's human life expectancy has been varying since 1990 when it was 62 years to 2007 when it dropped to 50 years [55]. According to the same report, the life expectancy of KZN for males was 48.8 and 49.1 for the duration 2001-2006 and 2006-2011 respectively. The average life expectancy for females was slightly higher at 50.3 and 50.2 for the years 2001-2006 and 2006-2011 respectively. This rather low life expectancy of KZN region has also been influenced by the high prevalence of HIV. In our parametrisation of the model we therefore choose the average life expectancy of 50 years synonymous with that of sub-Saharan Africa [56]. This value therefore translates in an average mortality rate of approximately 5.48×10^{-5} per day.

The survival of the bacteria in the aquatic environment varies with the habitat ranging from brackish, estuarine waters to highly saline sea and ocean waters. In a study by Bertuzzo *et al.* [45] in Thukela basin of KwaZulu Natal, they reported a net mortality rate of $\mu_p = 0.228$ per day. Note that the value 0.228 per day corresponds to a net survival time of approximately 5 days. This net survival time seems low with reference to reported values from other studies. According to Hartley *et al.* [42], the considered survival of vibrios was 30 days. On the other hand, Munro and Colwell [57] in their studies where they employed microcosms,

demonstrated that the bacteria can remain viable for more than 50 days upto 60 days even in absence of organic nutrients. We note that, even in the wake of hypoxia or extreme oxygen depletion, *V. cholerae* can still survive for a long time since they are facultatively anaerobic. We consider an estimated mortality rate of vibrios to be 0.02 on the interval $(0.017 - 0.033)$ per day corresponding to survival of upto 50 days on average. The lower limit of the intervals corresponds maximum survival of approximately 60 days [57], whereas the upper limit correspond to low survival of about 30 days [42].

Given the long term survival of *V. cholerae* in the environment, the disappearance and re-emergence of cholera disease, the association of the pathogen with zooplankton, phytoplankton and copepods, it reasonably indicates that the pathogen is always present in the environment and some net growth rate associated with its population evolution. In Codeço's work when studying the role of the aquatic reservoir in cholera dynamics, she used net growth rate of *V. cholera* of 0.73 day^1.

Bertuzzo *et al.* [45] also estimated the additional mortality rate attributed to cholera to be 4.0×10^{-1} per day. In the study by Bertuzzo *et al.* [45], the authors did not distinguish the cholera infected population into symptomatic and asymptomatic. We assume that this value is related to only the symptomatic individuals since asymptomatic cholera infected individuals are reported to have no cholera aggravated mortality [20, 58]. Studies from different authors indicate that symptomatic and asymptomatic cholera infected individuals have different recovery rates. Hendrix [59] reported about studies by Lindenboum and his colleagues in Pakistan in 1964 who indicated that the average duration of diarrhoea to range between 2.7 to 6.3 days with the average at 4.5 days. From this reported diarrhoeal duration, Neilan *et al.* [20] attributed the maximum duration of 6.3 days asymptomatically affected individuals. This value gives a recovery rate of $\gamma_2 = 0.15$ day^{-1}, for asymptomatic individuals [20]. In our model however, we consider a nominal value of $\gamma_2 = 0.2$ day^{-1} which corresponds to the average recovery time of 5 days. This value is well within the range reported by Hendrix [59] and the period of 3 to 7 days [38] for which copious diarrhoea due to cholera lasts.

The duration of immunity for individuals affected by cholera was estimated to be 9.3 ± 8.3 weeks [58]. If we consider a maximum waning period of 17.6 weeks, this value gives the minimum waning rate, $\omega = 8.12\times10^{-3}$ day^{-1} which is still within the range considered in [58].

The symptomatic and asymptomatic individuals have been shown to have variable rates of shedding the pathogen into aquatic environment. This shedding rate is characterised by the concentration of vibrios in the stool as well as the length of time for which the individual

sheds. Where as symptomatic individuals shed large concentration of the pathogen in the rice water stool, asymptomatic individuals shed relatively lower concentrations. However, asymptomatic individuals stay infectious for a relatively longer time with lower recovery rate compared to their symptomatic counterparts. According to Neilan *et al.* [20], the average shedding rate of the pathogen obtained from [36, 60, 61] is 0.5 day^{-1} for asymptomatic individuals. On the others hand the average shedding rate of 50.0 day^{-1} has been observed for symptomatic individuals [20, 60, 61]. King *et al.* [58] indicated that asymptomatic cholera infected individuals do not suffer cholera related death. However, in the study by Neilan *et al* [20] when comparing two study areas, Bogra and Calcuta, the cholera related mortality rates (symptomatic) used were 0.240 year^{-1} and 4.662 year^{-1} respectively. Owing to the relatively big difference between the two values, we can claim that cholera related mortality rates for symptomatic individual varies with the population group affected. It is ideal to believe that this maybe related to the level of hygiene, healthcare and emergency Medical care for symptomatic individuals. It is already clear that in communities where the level of hygiene is very poor, high mortality due to water-borne infections is often not a surprise.

The worst-case scenario exposure of people to contaminated water has been estimated to be at most once a day [36, 62, 63]. We use a similar value of $\beta = 1$ day^{-1} as the constant contact rate, i.e at least one contact per day.

Parameter	Range	Norminal Value	Units	Source
π		6	day^{-1}	Assumed
w		8.12×10^{-3}	day^{-1}	[58]
β	0-1	1	day^{-1}	[36, 62, 63]
K	$10^6 - 10^9$	10^6	cells L^{-1}	[36]
μ		5.48×10^{-5}	day^{-1}	[55, 56]
δ_1	$6.58\times10^{-4} - 0.015$	0.012	day^{-1}	[20, 64]
δ_2		0	day^{-1}	[20, 58]
γ_1	0.031-0.059	0.045	day^{-1}	[20, 64]
γ_2	$0.16 - 0.22$	0.20	day^{-1}	[20, 59]
K_p		10^8	cells L^{-1}	Assumed
α_1		0.5	day^{-1}	[36, 60, 61]
α_2		50.0	day^{-1}	[20, 60, 61]
r		0.73	day^{-1}	[36]
μ_p	$0.017 - 0.033$	0.02	day^{-1}	[42, 57]
ρ		0.2		[58]

3.3.2 Sensitivity analysis

The model system (3.3) has many parameters whose nominal values or parameter ranges are carefully estimated from published work. Since many of these parameters were not determined experimentally, their accuracy is not guaranteed. In the same way the chosen parameter values are not chosen with absolute certainty but with reasonable estimation. It is therefore necessary to establish the observed responses and influence of such parameters on the model. Establishment of such responses can be achieved through uncertainty or sensitivity analysis of the model parameters to the disease dynamics in case of an outbreak. We perform sensitivity analysis to determine the role of different parameter values in the dynamics of cholera epidemic. Therefore, sensitivity analysis is a process of ascertaining the degree to which an input parameter affects the output of the model [65]. Various methods for sensitivity analysis have been highlighted in [65], including the use sensitivity indexes and Partial rank correlation coefficients (PRCCs) and their application in previous studies. In the same line simulation software programs are continuously being developed devoted to risk and sensitivity analysis. One of the recent developments is SaSAT [66] which uses the Latin hypercube sampling scheme (LHS). Although the LHS may have limited control on the accuracy of the model output, it can be reliably used to predict the most influential parameters. In our model sensitivity analysis, we use the LHS implemented in Matlab to ascertain the major contributors to the model output in relation to other parameters in the model. Since we need a baseline or predictor of whether the disease may break out or not if new infective individuals get into the vulnerable population, we capitalise on the model basic reproduction number. This is ideal since the reproduction number is the “average number of secondary cases that an infectious individual may cause if they were introduced in a purely susceptible population". Since the nominal values of some model parameters are chosen from a respective parameter range, we set such nominal values as the peak values during the sampling of the such parameter intervals. For each of these parameter ranges, we assume statistical independence. We then equitably and simultaneously sample the parameter space [8] without replacement. At each run, we perform 1000 simulations and evaluate the partial rank correlation coefficients (PRCCs) of the parameters of interest. The results of simulation are given in the Tornado plot, Figure (3.3).

The parameters with negative PRCCs are observed to reduce the severity of the disease if they increased. On the other hand, the processes which lead to increase in the parameters with positive partial rank correlation coefficients also aggravate the severity of the disease. Increased decay of the pathogen, improved hygiene and recovery of both symptomatic and

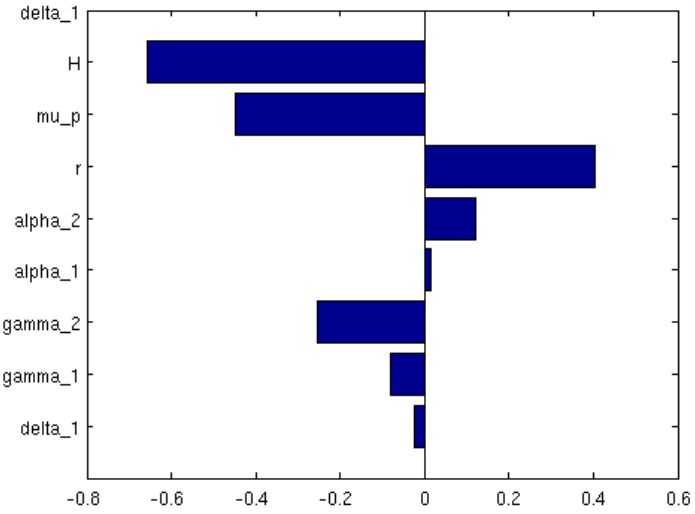

Figure 3.3: Tornado plot showing some important parameters driving the cholera epidemic.

asymptomatically infected individuals are observed to reduce the severity of the disease if such parameters are increased. Recovery of infected individuals has a two fold benefit in the fight against the infection; (i) it leads to reduction the likelihood getting new infections through direct person to person transmission, and (ii) a negligible amount of the pathogen would be shed into the aquatic reservoir greatly reducing the infection risk, most especially for the community that may have direct contact with a potentially contaminated water source. In addition, recovering individuals acquire some immunity to the disease which only wanes over a reasonable period of time hence reducing the susceptible. On the other hand, increased growth in the population of vibrios, and increased discharge of fresh bacteria into the aquatic environment by either the symptomatic or asymptomatic individuals, increase the severity of the infection. From the Figure 3.3, we observe that the level of hygiene plays a very significant role in reducing spread of the disease. On the contrary, the growth rate of the pathogen has been observed to be instrumental in aggravating the spread and severity of the disease.

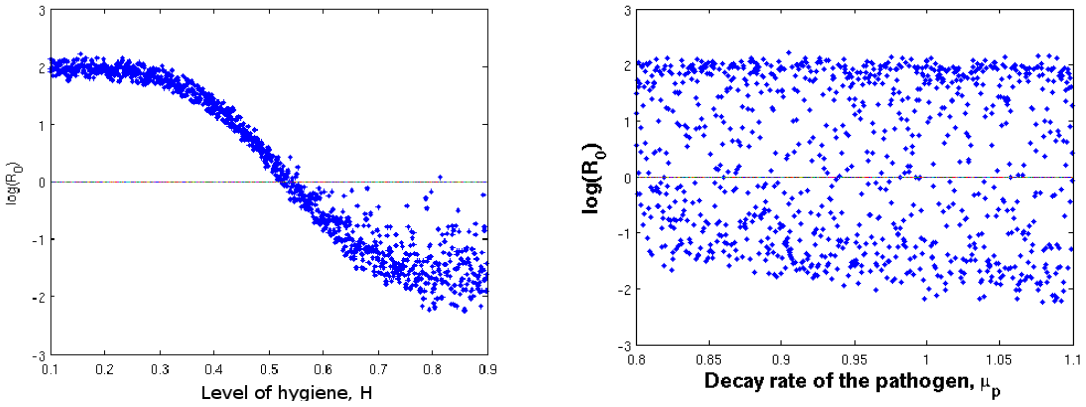

Figure 3.4: Scatter plots of parameters with the more negative PRCCs.

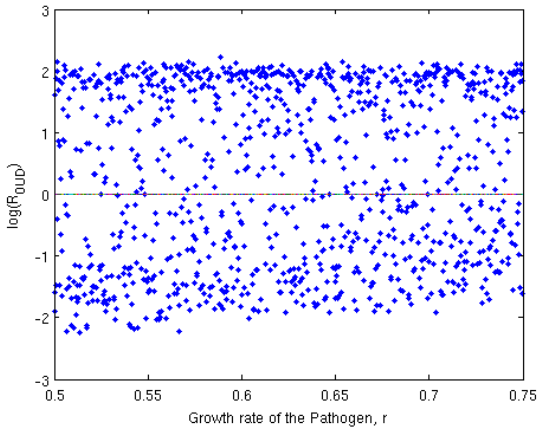

Figure 3.5: Scatter plot of the relationship between $\mathcal{R}_0$ and the growth rate of the pathogen, r, parameter with the more positive PRCC.

3.3.3 Numerical simulations

The model system of equations (3.3) is numerically integrated in python-scipy, using the standard ordinary differential equations solver *odeint*.

The plot in Figure 3.6 is obtained by replacing the nominal value of hygiene dependent contact rate in expression (3.30) with the functional response $f(H)$, for variable H while keeping other parameters constant. The observed inverse proportionality between $\mathcal{R}_0$ and H, shows the importance of improving hygiene if infections are to be contained or prevented.

From Figure 3.7, with poor hygiene, a negligible number of susceptible individuals is required for the disease to break out or become endemic. On the contrary, if the level of hygiene is high, a very big population of susceptible individuals will be required for an outbreak. Therefore, a high level of hygiene reduces the likelihood of an outbreak of cholera if new infected individuals are introduced in the community. In Figure 3.7, the values on

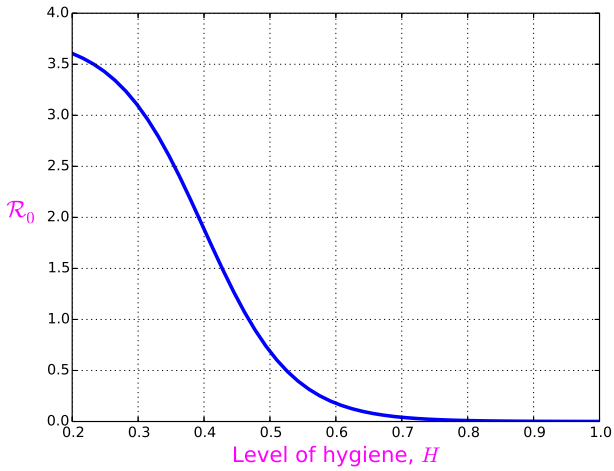

Figure 3.6: $\mathcal{R}_0$ as a function of level of hygiene H. The rest of the parameter values used are: $\beta = 0.05$, $\pi = 0.9 * 5.8\times10^{-5}$, $\mu = 5.8\times10^{-5}$, $K = 10\times^6$, $\rho = 0.2$, $\alpha_1 = 0.05$, $\alpha_2 = 50$, $\gamma_1 = 0.25$, $\gamma_2 = 0.2$, $r = 0.73$, $\mu_p = 1.06$, $\omega = 8.12\times10^{-3}$, $\delta_1 = 0.022$, $K_p = 1\times10^8$. For these parameter values, $\mathcal{R}_0 = 1$ when $H \approx 0.463$.

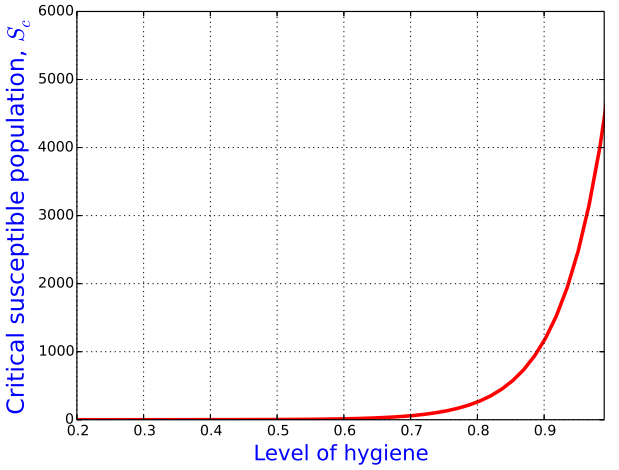

Figure 3.7: Variation of the critical susceptible population with the level of hygiene H. The parameter values used are as follows: $\beta = 0.05$, $\pi = 0.9 * 5.8\times10^{-5}$, $\mu = 5.8\times10^{-5}$, $K = 10\times^6$,$\rho = 0.2$, $\alpha_1 = 0.05$, $\alpha_2 = 50$, $\gamma_1 = 0.25$, $\gamma_2 = 0.2$, $r = 0.73$, $\mu_p = 1.06$, $\omega = 8.12\times10^{-3}$, $\delta_1 = 0.022$, $K_p = 1\times10^8$.

the vertical axis represent arbitrary values not actual numbers of individuals. Therefore, the major important feature to observe in this figure is the trend in the critical susceptible population with the level as the independent variable, which is hygiene in this case. It is obtained by replacing the nominal value f_h in expression (3.34) with the original person-to-person contact functional response for the specified level of hygiene.

We observe that the outbreak is so explosive at the beginning and then followed by a self-limiting phase. The explosive nature has been associated with the two infectious states of the pathogen, i.e the hyper-infectious and less infectious states [42]. The hyper-infectious vibrios being newly shed into the environment, susceptible individuals would have a higher potential of contact with such pathogen as opposed to the less hyper-infectious that might have stayed longer in the environment and whose virulence is relatively low. Although, at both extreme ends of hygiene level the outbreak is explosive, we observe a faster and

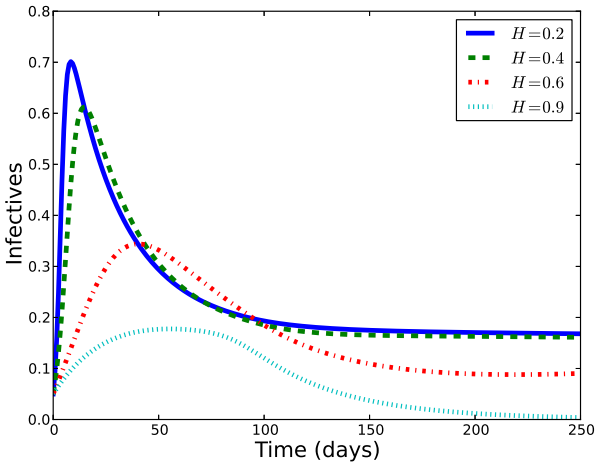

Figure 3.8: Evolution of the population of infectives, for different levels of hygiene H. The rest of the parameter values used are: $\beta = 0.05$, $\pi = 0.9 * 5.8\times10^{-5}$, $\mu = 5.8\times10^{-5}$, $K = 10\times^{6}$, $\rho = 0.2$, $\alpha_1 = 0.05$, $\alpha_2 = 50$, $\gamma_1 = 0.25$, $\gamma_2 = 0.2$, $r = 0.73$, $\mu_p = 1.06$, $\omega = 8.12\times10^{-3}$, $\delta_1 = 0.022$, $K_p = 1\times10^{8}$. For these parameter values, $\mathcal{R}_0 = 1$ when $H \approx 0.463$.

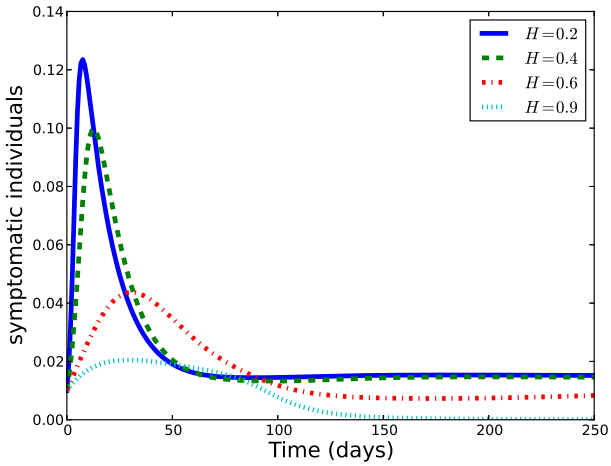

Figure 3.9: Evolution of the symptomatic population, for different levels of hygiene H. The parameter values used are as follows: $\beta = 0.05$, $\pi = 0.9 * 5.8\times10^{-5}$, $\mu = 5.8\times10^{-5}$, $K = 10\times^{6}$, $\rho = 0.2$, $\alpha_1 = 0.05$, $\alpha_2 = 50$, $\gamma_1 = 0.25$, $\gamma_2 = 0.2$, $r = 0.73$, $\mu_p = 1.06$, $\omega = 8.12\times10^{-3}$, $\delta_1 = 0.022$, $K_p = 1\times10^{8}$.

higher explosive nature in case of very poor hygiene (see Figures 3.8, 3.9 and 3.10). At the self-limiting phase which happens near the endemic steady state, it is clear that the infection will have a more devastating effect in the case when the hygiene levels are appalling. The self-limiting phase observed in Figures 3.8, 3.9 and 3.10 is a result of depletion of the susceptible population which reduced the likelihood of person to person contact as well as contact with the aquatic reservoir. We note also that the ratio of asymptomatic to symptomatically infected individuals is four to one and this is maintained for either level of hygiene. For this comparison see, the infected population phase space trajectories in Figures 3.9 and 3.10. Our model gives uni-modal outbreak with no recurrences. We acknowledge the fact that in some areas, outbreaks have bimodal patterns with variable inter-annual variability [9, 67]. However, these patterns depend on the parameter values specific to the locations whose epidemic is being modelled. For the Figures 3.8, 3.9 and 3.10 the given values of $H = [0.2, 0.4, 0.6, 0.9]$

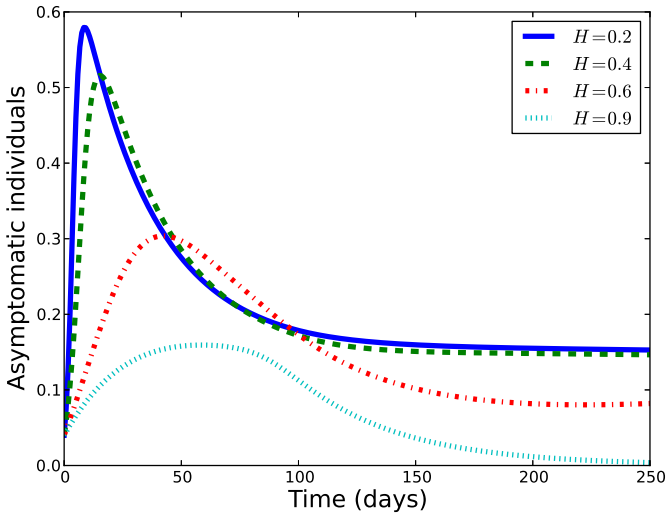

Figure 3.10: Evolution of the asymptomatic population, for different levels of hygiene H. The parameter values used are as follows: $\beta = 0.05$, $\pi = 0.9 * 5.8\times10^{-5}$, $\mu = 5.8\times10^{-5}$, $K = 10\times^{6}$,$\rho = 0.2$, $\alpha_1 = 0.05$, $\alpha_2 = 50$, $\gamma_1 = 0.25$, $\gamma_2 = 0.2$, $r = 0.73$, $\mu_p = 1.06$, $\omega = 8.12\times10^{-3}$, $\delta_1 = 0.022$, $K_p = 1\times10^{8}$.

have associated $\mathcal{R}_0 = [27.4, 14.1, 3.6, 0.87]$. This clearly affirms the importance of hygiene improvement in the fight against water-borne infections. We assert therefore that, although sporadic cases of cholera may occur with high levels of hygiene in place, an outbreak may be less likely. This is due to the fact that, at high hygiene levels, the health systems of the community affected would be having effective control, surveillance and proper ways of managing sporadic cases. This would result in lower subsequent generations of the infective than their predecessors, hence containing the impending outbreak.

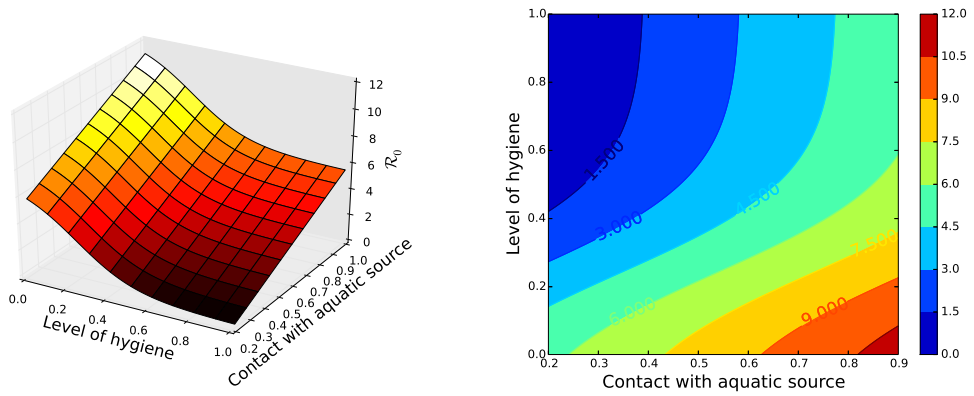

(a) 3D plot of $\mathcal{R}_0$ as a function hygiene level and contact rate with the contaminated source

(b) Contour plot of $\mathcal{R}_0$ as a function hygiene level and contact rate with the contaminated source

Figure 3.11: Disease threshold as a function of water-person and person-to-person contact rates

The worst case scenario in case of epidemic outbreak may be experienced when the level of hygiene is poor; maximizing person-to-person contact rate and when there is no accesses to

clean water; which maximises disease transmission through contact with the contaminated reservoir. The arbitrary values of $\mathcal{R}_0$ on the $\mathcal{R}_0$-axis in Figure 3.11(a) indicate the corresponding relationship between hygiene level and contact with a contaminated reservoir. At high values of $\mathcal{R}_0$, the outbreak may devastate the affected community and at low values of $\mathcal{R}_0$, the outbreak can be contained. Note that the contact rate and level of hygiene may not be discrete but on a continuous scale (see Figure 3.11(b)) of time. Therefore, a combination of factors may result into a disease threshold in a particular colour band. Given reliable data on cholera cases and influential factors, credible values of the disease threshold can be explicitly determined.

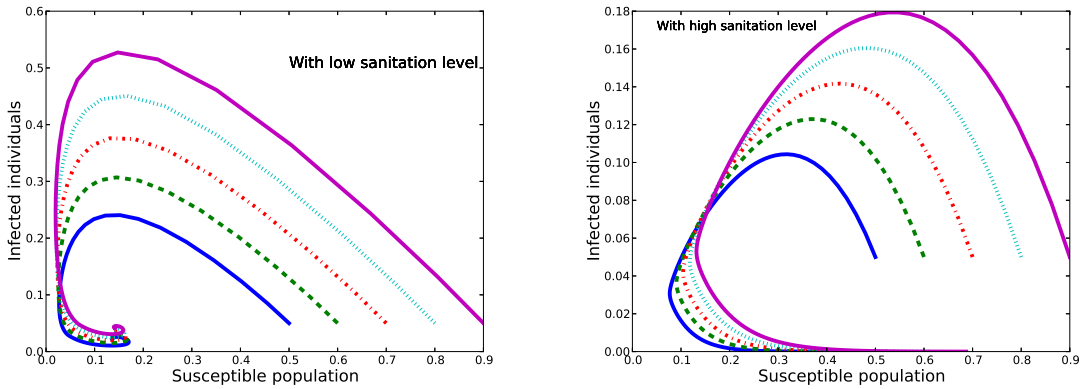

(a) (b)

Figure 3.12: Phase-portraits for the susceptible and infected population, at low and high hygiene levels

It can be observed from the phase-portraits (Figures 3.12(a) and 3.12(b)) that $\liminf_{t\to\infty} S(t) > 0$ irrespective of the level of hygiene. We note that, from Figure 3.12(b) that all solutions end on the susceptible population's-axis ($I \to 0$ as $t \to \infty$). On the other hand, when the level of hygiene is low, solutions approach a non negative steady state which is dependent on the initial conditions. At both low and high levels of hygiene, the higher the immunologically naive population there is, the more devastating the infection can be. Although in both cases the outbreak may be explosive in nature, it is way so devastating when the level of hygiene is poor. At high levels of hygiene, the solution trajectories starting in Ω, approach the disease free equilibrium. This reiterates the importance of good hygiene practices in containing cholera spread.

3.4 Conclusion

In this Chapter, a simple deterministic model which incorporates hygiene dependent person-to-person contact rate was presented and analysed. Important mathematical features of the models such as the threshold for the epidemic, steady states, positivity and boundedness of solutions as well as the region of biological significance were determined. The model was shown to have a disease free equilibrium which is both locally and globally asymptotically stable when the reproduction number is less than unity. This disease free equilibrium is unstable when the disease threshold is greater than unity. The model has a unique endemic equilibrium for $\mathcal{R}_0 > 1$.

Sensitivity analysis of the model parameters was carried out using the basic reproduction number as the threshold value with sampling based on the Latin hypercube Sampling scheme. The output of results of sensitivity analysis were indicated in the Tornado plot as well as the scatter plots. The tornado plot indicates relative sensitivity of the parameters based on the obtained values of partial rank correlation coefficients. Of all the parameters, the level of hygiene with a PRCC of less than -0.6 and the decay rate of the pathogen with PRCC of approximately -0.5, are the most sensitive parameters. These two are therefore influential in containing the epidemic if they are increased owing to their negative PRCCs. Of the parameters with positive PRCCs, the growth rate of the pathogen was shown to be more influential but with a slightly lower PRCC of approximately PRCC ≈ 0.4. Therefore, reducing the growth of the pathogen, would help contain the epidemic. In general, the level of hygiene has been shown to be instrumental if water-borne infections are to be contained. Therefore, this inverse relationship exhibited between a high level of hygiene and the likelihood of disease outbreak should be exploited, to prevent infections. Although many factors are influential in reducing spread of cholera, these factors such as recovery of infected individuals, decay of the pathogen which when increased reduce the severity of the infection may not easily be controlled. It is therefore, vital to focus on the preventive measures related to improved hygiene and general hand-hygiene.

In our results, there was no observable significant difference in the concentration of the pathogen with varying levels of hygiene, when the growth of the pathogen was assumed to be either exponential or logistic. The pathogen growth is also dependent on the balance between its intrinsic growth rate and mortality rate and this would result in either exponential decay or increase. The main observed difference in the two cases is simply faster decay when in the case of pathogen logistic growth as opposed to when the growth terms is assumed to be exponential. The lack of significant difference in pathogen concentration with

varying hygiene level is partly because, the major rates at which the pathogen is shed into the aquatic environment are constant and do not depend on the level of hygiene in our case. This same low sensitivity has been detected with respect to disease threshold shown in Figure 3.5. This could be one of the reasons that no significant emphasis is put on investigating the growth of the pathogen in the aquatic environment in some previous work [36, 42, 50] among others.

We acknowledge the fact that this work may have shortfalls as follows. The models does not take into account vaccination. However, vaccination is recommended as a preventive measure for cholera. Some emphasis on vaccination is given in Chapter 5 with respect to optimal control. In addition the model does not consider the role played by the bacteriophage in reducing the concentration of vibrios [37, 38], which in turn reduces the probability of immunologically naive individuals getting infected. The model considers a uni-modal epidemic although in some cases the cholera epidemic has been observed to be recurrent with reducing severity. Proposed improvements of the model include, consideration of a combination of hygiene, vaccination and biological control with vibrio specific bacteriophage.

Chapter 4

Metapopulation model for cholera transmission

4.1 Introduction

Similar to ecological studies of persistence and extinction of species, there is great interest in ascertaining why infections persist in the population. This concern has shaped the history of epidemiological research as well as population dynamics studies. For a long time now, homogeneity of the population in dynamics of infectious diseases has always been assumed. It however does not account for vital heterogeneous aspects related to spatial structure. When spatial information is required, or when spatial homogeneity does not adequately account for the observed behaviour or disease transmission, then spatial modelling becomes handy in accounting for spatially distinct individual characteristics. Some of these characteristics include differences in mixing behaviour as well as migration which results into heterogeneity [68]. Spatial structure and the spatial scales roughly operate in three broad classes of heterogeneities which are as described in [69];

1. environmental (covering geography and space including climate and hydrological factors)
2. contact (which involves contact patterns between hosts and pathogens including movement of hosts), and
3. host/pathogen heterogeneity (related to genetic factors and resistance to the disease)

It is for this reason that spatial modelling has taken great shape in the study of disease dynamics while accounting for the degree of uniqueness in one patch relative to another.

Different approaches used in spatial modelling range from the use of systems of reaction-diffusion equations (RDEs) [52] to meta-population model framework. Use of RDEs is often faced with a challenge of complexity, and is based on an assumption of continuous movement of organisms in space in a random walk fashion which may not be entirely realistic [68]. Meta-population (patch) models are however, based on the assumption of homogeneity within a patch and spatial heterogeneity is accounted for by migration between patches. This assumption is plausible since humans often frequent a home range, as opposed to random walk which is assumed in RDEs. We note that the above two mentioned approaches may not be the only ways in which to account for spatial heterogeneity. For instance, Lloyd and May [70] in their multi-patch model accounted for heterogeneity through mixing of individuals from separate patches without explicit migration.

Populations in spatially disjunct locations exhibit spatial synchrony if they fluctuate in a similar manner [71]. Synchronous fluctuation is characterised by coincident changes in the abundance, population cycles or other varying characteristics of geographically adjunct populations. These fluctuations in populations may be predominantly quantitative or qualitative. According to Matter [72], populations or local populations within a metapopulation often vary together in population size. In addition, in theoretical assessment of synchrony, identical ability of populations to absorb and produce dispersing individuals is assumed. In ecological studies, spatial synchrony is attributed to dispersal (migration) or environmental stochasticity ("moran effect"). In accordance with the Moran effect, "if two populations have the same density-dependent structure, then correlated density-dependent structures can bring fluctuations in populations into synchrony [73]". In this effect therefore, the dynamics of the population may congruently depend on some asynchronous exogenous factors which may include temperature and rainfall among others. These factors are important drivers of the cholera epidemic most especially in areas where it is endemic. Migration has also been observed as a potential mechanism by which an infection may be transmitted from one community to another. However, there has been no explicit study on the would be anticipated consequences of migration between communities in times of cholera epidemic. Our study is motivated by the recent major cholera out break in South Africa during 2000-2002, that spread to eight out of the nine provinces [74] in the country. See also Table 1.2 for the reported cases and the associated case fatality ratios. The provinces are not all connected by a common river network and neither did the epidemic start at the same time in all the affected provinces. First cases were reported in KwaZulu Natal province and later in other regions. Since the disease is water-borne and human-to-human transmission is known as a potential route, this raises speculations that human movement must have played a significant role in

disease transmission. In the recent work by Bertuzzo *et al.* [45], a spatial transmission model developed and analysed indicated hydrologic networks and human mobility as drivers of the dispersal of the pathogen.

The work in this chapter is motivated by the desire to understand the possible effect of migration between communities on the spread of cholera. Although substantial work has been done in the study of cholera transmission dynamics, no explicit consideration of meta-population study has been previously done. We consider an SIR meta-populations model for cholera describing disease transmission between two communities (patches) connected by a transport network. Although, the communities are assumed to be connected with exchange of populations between communities, cross community transmission is assumed not to exist. In the cholera transmission dynamics which involve both symptomatically infected and asymptomatic carriers, we assume that it is only the asymptomatically infected who can move from one community to another, most especially if the separating distance is large. In general the transmission dynamics of the *vibrios* in humans in a metapopulation framework may be complex due to the local and long-range movements of individuals. In addition, the non human source of the *vibrios* i.e that aquatic reservoir is also complex. This is depended on the rate at which the water is flowing, the volume which is related to the dilution of the pathogen concentration, its virulence and the salinity of the aquatic reservoir. In addition it is important to note that the movement between populations depends on the density of the population and the distance separating the adjunct communities. However, incorporating all factors, in an all inclusive model can be a daunting task and the resulting model may be mathematically intractable.

4.2 Model formulation

We consider a simple SIR meta-populations model for cholera transmission dynamics. The model describes two sub-populations which represent two communities connected by the transport network. In the cholera transmission dynamics which involves both symptomatic and asymptomatic (healthy) *vibrio* carriers, we assume that it is only the healthy carriers who can move from one place to another, most especially if the separating distance is large. The restriction on the movement ability is due to the fact that, once an individual consumes the pathogen in water or contaminated food, the symptoms appear within a short period of time. This may be much shorter than the time required for an individual to move from one population sub-group to another. This condition applies well to inter-provincial movements. The inter-provincial movement is predominantly by road transport. Transmission resulting

from individuals travelling by air transport means is assumed to be less likely, given the conditions and sanitary weaknesses of how cholera is easily spread. The major exception here could be with migrant workers who could be living in poor conditions with no access to clean, treated water. Sometimes the transmission could occur en route at stop overs as travellers buy food staffs along the route. In general the transmission dynamics of the *vibrios* in humans is complex due to the local and long-range movements of individuals. In addition, the non human source of the *vibrios* i.e the aquatic reservoir is also complex. This is depended on the rate at which the water is flowing and the and the volume, which is related to the dilution of the pathogen, its virulence and the salinity of the aquatic reservoir. In the same way it is important to note that the movement between populations depends on the size as well as the distance between the populations.

4.3 The mathematical model

In the model formulation, the general population considered is divided in two main communities and each community divided into three compartments with reference to *vibrio* transmission and disease states of the individuals. The compartmentalisations in a single community involves individuals who are immunologically naive (Susceptible population) S, those infected I and those individuals who have recovered R but with temporary immunity. Within a community, the subpopulations within a compartment are assumed to be homogeneous and thus mix homogeneously. In addition, we assume that in a case when cholera is endemic, acquired immunity wanes in a relatively shorter time than the duration of the infection in the population. This motivates the need to consider a SIRS model for the dynamics within a community considered, in the case of endemic cholera. Our metapopulations model for cholera accounts for two movement patterns. First, the movement of susceptible individuals from one community to the other. In this respect susceptible individuals can move from one community to the other and back. During the migration of susceptible individuals, we assume that no infection occurs en route. The recruitment of new susceptibles into communities is at a rates π_1 and π_2 for the first and second communities respectively. This recruitment is mainly through immigration and new births during the modelling time. Once individuals are away from their home community, they follow the disease dynamics of destination community. Secondly, the movement of infective individuals is typically by those who do not show symptoms. These play a vital role in metapopulation transmission modelling of cholera dynamics since they contribute to the disease transmission for a relatively long time. The role played by those infected but without symptoms may range

from person to person transmission as well as shedding of the pathogen into the aquatic reservoir. The overall dynamics of the general population are accounted for by the contribution from both subpopulations. We assume that the recovered individuals are more likely to be confined in their home communities as they would be recovering from the trauma and weakness caused by the disease. Therefore, movement of recovered individuals across communities is less likely. The susceptible population is depleted following contact with the aquatic reservoir at rate β_1 and β_2 as well as through person-to person contact at rates α_1 and α_2 in the first and second community respectively. We note that an individual must consume atleast the concentration (K) of *vibrios* equivalent to an amount that increases the possibility of being infected to about 50%, if they are to contract the infection [36]. The infected individuals recover from cholera at rates γ_1 and γ_2 respectively for the two communities. The recovered population in each of the communities acquire some immunity due to exposure to cholera but this immunity wanes at a similar rate ω. Individuals in each compartment suffer natural mortality at rates μ_1 and μ_2 for the first and second community respectively. Infected individuals suffer disease induced mortality at rates δ_1 and δ_2 for the two communities respectively. Infected individuals in the first and second communities shed the pathogen into the aquatic environment at rates σ_1 and σ_2 respectively. This shedding rate varies with communities depending on the level of sanitation, infrastructure development and general lifestyle. The flow diagram of disease progression is given in Figure 4.3.

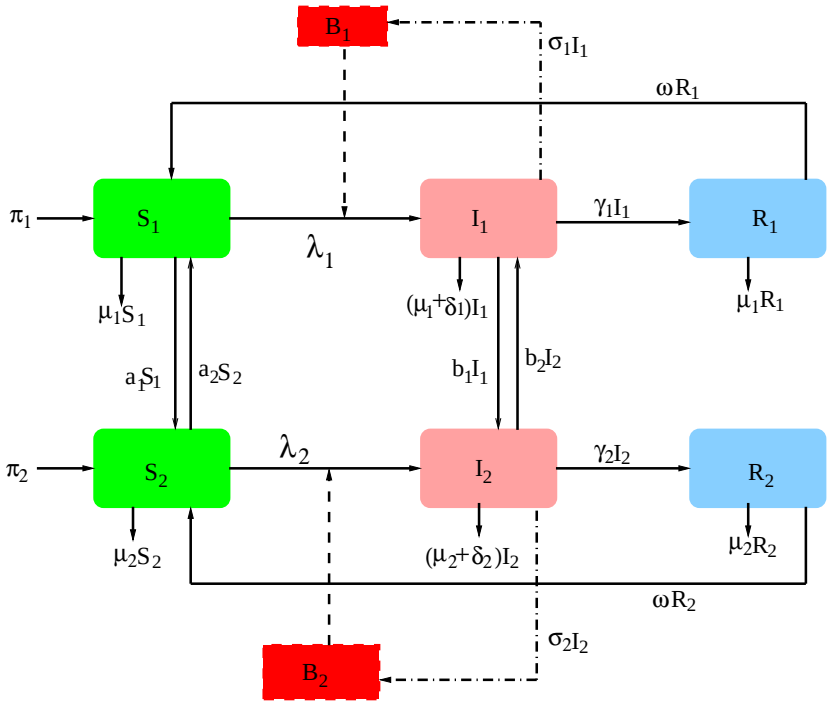

Figure 4.1: Flow diagram of disease dynamics in two sub-populations

The model system of equations for the first sub-population is given by

$$\begin{aligned}
\frac{dS_1}{dt} &= \pi_1 + a_2 S_2 + \omega R_1 - \beta_1 \frac{B_1}{K + B_1} S_1 - \alpha_1 I_1 S_1 - (a_1 + \mu_1) S_1, \\
\frac{dI_1}{dt} &= \beta_1 \frac{B_1}{K + B_1} S_1 + \alpha_1 I_1 S_1 + b_2 I_2 - Q_1 I_1, \\
\frac{dR_1}{dt} &= \gamma_1 I_1 - (\mu_1 + \omega) R_1, \\
\frac{dB_1}{dt} &= \sigma_1 I_1 - Q_2 B_1
\end{aligned} \tag{4.1}$$

and for the second sub-population given by

$$\begin{aligned}
\frac{dS_2}{dt} &= \pi_2 + a_1 S_1 + \omega R_2 - \beta_2 \frac{B_2}{K + B_2} S_2 - \alpha_2 I_2 S_2 - (a_2 + \mu_2) S_2, \\
\frac{dI_2}{dt} &= \beta_2 \frac{B_2}{K + B_2} S_2 + \alpha_2 I_2 S_2 + b_1 I_1 - Q_3 I_2, \\
\frac{dR_2}{dt} &= \gamma_2 I_2 - (\mu_2 + \omega) R_2, \\
\frac{dB_2}{dt} &= \sigma_2 I_2 - Q_4 B_2,
\end{aligned} \tag{4.2}$$

where $Q_1 = (\mu_1 + \delta_1 + \gamma_1 + b_1)$, $Q_2 = (\mu_p - g_1)$, $Q_3 = (\mu_2 + \delta_2 + \gamma_2 + b_2)$, $Q_4 = (\mu_p - g_2)$. The initial conditions of the model are such that $S_1(0) > 0, I_1(0) \geq 0, R_1(0) \geq 0$ and $B_1(0) \geq 0$ for the first patch and $S_2(0) > 0, I_2(0) \geq 0, R_2(0) \geq 0$ and $B_2(0) \geq 0$ for the second patch.

The local population are connected by migration of individuals from one sub-population to the next and back. Some of the key issues of interest include extinction of the disease in one population and re-emergence in the other. In this respect the scale of the infection may differ between metapopulations. The population of community 1, i.e N_1 evolves according to the sum of the first three equations of system (4.1) and N_2 evolves according to the sum of the first three equations of system (4.2). If we consider each of the sub-populations as a closed community with respect to the adjacent community, i.e, there are no emigrations and immigrations of individuals, the evolution of each of the sub- populations is given by

$$\frac{dN_1}{dt} = \pi_1 - \mu_1 N_1 - \delta_1 I_1 \leq \pi_1 - \mu_1 N_1, \tag{4.3a}$$

$$\frac{dN_2}{dt} = \pi_2 - \mu_2 N_2 - \delta_2 I_2 \leq \pi_2 - \mu_2 N_2. \tag{4.3b}$$

The solution to each of the equation in system (4.3) is given by $N_i \leq \frac{\pi_i}{\mu_i} + \left(N_{0i} - \frac{\pi_i}{\mu_i}\right) e^{-\mu_i t}$, where N_{0i} are the initial populations for $i = \{1, 2\}$. The solution of all the equations from systems (4.1) and (4.2) all remain non negative for all $t \geq 0$. The total population (N_1, N_2) in each of the sub-populations is bounded by $\frac{\pi_i}{\mu_i}$, for $i = \{1, 2\}$. The total population in both

sub populations is given by $N = N_1 + N_2$ such that the evolution of the total time over a specified period is given by

$$\frac{dN}{dt} \leq \pi_1 + \pi_2 - (\mu_1 N_1 + \mu_2 N_2). \tag{4.4}$$

If we let $\mu^\star = \min\{\mu_1, \mu_2\}$, then it can be shown that

$$\limsup_{t\to\infty} N \leq \frac{\pi_1 + \pi_2}{\mu^\star}. \tag{4.5}$$

From the last equation of system (4.1) and using the upper bound on the total population in equation (4.5), the evolution of vibrios B_1 satisfy the inequality

$$\frac{dB_1}{dt} \leq \sigma_1 \left(\frac{\pi_1 + \pi_2}{\mu^\star}\right) - Q_2 B_1. \tag{4.6}$$

If we assume that $B_1(0) = B_{10}$, then we have

$$B_1(t) \leq \frac{\sigma_1}{Q_2}\left(\frac{\pi_1 + \pi_2}{\mu^\star}\right) + \left(B_{10} - \frac{\sigma_1}{Q_2}\left(\frac{\pi_1 + \pi_2}{\mu^\star}\right)\right) e^{-Q_2 t}.$$

This implies that

$$\lim_{t\to\infty} B_1(t) = \frac{\sigma_1}{Q_2}\left(\frac{\pi_1 + \pi_2}{\mu^\star}\right).$$

Using a similar approach with the fourth equation of system (4.2) and that $B_2(0) = B_{20}$, it can be shown that

$$B_2(t) \leq \frac{\sigma_2}{Q_4}\left(\frac{\pi_1 + \pi_2}{\mu^\star}\right) + \left(B_{20} - \frac{\sigma_2}{Q_4}\left(\frac{\pi_1 + \pi_2}{\mu^\star}\right)\right) e^{-Q_4 t},$$

and that

$$\lim_{t\to\infty} B_2(t) = \frac{\sigma_2}{Q_4}\left(\frac{\pi_1 + \pi_2}{\mu^\star}\right).$$

Therefore, the phase space of the model is given by

$$\Omega := \left\{(S_1, I_1, R_1, B_1, S_2, I_2, R_2, B_2) : S_1 + I_1 + R_1 + S_2 + I_2 + R_2 \leq \frac{\pi_1 + \pi_2}{\mu^\star}\right\}. \tag{4.7}$$

The solutions in Ω are all non negative and bounded. Hence the domain of biological significance is positively invariant and attracting. Therefore all solutions starting in Ω remain in Ω. The guide to the proof of positivity and boundedness of solution can be found in [75, 76, 77].

4.4 Equilibrium points

The model has four equilibrium points given by

$$\mathbb{E}_0 = \{S_1^*, 0, 0, 0, S_2^*, 0, 0, 0\} \in \mathbb{R}_+^8, \tag{4.8a}$$
$$\mathbb{E}_1 = \{S_1^{**}, I_1^{**}, R_1^{**}, B_1^{**}, S_2^{**}, 0, 0, 0\} \in \mathbb{R}_+^8, \tag{4.8b}$$
$$\mathbb{E}_2 = \{\bar{S^*}_1, 0, 0, 0, \bar{S^*}_2, \bar{I^*}_2, \bar{R^*}_2, \bar{B^*}_2\} \in \mathbb{R}_+^8, \tag{4.8c}$$
$$\mathbb{E}_3 = \{\bar{S_1^{**}}, \bar{I_1^{**}}, \bar{R_1^{**}}, \bar{B_1^{**}} \bar{S_2^{**}}, \bar{I_2^{**}}, \bar{R_2^{**}}, \bar{B_2^{**}}\} \in \mathbb{R}_+^8, \tag{4.8d}$$

of which $\mathbb{E}_0$ is the disease free equilibrium. The equilibrium points $\mathbb{E}_1$ and $\mathbb{E}_2$ are referred to as the first and second boundary endemic equilibria, whereas $\mathbb{E}_3$ is referred to as the interior endemic equilibrium.

The disease free equilibrium $\mathbb{E}_0$ in both sub-populations is obtained by reducing the systems of equations (4.1) and (4.2). At this equilibrium, we also assume that in both the accessed aquatic environments, there is no pathogen. Therefore, the systems of equation (4.1) and (4.2) reduce to

$$\begin{aligned} \frac{dS_1}{dt} &= \pi_1 + a_2 S_2 - (\mu_1 + a_1) S_1, \\ \frac{dS_2}{dt} &= \pi_2 + a_1 S_1 - (\mu_2 + a_2) S_2. \end{aligned} \tag{4.9}$$

Equating the right hand side of the system of equations (4.9) to zero and solving for the equilibrium points we obtain

$$S_1^* = \frac{\pi_1(a_2 + \mu_2) + a_2\pi_2}{\mu_1\mu_2 + \mu_1 a_2 + a_1\mu_2}, \quad S_2^* = \frac{\pi_2(a_1 + \mu_1) + a_1\pi_1}{\mu_1\mu_2 + \mu_1 a_2 + a_1\mu_2}. \tag{4.10}$$

4.4.1 The reproduction number

The reproduction number for the model is obtained using the next generation method described in [51]. If the infection is existent in a single isolated patch, then the corresponding threshold numbers for its persistence is given by

$$\mathcal{R}_{01} = \frac{\pi_1(\alpha_1 Q_2 K + \beta_1\sigma_1(\mu_1+\delta_1+\gamma_1))}{\mu_1(\mu_1+\delta_1+\gamma_1)Q_2 K}, \quad \text{and} \quad \mathcal{R}_{02} = \frac{\pi_2(\alpha_2 Q_4 K + \beta_2\sigma_2(\mu_2+\delta_2+\gamma_2))}{\mu_2(\mu_2+\delta_2+\gamma_2)Q_4 K} \tag{4.11}$$

respectively for the first and second community. Such values, $\mathcal{R}_{01}$ and $\mathcal{R}_{02}$ of the disease threshold apply to completely isolated communities. On the contrary, if the infection exists in a single community which is connected to another patch through movement, the phe-

nomenon related to the movement of individuals should be reflected in the disease threshold.

When the communities are connected by migration, the community specific reproduction numbers are given by

$$\mathcal{R}_{01M} = \frac{(\pi_1(\mu_2+a_2)+a_2\pi_2)(\beta_1\sigma_1+Q_2\alpha_1 K)}{Q_1Q_2(\mu_1+a_1)(\mu_2+a_2)(1-\Phi_1)K} \text{ and}$$
$$\mathcal{R}_{02M} = \frac{(\pi_2(\mu_1+a_1)+a_1\pi_1)(\beta_2\sigma_2+Q_4\alpha_2 K)}{Q_2Q_4(\mu_1+a_1)(\mu_2+a_2)(1-\Phi_1)K},$$

for first and second community respectively, where

$$\Phi_1 = \frac{a_1a_2}{(\mu_1+a_1)(\mu_2+a_2)} < 1.$$

The term $\Phi_1 = \frac{a_1}{\mu+a_1}\cdot\frac{a_2}{\mu_2+a_2}$ indicates the fraction of immunologically naive individuals who move from either the first community or the second and back. The values $\frac{1}{\mu_1+a_1}$, $\frac{1}{\mu_2+a_2}$ indicate the average time individuals in compartments S_1 and S_2 stay in their respective compartments. Therefore, $(1-\Phi_1)$ indicates the fraction of individuals who do not cycle between compartments S_1 and S_2. The model reproduction number $\mathcal{R}_{0M}$, is given as the maximum of the patch specific reproduction numbers

$$\mathcal{R}_{0M} = \max\{\mathcal{R}_{01M}, \mathcal{R}_{02M}\}. \tag{4.12}$$

Global stability of the disease free equilibrium $\mathbb{E}_0$

Lemma 4.4.1. *The disease free equilibrium $\mathcal{E}_0$ is globally stable whenever, $\mathcal{R}_{0M} < 1$ and unstable otherwise.*

Let $V = \theta_1 I_1 + \theta_2 B_1 + \theta_3 I_2 + \theta_4 B_2$ be a candidate Lyapunov function. The constants θ_i for $i = 1,2,3,4$ are non negative. We can find the constants θ_1 such that the Lyapunov candidate is positive definite. The derivative of the Lyapunov function is given by

$$\begin{aligned}\frac{dV}{dt} &= \theta_1\frac{dI_1}{dt} + \theta_2\frac{dB_1}{dt} + \theta_3\frac{dI_2}{dt} + \theta_4\frac{dB_2}{dt},\\ &= \theta_1\left[\beta_1\frac{B_1}{K_1+B_1}S_1 + \alpha_1 I_1 S_1 + b_2 I_2 - b_1 I_1 - (\mu_1+\delta_1+\gamma_1)I_1\right] + \theta_2\left[\sigma_1 I_1 - Q_2 B_1\right]\\ &+ \theta_3\left[\beta_2\frac{B_2}{K_2+B_2}S_2 + \alpha_2 I_2 S_2 + b_1 I_1 - b_2 I_2 - (\mu_2+\delta_2+\gamma_2)I_2\right] + \theta_4\left[\sigma_2 I_2 - Q_4 B_2\right].\end{aligned}$$

We note that for all $t \in [0,t)$, $\frac{B_1}{K+B_1} < \frac{B_1}{K}$ and $\frac{B_2}{K+B_2} < \frac{B_2}{K}$. From the disease free equilibrium,

we can re-write the values for susceptible individuals as

$$S_1^* = \frac{\pi_1(a_2+\mu_2)+a_2\pi_2}{(\mu_1+a_1)(\mu_2+a_2)(1-\Phi_1)},\ \ S_2^* = \frac{\pi_2(a_1+\mu_1)+a_1\pi_1}{(\mu_1+a_1)(\mu_2+a_2)(1-\Phi_1)}, \tag{4.13}$$

where

$$\Phi_1 = \frac{a_1 a_2}{(\mu_1+a_1)(\mu_2+a_2)} < 1.$$

Therefore, the derivative of the Lyapunov function satisfies the inequality

$$\begin{aligned}\frac{dV}{dt} \leq & \left[\theta_1\frac{\beta_1 S_1^*}{K} - \theta_2 Q_2\right] B_1 + \left[\theta_1\alpha_1 S_1^* - \theta_1 Q_1 + \theta_2\sigma_1\right] I_1 \\ & + \left[\theta_3\frac{\beta_2 S_2^*}{K} - \theta_4 Q_4\right] B_1 + \left[\theta_3\alpha_2 S_2^* - \theta_3 Q_3 + \theta_4\sigma_2\right] I_2.\end{aligned}$$

We now set the coefficients to B_1 and B_2 to zero and evaluate to obtain

$$\theta_1 = KQ_2,\ \ \theta_2 = \beta_1 S_1^*,\ \ \theta_3 = KQ_4 \ \text{ and } \ \theta_4 = \beta_2 S_2^*. \tag{4.14}$$

We then use the coefficients obtained (4.14) into the candidate Lyapunov function. The derivative of the resulting Lyapunov function is given by

$$\begin{aligned}\frac{dV}{dt} \leq & KQ_2\left[\beta_1\frac{B_1}{K_1}S_1^* + \alpha_1 I_1 S_1^* + b_2 I_2 - b_1 I_1 - (\mu_1+\delta_1+\gamma_1)I_1\right] + \beta_1 S_1^*\left[\sigma_1 I_1 - Q_2 B_1\right] \\ & + KQ_4\left[\beta_2\frac{B_2}{K}S_2^* + \alpha_2 I_2 S_2^* + b_1 I_1 - b_2 I_2 - (\mu_2+\delta_2+\gamma_2)I_2\right] + \beta_2 S_2^*\left[\sigma_2 I_2 - Q_4 B_2\right]\end{aligned}$$

Collecting like terms, we obtain

$$\begin{aligned}\frac{dV}{dt} &\leq \left[S_1^*(\beta_1\sigma_1 + Q_2\alpha_1 K) - KQ_1Q_2\right] I_1 + \left[S_2^*(\beta_2\sigma_2 + Q_4\alpha_2 K) - KQ_3Q_4\right] I_2 \\ &= KQ_1Q_2\left[\frac{(\pi_1(\mu_2+a_2)+a_2\pi_2)(\beta_1\sigma_1+Q_2\alpha_1 K)}{Q_1Q_2(\mu_1+a_1)(\mu_2+a_2)(1-\Phi_1)K} - 1\right] I_1 \\ &\quad + KQ_3Q_4\left[\frac{(\pi_2(\mu_1+a_1)+a_1\pi_1)(\beta_2\sigma_2+Q_4\alpha_2 K)}{Q_3Q_4(\mu_1+a_1)(\mu_2+a_2)(1-\Phi_1)K} - 1\right] I_2 \\ &= KQ_1Q_2\left(\mathcal{R}_{01M} - 1\right) I_1 + kQ_3Q_4\left(\mathcal{R}_{02M} - 1\right) I_2.\end{aligned}$$

We note that whenever $\mathcal{R}_{01M} < 1$ and $\mathcal{R}_{02M} < 1$ then $\frac{dV}{dt} < 0$. Equality holds when $\mathcal{R}_{01M} = \mathcal{R}_{02M} = 1$ or when $I_1 = I_2 = 0$. Therefore, by the LaSalle Invariance principle [53], the disease free equilibrium is globally stable whenever $\mathcal{R}_0 < 1$. This completes the proof.

4.4.2 Endemic steady state $\mathbb{E}_1$

Lemma 4.4.2. *The model system (4.1) and (4.2) has a unique boundary endemic equilibrium $\mathbb{E}_1$ in Ω whenever $\mathcal{R}_{01M} > 1$ and $\mathcal{R}_{02m} < 1$.*

Lemma 4.4.2 implies that cholera persists in the first sub-population but dies out in the second sub-population.

Proof. We note that with absence of the infections in the second sub-population, then $I_2 = 0$. Then

$$\begin{cases} \pi_1 + a_2 S_2^{**} + \omega R_1^{**} = \left(\beta_1 \frac{B_1^{**}}{K+B_1^{**}} + \alpha_1 I_1^{**}\right) S_1^{**} + (a_1 + \mu_1) S_1^{**}, \\ \left(\beta_1 \frac{B_1^{**}}{K+B_1^{**}} + \alpha_1 I_1^{**}\right) S_1^{**} = Q_1 I_1^{**}, \\ \gamma_1 I_1^{**} = (\mu_1 + \omega) R_1^{**} \\ \sigma_1 I_1^{**} = Q_2 B_1^{**} \\ \pi_2 + a_1 S_1^{**} = (\mu_2 + a_2) S_2^{**} \end{cases} \tag{4.15}$$

From the fifth equation of (4.15), S_2 can be given as

$$S_2^{**} = \frac{\pi_2 + a_1 S_1^{**}}{\mu_2 + a_2}. \tag{4.16}$$

Similarly, from the fourth and the third equations of (4.15), we obtain

$$B_1^{**} = \frac{\sigma_1 I_1^{**}}{Q_2}, \tag{4.17}$$

$$R_1^{**} = \frac{\gamma_1 I_1^{**}}{\mu_1 + \omega} \quad \text{respectively.} \tag{4.18}$$

When we substitute (4.17) into the second equation of (4.15), we obtain

$$\left(\frac{\beta_1 \sigma_1 I_1^{**}}{Q_2 K + \sigma_1 I_1^{**}} + \alpha_1 I_1^{**}\right) S_1^{**} = Q_1 I_1^{**}. \tag{4.19}$$

This gives $I_1^{**} = 0$ as one of the solutions. This solution corresponds to the disease free equilibrium (4.8a). If $I_1^{**} \neq 0$ the other solution gives the relationship between the susceptible population S_1^{**} and the population of infected I_1^{**} in metapopulation one such that

$$S_1^{**} = \frac{Q_1 Q_2 K + Q_1 \sigma_1 I_1^{**}}{(\beta \sigma_1 + \alpha_1 Q_2 K) + \alpha_1 \sigma_1 I_1^{**}} \tag{4.20}$$

If we substitute for B_1^{**}, and R_1^{**} in the first equation of (4.15), we obtain

$$\Phi_3 = Q_1(1 - \Phi_2) I_1^{**} + (\mu_1 + a_1)(1 - \Phi_1) S_1^{**}, \tag{4.21}$$

where

$$\Phi_3 = \frac{\pi_1(\mu_2 + a_2) + a_2\pi_2}{\mu_2 + a_2}, \quad \Phi_2 = \frac{\omega\gamma_1}{(\mu_1 + \omega)Q_1}.$$

The terms $\frac{\gamma_1}{Q_1}$ and $\frac{\omega}{\mu_1+\omega}$ indicate fraction of individuals who move out of the compartments I_1 and R_1 respectively. We note that, since there is no direct reverse route from R_1 to I_1, there is no direct cycling of individuals between these two compartments.

Then we substitute for S_1 (equation (4.20)) into equation (4.21) to obtain a quadratic equation given by

$$\mathcal{A}_2 I_1^2 + \mathcal{A}_1 I_1 + \mathcal{A}_0 = 0 \tag{4.22}$$

where

$$\begin{cases} \mathcal{A}_2 &= \alpha_1\delta_1 Q_1(1-\Phi_2) \\ \mathcal{A}_1 &= Q_1(\Phi_2)(\beta_1\sigma_1 + \alpha_1 Q_2 k) + \sigma_1 Q_1(\mu_1 + a_1)(1-\Phi_1)(1-\mathcal{R}_{01c}) \\ \mathcal{A}_0 &= Q_1 Q_2(\mu_1 + a_1)(1-\Phi_1)k\,(1-\mathcal{R}_{01m}) \end{cases}$$

where

$$\mathcal{R}_{01M} = \frac{\Phi_3(\beta_1\sigma_1 + \alpha_1 Q_1 k)}{Q_1 Q_2(\mu_1 + a_1)(1-\Phi_1)k}, \quad \text{and} \quad \mathcal{R}_{01c} = \frac{\Phi_3\alpha_1}{Q_1(\mu_1 + a_1)(1-\Phi_1)}$$

We note that the solution of the polynomial (4.22) depends on the signs of $\mathcal{A}_1$ and $\mathcal{A}_0$. We there for have the following observations

- when $\mathcal{A}_0 < 0$ (i.e when $\mathcal{R}_{01M} > 1$) we have exactly one solution for all values of $\mathcal{A}_1$.
- When $\mathcal{A}_0 > 0$ (i.e when $\mathcal{R}_{01M} < 1$) we have no positive solution if $\mathcal{A}_1 > 0$ and two distinct positive roots when $\mathcal{A}_1 < 0$.

Therefore, when $\mathcal{R}_{01M} > 1$ we have a unique disease persistent equilibrium localised in sub-population 1. □

4.5 Local stability of the endemic equilibrium $\mathbb{E}_1$

We use the center manifold theory (CMT) described in [78]to ascertain whether the boundary equilibrium $\mathbb{E}_1$ is locally stable. We not that if the disease is localised only in the first community, we assume no immigration of infects from the second community as well as no pathogen exists in that community. Let us consider the system of equations (4.1) and the first equation of system (4.2) with the bifurcation parameter ϕ such that

$$\frac{dx}{dt} = f(x,\phi), f : \mathbb{R}^5 \times \mathbb{R} \to \mathbb{R} \quad \text{and} \quad f \in C^2(\mathbb{R}^5 \times \mathbb{R}). \tag{4.23}$$

Assume that 0 is a non-hyperbolic steady state of the first community, then $f(0,\phi) = 0$ for all ϕ. Let the linearisation matrix, $\mathbf{A}$ be such that

$$\mathbf{A} = D_x f(0,0), \tag{4.24}$$

has a left eigenvector denoted by y and the right eigenvector denoted by v. Then the local dynamics of the model around 0 is totally governed by $\mathbf{a}$ and $\mathbf{b}$ [78, 79], where

$$\mathbf{a} = \sum_{k,i,j=1} y_k v_i v_j \frac{\partial^2 f_k}{\partial x_i \partial x_j}(0,0) \tag{4.25}$$

$$\mathbf{b} = \sum_{k,i,j=1} y_k v_i \frac{\partial^2 f_k}{\partial x_i \partial \phi}(0,0) \tag{4.26}$$

According to [78], the local dynamics of the model around 0 is determined by the signs of $\mathbf{a}$ and $\mathbf{b}$. We detail the condition on the signs of $\mathbf{a}$ and $\mathbf{b}$ and the bifurcation parameter for convenience of interpretation of the stability.

i. $\mathbf{a} > 0$, $\mathbf{b} > 0$, when $\phi < 0$ with $|\phi| \ll 1$, 0 is locally asymptotically stable, and there exists a positive unstable equilibrium; when $0 < \phi \ll 1$, 0 is unstable and there exists a negative and locally asymptotically stable equilibrium.

ii. $\mathbf{a} < 0$, $\mathbf{b} < 0$, when $\phi < 0$ with $|\phi| \ll 1$, 0 is unstable; when $0 < \phi \ll 1$, 0, is locally asymptotically stable, and there exists a positive unstable equilibrium.

iii. $\mathbf{a} > 0$, $\mathbf{b} < 0$, when $\phi < 0$ with $|\phi| \ll 1$, 0 is unstable, and there exists a locally asymptotically stable negative equilibrium; when $0 < \phi \ll 1$, 0 is stable and a positive unstable equilibrium appears.

iv. $\mathbf{a} < 0$, $\mathbf{b} > 0$, when ϕ changes from negative to positive, 0 changes its stability from stable to unstable. Correspondingly, a negative unstable equilibrium becomes positive and locally asymptotically stable.

Let us now redefine the state variables $(S_1, I_1, R_1, B_1, S_2)$ as $(x_1, x_2, x_3, x_4, x_5)$. Then the associated system of equations obtained from systems (4.20) and (4.38) is given by

$$\begin{aligned}
\frac{dx_1}{dt} &= f_1 = \pi_1 + a_2x_5 + \omega x_3 - \beta_1\frac{x_4}{K+x_4}x_1 - \alpha_1x_2x_1 - (a_1+\mu_1)x_1\\
\frac{dx_2}{dt} &= f_2 = \beta_1\frac{x_4}{K+x_4}x_1 + \alpha_1x_2x_1 - Q_1x_2,\\
\frac{dx_3}{dt} &= f_3 = \gamma_1x_2 - (\mu_1+\omega)x_3,\\
\frac{dx_4}{dt} &= f_4 = \sigma x_2 - Q_2x_4,\\
\frac{dx_5}{dt} &= f_5 = \pi_2 + a_1x_1 - (a_2+\mu_2)x_5.
\end{aligned} \tag{4.27}$$

We evaluate the bifurcation parameter ϕ by equating R_{01m} to one to obtain

$$\phi = {\beta_1}^* = \frac{Q_1Q_2(\mu_1+\mu_1)(\mu_2+\mu_2)(1-\Phi_1)K - Q_2\alpha_1K(\pi_1(\mu_2+a_2)+a_2\pi_2)}{\sigma_1(\pi_1(\mu_2+a_2)+a_2\pi_2)}. \tag{4.28}$$

We linearise the system of equations (4.27) to the first community at the disease free equilibrium and with the bifurcation parameter ϕ to obtain

$$J(\mathbb{E}_1) = \begin{pmatrix}
-(a_1+\mu_1) & -\alpha_1S_1^* & \omega & \frac{-\phi^*S_1^*}{K} & a_2\\
0 & -(Q_1-\alpha_1S_1^*) & 0 & \frac{\phi^*S_1^*}{K} & 0\\
0 & \gamma_1 & -(\mu_1+\omega) & 0 & 0\\
0 & \sigma_1 & 0 & -Q_4 & 0\\
a_1 & 0 & 0 & 0 & -(a_2+\mu_2)
\end{pmatrix}. \tag{4.29}$$

The characteristic polynomial of the matrix (4.29) is given by

$$P(\lambda) = (\lambda+\mu_1+\omega)\left(\lambda^4 + \mathcal{G}_3\lambda^3 + \mathcal{G}_2\lambda^2 + \mathcal{G}_1\lambda + \mathcal{G}_0\right) = 0, \tag{4.30}$$

where

$$\begin{cases}
\mathcal{G}_0 &= (\mu_1+a_1)(\mu_2+a_2)(1-\Phi_1)\left[Q_1Q_2 - \left(\alpha_1Q_2 + \frac{\sigma_1\phi^*}{K}\right)S^*\right],\\
\mathcal{G}_1 &= (\mu_1+a_1)(\mu_2+a_2)(1-\Phi_1)\left[Q_2 + Q_1\left(1-\mathcal{R}_{01M}^p\right)\right],\\
\mathcal{G}_2 &= (\mu_1+a_1)(\mu_2+a_2)(1-\Phi_1) + (\mu_1+a_1)\sigma_1 + (\mu_2+a_2)Q_2\\
&\quad + Q_1(\mu_1+a_1+\mu_2+a_2)\left(1-\mathcal{R}_{01M}^p\right)\\
\mathcal{G}_3 &= \mu_1+a_1+\mu_2+a_2+Q_1\left(1-\mathcal{R}_{01M}^p\right),
\end{cases}$$

and $\mathcal{R}_{01M}^p = \dfrac{\pi_1(\mu_2+a_2)+a_2\pi_2}{Q_1(\mu_1+a_1)(\mu_2+a_2)(1-\Phi_1)}$.

Substituting for ϕ^* and S^* in the expression for $\mathcal{G}_0$, we obtain $\mathcal{G}_0 = 0$. In addition, close

to the disease free equilibrium, $\mathcal{R}^{p}_{01M}$ is less than one and the coefficients $\mathcal{G}_1$, $\mathcal{G}_2$, $\mathcal{G}_3$ of the polynomial (4.30) are all positive. Therefore, using Descartes rule of signs, the resultant characteristic polynomial gives a zero eigenvalue and the rest of the eigenvalues are all negative. The matrix (4.29) has left eigenvectors $y = (y_1, y_2, y_3, y_4)^T$ corresponding to the zero eigenvalue, where

$$\begin{cases} y_1 &= 0, \\ y_2 &= \sigma_1(\mu_1 + a_1)(\mu_2 + a_2)(1 - \Phi_1), \\ y_3 &= 0, \\ y_4 &= Q_1(\mu_1 + a_1)(\mu_2 + a_2)(1 - \Phi_1) - \alpha_1\left(\pi_1(\mu_2 + a_2) + a_2\pi_2\right) \\ y_5 &= 0. \end{cases}$$

The right eigenvector associated with the zero eigenvalue of (4.29) is $v = (v_1, v_2, v_3, v_4)^t$ where

$$\begin{cases} v_1 &= Q_1Q_2Q_3(1 - \Phi_1 - \Phi_2), \\ v_2 &= Q_2, \\ v_3 &= \frac{\gamma_1 Q_2}{(\mu_1+\omega)}, \\ v_4 &= \sigma_1, \\ v_5 &= \frac{a_1}{\mu_2+a_2}v_1. \end{cases} \tag{4.31}$$

We now evaluate the non-zero second order mixed derivatives of with respect to the variables where we obtain

$$\frac{\partial^2 f_1}{\partial x_1 \partial x_2} = \frac{\partial^2 f_1}{\partial x_2 \partial x_1} = -\alpha, \qquad \frac{\partial^2 f_1}{\partial x_1 \partial x_4} = \frac{\partial^2 f_1}{\partial x_4 \partial x_1} = -\frac{\phi^*}{K}, \tag{4.32}$$

$$\frac{\partial^2 f_2}{\partial x_1 \partial x_2} = \frac{\partial^2 f_2}{\partial x_2 \partial x_1} = \alpha, \qquad \frac{\partial^2 f_2}{\partial x_1 \partial x_4} = \frac{\partial^2 f_2}{\partial x_4 \partial x_1} = \frac{\phi^*}{K}. \tag{4.33}$$

The non-zero partial derivatives to used in calculating **b** are

$$\frac{\partial^2 f_1}{\partial x_4 \partial \phi} = -\frac{S_1^*}{K}, \qquad \frac{\partial^2 f_2}{\partial x_4 \partial \phi} = \frac{S_1^*}{K}. \tag{4.34}$$

We now substitute the expressions into (4.25) and (4.26) to obtain

$$\mathbf{a} = -\frac{2\beta^*\mu y_2}{\pi}\left[v_2v_4(1 + \eta_2) + v_2v_3(1 + \eta_1) + v_3v_4(\eta_1 + \eta_2)\right],$$
$$\mathbf{b} = \mu Q_2Q_3(1 - \Phi_1)\left[Q_2Q_3(1 - \Phi_1) + \eta_1\sigma Q_3 + \eta_2\sigma\rho\right].$$

Clearly, we observe that $\mathbf{a} < 0$ and $\mathbf{b} > 0$. Thus, the drug persistent steady state is locally asymptotically stable close to $R_0 = 1$. We can summarise the results in the following Lemma.

Lemma 4.5.1. *The drug persistent steady state is locally asymptotically stable when $R_0 > 1$ but only if R_0 is close to 1.*

4.5.1 Endemic steady state $\mathbb{E}_2$

Lemma 4.5.2. *The model system (4.1 and 4.2) has a unique boundary endemic equilibrium $\mathbb{E}_2$ in Ω whenever $\mathcal{R}_{02M} > 1$ and $\mathcal{R}_{01M} < 1$.*

Lemma 4.5.2 implies that cholera persists in the second sub-population $(I_2 > 0)$ but dies out in the first sub-population.

Proof. We note that in the absence of the infections in the first sub-population, $I_1 = 0$. Then from equations (4.1) and (4.2) at $\mathbb{E}_2$, we have

$$\begin{cases} \pi_1 + a_2\bar{S^*}_2 = (\mu_1 + a_1)\bar{S^*}_1, \\ \pi_2 + a_1\bar{S^*}_1 + \omega\bar{R^*}_2 = \left(\beta_2\frac{\bar{B_2^*}}{K+\bar{B_2^*}} + \alpha_2\bar{I^*}_2\right)\bar{S^*}_2 + (a_2 + \mu_2)\bar{S^*}_2, \\ \left(\beta_2\frac{\bar{B_2^*}}{K+\bar{B_2^*}} + \alpha_2\bar{I^*}_2\right)\bar{S^*}_2 = Q_3\bar{I^*}_2, \\ \gamma_2\bar{I^*}_2 = (\mu_2 + \omega)\bar{R^*}_2 \\ \sigma_2\bar{I^*}_2 = Q_4\bar{B_2^*} \end{cases} \tag{4.35}$$

Using the first, fourth and fifth equations of the system of equations (4.35), we obtain expressions for $\bar{S_1^*}$, $\bar{R_2^*}$, and $\bar{B_2^2}$ as

$$\bar{S_1^*} = \frac{\pi_1 + a_2 S_2}{\mu_1 + a_1}, \tag{4.36a}$$

$$\bar{R_2^*} = \frac{\gamma_2 I_2}{\mu_2 + \omega}, \tag{4.36b}$$

$$\bar{B_2^*} = \frac{\sigma_2 I_2}{Q_4} \quad \text{respectively.} \tag{4.36c}$$

Substituting for $\bar{B_2^*}$ in the third equation of system (4.35) we obtain

$$\left(\frac{\beta_2\sigma_2 I_2^*}{Q_4 K + \sigma_2\bar{I_2^*}} + \alpha_2\bar{I_2^*}\right) S_2 = Q_3 I_2^*. \tag{4.37}$$

This gives $\bar{I_2^*} = 0$ as one of the solutions. This solution corresponds to the disease free steady state. If $\bar{I_2^*} \neq 0$,then remaining part of the expression gives the relationship between $\bar{S_2^*}$ and $\bar{I_2^*}$ such that

$$\bar{S_2^*} = \frac{Q_3 Q_4 K + Q_3\delta_2\bar{I_2^*}}{(\beta_2\delta_2 + \alpha_2 Q_4 K) + \delta_2\alpha_2\bar{I_2^*}} \tag{4.38}$$

We substitute for $\bar{B}_2^*$, and $\bar{R}_2^*$ in the second equation of (4.35), we obtain

$$\Phi_5 = Q_1(1-\Phi_4)\bar{I}_2^* + (\mu_1+a_1)(1-\Phi_1)\bar{S}_2^*, \tag{4.39}$$

where

$$\Phi_5 = \frac{\pi_2(\mu_1+a_1)+a_1\pi_1}{\mu_1+a_1}, \quad \Phi_4 = \frac{\omega\gamma_1}{(\mu_2+\omega)Q_3}.$$

Then we substitute for $\bar{S}_2^*$ (equation (4.38)) into equation (4.39) we obtain a quadratic equation given by

$$\mathcal{C}_2\bar{I}_2^{*2} + \mathcal{C}_1\bar{I}_2^* + \mathcal{C}_0 = 0 \tag{4.40}$$

where

$$\begin{cases} \mathcal{C}_2 &= \alpha_2\sigma_2 Q_3(1-\Phi_4) \\ \mathcal{C}_1 &= Q_3(1-\Phi_4)(\beta_2\sigma_2+\alpha_2 Q-4K)+\sigma_2 Q_3(\mu_2+a_2)(1-\Phi_1)(1-\mathcal{R}_{02c}) \\ \mathcal{C}_0 &= Q_3Q_4K(\mu_2+a_2)(1-\Phi_1)(1-\mathcal{R}_{02M}) \quad \text{where} \end{cases}$$

$$\mathcal{R}_{02M} = \frac{\Phi_5(\beta_2\sigma_2+\alpha_2Q_4K)}{Q_3Q_4K(\mu_2+a_2)(1-\Phi_1)} \quad \text{and} \tag{4.41}$$

$$\mathcal{R}_{02c} = \frac{\Phi_5\alpha_2}{Q_3(\mu_2+a_2)(1-\Phi_1)} \tag{4.42}$$

We note that the solutions of the polynomial (4.40) depends on the signs of $\mathcal{C}_1$ and $\mathcal{C}_0$. We there for have the following observations

- When $\mathcal{C}_0 < 0$ (i.e when $\mathcal{R}_{02M} > 1$), we have exactly one positive solution for all values of $\mathcal{C}_1$.
- When $\mathcal{C}_0 > 0$ (i.e when $\mathcal{R}_{02M} < 1$) the polynomial (4.40) has no positive roots since $\mathcal{A}_1 > 0$.

Therefore, the model has a unique disease persistent equilibrium $\mathbb{E}_2$ whenever $\mathcal{R}_{02M} > 1$ and $\mathcal{R}_{01M} < 1$ □

Owing to the complexity of the model and increased non-linearity of the terms involved, attempts to explicitly determine existence and stability of the interior equilibrium (disease persistent equilibrium) were rendered futile. We now resort to numerical simulations to ascertain the phase space trajectories of the compartments involved.

4.6 Numerical simulations

The numerical simulations of the model are performed using the ordinary differential equations numerical integration routine *odeint* in python-scipy. In our numerical simulations, the transmission dynamics of the infection in the considered communities are characterised by assumptions based on; social economic status, welfare, infrastructural development as well as difference in health care systems and awareness. In our model simulations, we assume that community 1 has better services compared to community 2. As result, the likelihood of disease severity and parameters related to transmission dynamics are assumed to be higher in sub-population 2 compared to community 1. Each of the communities is in contact with a distinct contaminated aquatic reservoir. Since we assume that the communities are not separated by a great distance, we assume that the abiotic and biotic factors that influence the multiplication of the pathogen are not significantly different. However, due to the relative difference in the standard of life, the shedding rate of the pathogen in the poorer community is expected to be higher. This would greatly affect the concentration of the pathogen in the corresponding aquatic reservoir.

4.6.1 Parameter estimation

The comprehensive selection of parameters values use in the simulation is outlined in Chapter 3. In this chapter however, some of the parameters have been selected within the specified ranges to cater for the differences in the communities mimicked in this study as well as the disease transmission dynamics. The full list of parameter values used in the simulation is given in Table 4.1. In the parameter values chosen, there are noticeably reasonable differences in the parameters for sub-populations 1 and 2. It is necessary to highlight that the parameter related to shedding of the pathogen typically affects the concentration of the pathogen and has less influence on the human population. We note that the symptomatic and asymptomatic individuals have markedly different shedding rates, i.e 50 day^{-1} and 0.5 day^{-1} respectively. It should be noted that of all infected individuals, often up to 80% are asymptomatic.

4.7 Sensitivity and uncertainty analysis

We carry out sensitivity analysis to quantify uncertainty of the parameters to the metapopulation model output. This is vital since it enables us identify critical input parameters that

Parameter	Range	Value	Units	Source
π_1		$\mu \times N_1$		Assumed
π_2		$\mu \times N_2$		Assumed
β_1	0-1	0.00125		Assumed
β_2	0-1	0.0125		Assumed
K	$10^6 - 10^9$	10^6	cells L^{-1}	[36]
μ_1		0.02	day^{-1}	[55, 56]
μ_2		0.02	day^{-1}	[55, 56]
δ_1	$6.58\times10^{-4} - 0.0182$	0.0125	day^{-1}	[20, 64]
δ_2	$6.58\times10^{-4} - 0.0182$	0.045	day^{-1}	[20, 64]
γ_1	$0.031 - 0.059$	0.045	day^{-1}	[20, 58]
γ_2	$0.031 - 0.059$	0.035	day^{-1}	[20, 58]
μ_p	$1.017 - 1.083$	1.06	day^{-1}	[36, 42, 50, 57]
g_1, g_2		0.73	day^{-1}	[36]
α_1	$0.031 - 0.059$	0.045	day^{-1}	Assumed
α_2	$0.031 - 0.059$	0.035	day^{-1}	Assumed
σ_1, σ_2	$10 - 100$	50.0	$cells ml^{-1} day^{-1} person^{-1}$	[36]

Table 4.1: Nominal values of estimated parameter values used in the simulations

should be the center of focus if the disease is to be contained. Sensitivity and uncertainty analysis are performed using the Latin hypercube sampling (LHS) scheme, a Monte-Carlo stratified sampling method that allows us to obtain an unbiased estimate of the model output for a given set of input parameter values [8]. The parameter space is simultaneously sampled without replacement and assuming statistical independence between the parameters. The selected samples is used to compute unbiased estimates of output values for disease thresholds specific to the communities under study as well as that of the model. The computed partial rank correlation coefficients of the specific output threshold values are graphically presented in tornado plots, see Figures 4.2 and 4.3.

A positive (negative) correlation coefficient corresponds to an increasing (decreasing) monotonic trend between the disease threshold and the parameter under consideration. Figures 4.2(a) and 4.2(b) are produced using disease threshold ratios $\mathcal{R}_{01M}$ and $\mathcal{R}_{02M}$ respectively. From the figures, the parameters related to movement of individuals from one community to another have reasonably significant PRCCs. We note that in both plots, person-to-person contact can not be ignored. The parameters μ_p, g_1 and g_2 have the lowest PRCCs with respect to the corresponding disease thresholds. However, their direction of influence is clearly visible. In this regard, since no effort toward reducing disease spread is rendered insignificant, any action that increases mortality of vibrios and reduces their multiplication eventually not only reduces the infection but also the risk. In addition the rates σ_1 and σ_2 at which infected

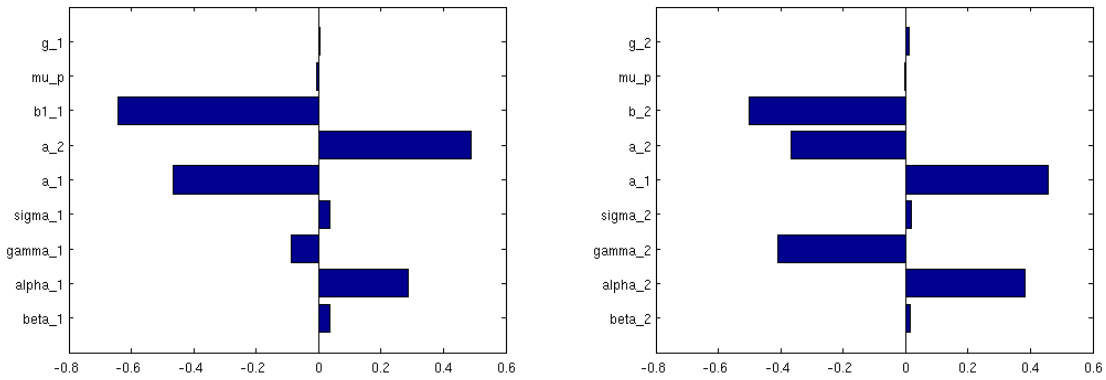

(a) (b)

Figure 4.2: Tornado plots showing PRCCs of the different parameter values. Figure 4.2(a), is produced assuming that the infection is localised only in community one and similarly for Figure 4.2(b).

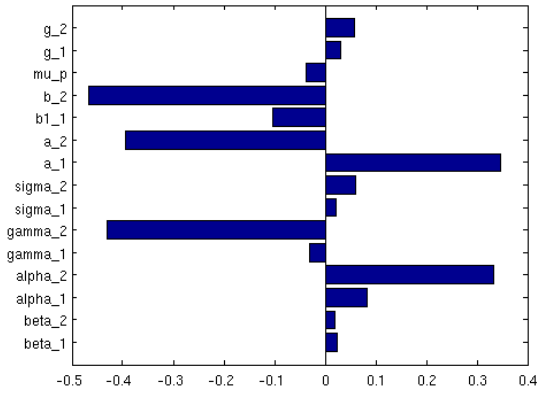

Figure 4.3: Tornado plot showing PRCCs of the parameter values and the model reproduction number.

individuals shed the pathogen into the aquatic environment as well as the contact β_1 and β_2 increase the severity of the disease when increased.

Increasing the migration of infected individuals from their corresponding subpolulations, results in the reduction in the total infective density. This eventually results in the reduction in the correlation of infective densities in the two communities and consequently a decrease in the epidemic coupling between the two communities [80]. However, continued in and outflow of both susceptible and the infected between the two communities potentially counteracts decorrelation that would be caused by emigration and reduced infective density in either community.

Endemic cholera in isolated patches

In this case endemicity of cholera in the model is accounted for by considering changes in the model parameters. Since infection with cholera confers some immunity, we assume that in the case of endemic cholera, the modelling time is long enough and that immunity may wane in the process leading to some recovered individuals becoming immunologically naive again. In the simulation therefore, the parameter ω is non-zero.

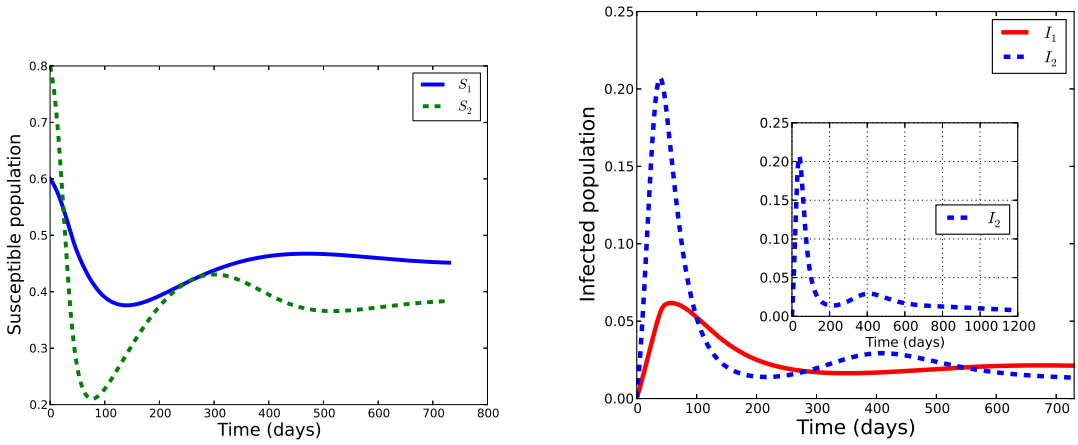

(a) (b)

Figure 4.4: Comparison of the susceptible and infected populations in homogeneous isolated sub-populations. The community specific disease thresholds evaluated using expressions $\mathcal{R}_{01}$ and $\mathcal{R}_{02}$ in equation (4.11) are 1.762 and 2.049 respectively.

In both the isolated sub-populations, the outbreak is explosive in nature. There is observed higher severity of the infection in community 2 with poorer facilities compared to community 1. We note that the infection reaches equilibrium much earlier in the community 2

compared to community , see Figure 4.4(b). This is due to the fact that; even though in a community 2 the initially susceptible population is much higher than that in community 1, the transmission parameters in community 2 are also high. This results in faster depletion of the susceptible pool (Figure 4.4(a)) hence reducing the likelihood of getting new infection. The rates are however, slower in community 1. Thus, the infection reaches a self-limiting phase much earlier in community 2 than in community 1. Long term dynamics indicate that, in the case of poorer conditions more than one episode of the epidemic may occur although the second episode may be much smaller than the first. Owing to the long term dynamics of the model, we predict that at equilibrium, the infected proportion in the patch with better facilities may be slightly higher than in the poorer patch. This is may be attributed to the fact that, in a poorer community, the infection would have greatly devastated the susceptible pool and that there may be far less people to infect. See Figure 4.4 for comparison. This disease devastating presumption is also depicted in the evaluated disease threshold values for the isolated communities.

Non endemic cholera in isolated communities

In the case of non endemic cholera, we assume that the waning rate is negligible. Over the modelling time,

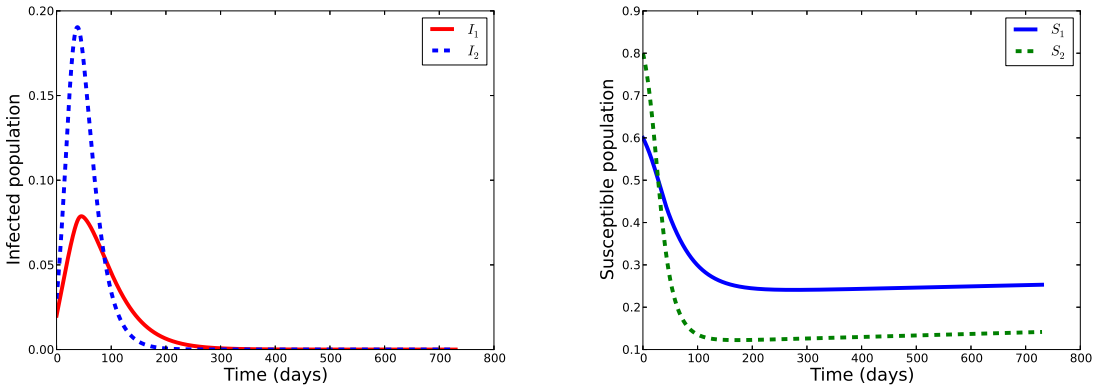

(a) (b)

Figure 4.5: Comparison of the susceptible and infected populations in homogeneous isolated sub-populations in the case of non-endemic cholera.

Similar to the case with endemic cholera, the outbreak is explosive followed by a self-limiting phase, see figure 4.5(a). This phase is also attributed to depletion in the susceptible population (Figure 4.5(b)) which reduces the likelihood of getting new infections. Unlike in the

case of endemic cholera, non-endemic cholera is characterised by as single outbreak and no recurring episodes.

Synchronous fluctuation of the sub-populations

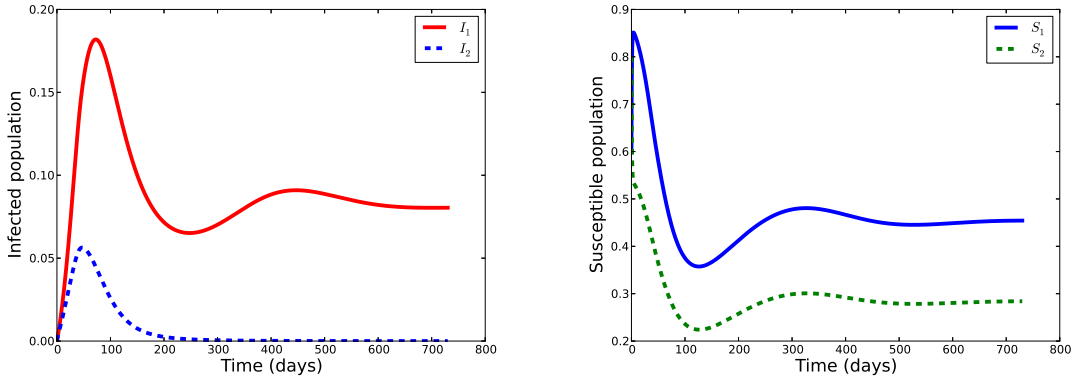

(a) (b)

Figure 4.6: Comparison of susceptible and infected populations across patches assuming movement of only susceptibles between patches. The parameters describing movement are such that $a_2 > a_1 > 0$, $b_2 = b_1 = 0$.

Increase in the susceptible population in the first community, is directly related to increasing the likelihood of an individual getting infected. This is due to the fact that increase in the susceptible population increases the probability of infected individuals transmitting the diseases to those uninfected through person-to person contact. In addition there is an increases chance that more immunologically naive individuals will come in contact with a vibrio contaminated aquatic source. It can clearly be observed that, when movement between compartments of susceptible population compartments is in existence, the is synchronous fluctuation of the populations in compartments of S_1 and S_2, see figure 4.6(b). No such scenario is observed in the compartments of I_1 and I_2, for which no migration has been accounted for, see figure 4.6(a).

Making an assertion that migration causes synchrony in metapopulation driven epidemics may be naive. This is owing to the fact that many other intrinsic and extrinsic factors including temperature and rainfall are vital contributors. As opposed to Figure 4.6(a), Figure 4.7(a) shows synchronous fluctuation of the population in compartments I_1 and I_2.

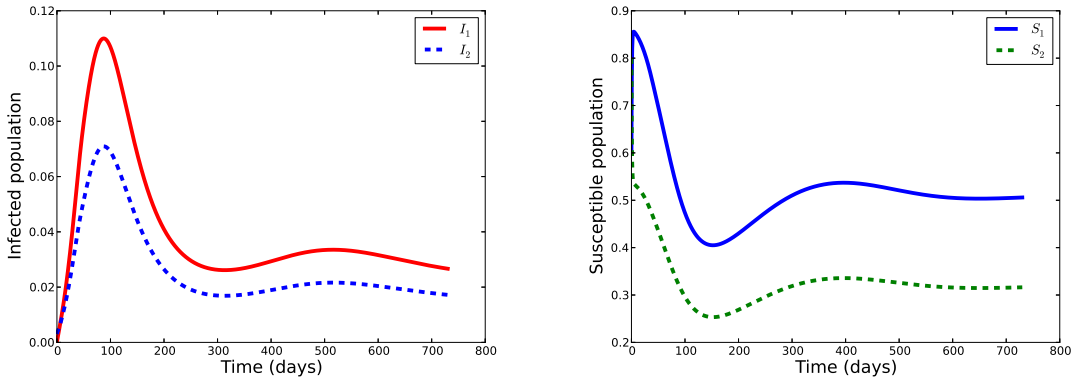

(a) (b)

Figure 4.7: Comparison of susceptible and infected populations across communities assuming movement of both susceptible and infected individuals between communities. The parameters describing movement are such that $a_2 > a_1 > 0$ and $b_2 > b_1 > 0$.

4.8 Conclusion

A deterministic model for cholera dynamics between connected communities is presented. Vital mathematical features including isolated patch specific disease thresholds were presented as well as disease thresholds accounting for migratory connection between patches. The effect of various process including migration on the dynamics of cholera have been examined. Sensitivity analysis has been performed to equitably ascertain the potential effect of vital parameters on the severity of the infection.

Understanding disease spread in non-isolated communities is important in containing of many communicable, infectious and childhood diseases. Movement of both susceptible and infected individuals influences the severity and persistence of the infection as well as synchronous fluctuation of the population in both communities. When the combined community disease threshold is greater than unity, the disease is more likely to persist in both communities if there is unrestricted migration. Otherwise, the disease will only persist in a community where the specific community disease threshold is greater than unity.

Chapter 5

Optimal control of cholera in connected communities

5.1 Introduction

Various controls for cholera have been recommended. These controls range from preventive measures to treatment protocols. Preventive measures are aimed at averting new infections by preventing the immunologically naive people from consuming or coming into contact with the bacteria. Treatment and control targets the infected persons reducing the number of those infected as well as reducing the case fatality rate. Such preventive and control measure are explained in detail with regard to the metapopulation model of two connected communities as follows. First, an Oral Cholera Vaccine (OCV) recently recommended [23] is now in use. Notably, it was recently used during the cholera outbreak that affected Haiti after the 2010-2011 earthquake [33]. Secondly, sanitation and hygiene reduce the rate of pathogen ingestion. Such controls include chemical treatment and boiling of water for cooking and drinking, proper storage and preparation of foods to prevent contamination. Thirdly, for the infected case management and treatment procedure which involves administering Oral Rehydration Salts (**ORS**) to restore ion balance, intravenous administration of fluids in serious cases and use of antibiotics is recommended.

Mathematical modelling of cholera transmission dynamics dates back to the 1970s with the work done by Capasso & Paveri-Fontana [41], but more profound work has been done in the last 1 to 2 decades. Most of the work done so far focuses on specific communities and not the metapopulation framework of the infection. An extensive highlight of the metapopulation framework in epidemic models involving both cross community infections as well as exchange of populations between communities is given in [81] but not a single case is spe-

cific to cholera. Optimal control of the infection has only been studied recently in [20] when comparing cholera transmission between two separate Indian communities of Bogra and Calcutta. To our knowledge, no optimal control study has been considered in the metapopulation framework for cholera transmission to date. However, general modelling of control of epidemics in metapopulations was recently done using an SIS model [82]. In this same work, the authors highlighted the likely difficulty and mathematical intractability to be faced if a SIR or SIRS model is to be used. In this paper, we consider a SIRS model with controls since cholera transmission typically follows such dynamics.

5.2 Mathematical model

In the model, we consider two routes of transmission. The primary route, characterised by consumption of vibrio infected water from aquatic sources. The secondary route (also referred to as person-to-person transmission), is characterised by consumption of food contaminated with vibrios from faecal matter. The human population is subdivided into three compartments depending on their status with respect to the infection. The Susceptible S, are those who are at risk of contracting cholera either through contaminated water of by the secondary route. Once infected, individuals move into compartment I. Those who recover from the infection move into compartment R at rates γ_1 and γ_2 for the first and second compartments respectively. The infection confers some temporary immunity which wanes at a rate ω. In the infection dynamics, the disease may be endemic or non-endemic. In the former case, the acquired immunity of those once infected is expected to wane at a faster rate resulting in a SIRS type of model as opposed to the SIR model in the latter case. It is assumed that the time delay between consumption of vibrio infected food or contaminated water and the commencement of infectiousness is negligible (see also [41]).

The flow diagram of disease progression in two communities is given in Figure 5.1.

The terms $\Lambda_1 = (1-u)\frac{\beta_1 B_1}{K+B_1} + (1-m)\alpha_1 I_1$ and $\Lambda_2 = (1-u)\frac{\beta_2 B_2}{K+B_2} + (1-m)\alpha_2 I_2$ are the incidence functions for the first and second community respectively. These two terms describe the rate of apparition of new cholera cases in the respective communities.

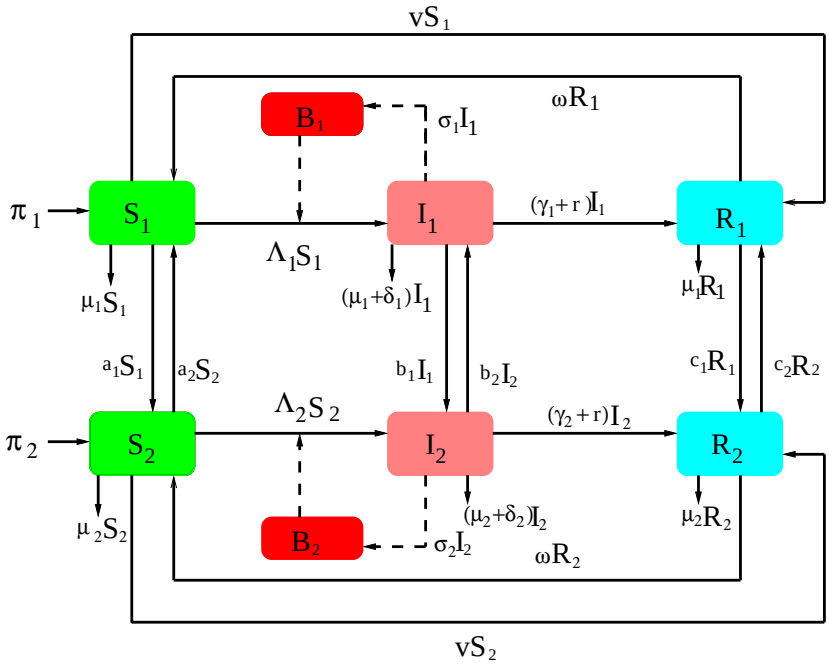

Figure 5.1: Flow diagram of disease dynamics in two communities.

The model system of equations for the first sub-population is given by

$$\frac{dS_1}{dt} = \pi_1 + a_2S_2 + \omega R_1 - (1-u)\beta_1\frac{B_1}{K+B_1}S_1 - (1-m)\alpha_1 I_1 S_1 - (a_1+\mu_1)S_1 - vS_1, \quad (5.1a)$$

$$\frac{dI_1}{dt} = (1-u)\beta_1\frac{B_1}{K+B_1}S_1 + (1-m)\alpha_1 I_1 S_1 + b_2 I_2 - Q_1 I_1 - rI_1, \quad (5.1b)$$

$$\frac{dR_1}{dt} = vS_1 + \gamma_1 I_1 + rI_1 - (\mu_1+\omega)R_1, \quad (5.1c)$$

$$\frac{dB_1}{dt} = \sigma_1 I_1 - Q_2 B_1, \quad (5.1d)$$

$$\frac{dS_2}{dt} = \pi_2 + a_1S_1 + \omega R_2 - (1-u)\beta_2\frac{B_2}{K+B_2}S_2 - (1-m)\alpha_2 I_2 S_2 - (a_2+\mu_2)S_2 - vS_2, \quad (5.1e)$$

$$\frac{dI_2}{dt} = (1-u)\beta_2\frac{B_2}{K+B_2}S_2 + (1-m)\alpha_2 I_2 S_2 + b_1 I_1 - Q_3 I_2 - rI_2, \quad (5.1f)$$

$$\frac{dR_2}{dt} = vS_2 + \gamma_2 I_2 + -(\mu_2+\omega)R_2, \quad (5.1g)$$

$$\frac{dB_2}{dt} = \sigma_2 I_2 - Q_4 B_2, \quad (5.1h)$$

where $Q_1 = (\mu_1 + \delta_1 + \gamma_1 + b_1)$, $Q_2 = (\mu_p - g_1)$, $Q_3 = (\mu_2 + \delta_2 + \gamma_2 + b_2)$, $Q_4 = (\mu_p - g_2)$. Note that all constants in the balance equations are non negative. In addition Q_2 and Q_4 are positive, indicating that in absence of faecal contribution from infective humans, the bacteria can not sustain itself in the aquatic environment [41]. The initial conditions of the model are such that S_{10}, I_{10}, R_{10}, B_{10},S_{20}, I_{20}, R_{20} and B_{20} are all non-negative.

5.2.1 Model analysis

The solution to model system of equations (5.1) with non-negative initial conditions are all non-negative and bounded. Interested readers can investigate positivity and boundedness of the solutions using the method based on the theory on differential equations outlined in Chapter 3.

Theorem 5.2.1. *The feasible region* Ω *given by*

$$\Omega := \left\{ (S_1(t), I_1(t), R_1(t), B_1(t), S_2(t), I_2(t), R_2(t), B_2(t)) \in \mathbb{R}^8_+ | \; 0 < N < \frac{\pi_1 + \pi_2}{\mu^\star} \right\}, \quad (5.2)$$

where, $\mu^\star = \min\{\mu_1, \mu_2\}$ *and* $N = S_1(t) + I_1(t) + R_1(t) + S_2(t) + I_2(t) + R_2(t)$*, with initial conditions* $S_{10} > 0, I_{10} \geq$*,* $R_{10} \geq 0, B_{10} \geq 0$*,* $S_{20} > 0, I_{20} \geq 0, R_{20} \geq 0$ *and* $B_{20} \geq 0$ *is positively invariant and attracting with respect to the model system* (5.1) *for all* $t > 0$*.*

We note that if both communities are free of the infection, no treatment control protocol may be implemented. However, vaccination may still be in place as will be indicated in the steady state points. Although, the permissible controls vary with time, to analyse the steady states, we assume that the controls are constant thereby analysing a non-autonomous system of differential equations, see also [83]. Therefore, the disease free equilibrium $\mathbb{E}_0$ given by

$$\mathbb{E}_0 = \{S_1^*, 0, 0, 0, S_2^*, 0, 0, 0\}, \quad (5.3)$$

where

$$S_1 = \frac{\pi_1(a_2 + \mu_2 + v) + a_2\pi_2}{(a_1 + \mu_1 + v)(a_2 + \mu_2 + v)(1 - \Phi_1)}, \quad S_2 = \frac{\pi_2(a_1 + \mu_1 + v) + a_1\pi_1}{(a_1 + \mu_1 + v)(a_2 + \mu_2 + v)(1 - \Phi_1)}. \quad (5.4)$$

The term $\Phi_1 = \frac{a_1}{(a_1+\mu_1+v)} \cdot \frac{a_2}{(a_2+\mu_2+v)}$ indicates the proportion of susceptible individuals who move back and forth in compartments S_1 and S_2. Therefore, $(1 - \Phi_1)$ indicates the fraction of susceptible individuals who don't move from their home compartments. We note also that the proportions of the susceptible S_1 and S_2 fall off as quadratic terms of the vaccination (in the denominator) and increase linearly (in the numerator). Therefore, if the higher the vaccination coverage, the lower fraction of the population that remains naive to the infection.

The community specific disease threshold numbers can be obtained using the next generation matrix method outlined in [51]. When computing the disease thresholds however, we assume that the controls are constant so that the model system of equations is non autonomous.

$$\mathcal{R}_{01oc} = \frac{(\pi_1(a_2 + \mu_2 + v) + a_2\pi_2)\left((1 - m)\alpha_1 Q_2 K + (1 - u)\beta_1\sigma_1\right)}{Q_1 Q_2 (a_1 + \mu_1 + v)(a_2 + \mu_2 + v)(1 - \Phi_1)K} \quad (5.5)$$

for the first community, and

$$\mathcal{R}_{02oc} = \frac{(\pi_2(a_1+\mu_1+v)+a_1\pi_1)\left((1-m)\alpha_2 Q_4 K+(1-u)\beta_2\sigma_2\right)}{Q_3Q_4(a_1+\mu_1+v)(a_2+\mu_2+v)(1-\Phi_1)K} \tag{5.6}$$

for the second community. Then the model basic reproduction $\mathcal{R}_{0oc}$ is given by

$$\mathcal{R}_{0oc} = \max\{\mathcal{R}_{01oc}, \mathcal{R}_{02oc}\}.$$

From the structure of the model used and the obtained community specific reproduction numbers controls are evident. From the expressions for community specific disease thresholds, it is evident that increasing access to clean water and enhancing proper hand hygiene reduces the disease threshold. Therefore, with enhanced controls, the subsequent number of those infected will be less than that of their predecessors hence reducing the severity of the infection.

It should also be noted that application of control strategies mainly reduces transmission of the infection related to contact with the aquatic reservoirs, hand hygiene mainly related to handling of foodstuffs and vaccination aimed at reducing the risk of immunologically naive persons from contracting the infection through any of the indicated routes. It is already known that during times of cholera, administration of ORS is important in resorting the ion balance in the body and fluids lost due to excessive diarrhoea.

Theorem 5.2.2. *The disease free steady state* (5.3) *of model* (5.1) *is globally asymptotically stable whenever,* $\mathcal{R}_{0oc} < 1$ *and unstable otherwise.*

The proof to Theorem 5.2.2 can be given using the approach to the proof for Lemma 1 in [39]. However, in this case the community specific reproduction numbers to be used are (5.5) and (5.6). In addition, any parameters related to control of the infection must be assumed constant. Similarly, the community specific endemic equilibrium points can be obtained following the approach in [39] as well as the proofs of local stability.

5.2.2 Optimal control

The general procedure of optimal control process in an epidemiological model involves the following process;

- identify permissible controls applicable to the model,
- set up the objective function with controls,

- construct the Hamiltonian,
- evaluate co-state variable (adjoint functions),
- identify the threshold controls that minimise the Hamiltonian.

This optimal control minimisation procedure follows Pontryagin's Maximum/Minimum principle [84].

In the general case, for a selected set of permissible controls u_1, u_2, and u_3 the objective function $\mathcal{J}$ can be set up as

$$\mathcal{J} = \min_{u_1,u_2,u_3} \int_0^{t_f} \left(e_1 I_1 + e_2 I_2 + q_1 u_1^2 + q_2 u^2 + q_3 u_3^2\right) dt, \tag{5.7}$$

where e_1, e_2 q_1, q_2 and q_3 are positive weights associated with minimising infections and the costs respectively. If we assume that the cost of controls to be non-linear, quadratic terms (for mathematical tractability) can be used. A detailed description of the optimal control process using both non-linear controls and linear controls, the challenges associated and and possible remedies are given in [85].

Let λ_{S_1}, λ_{I_1}, λ_{R_1}, λ_{B_1}, λ_{S_2}, λ_{I_2}, λ_{R_2} and λ_{B_2} be the adjoint functions or co-state variables associated with the states. We multiply each of the adjoint functions with the right side of the equation describing the evolution of each state variable. The objective function is given by

$$\mathcal{J}(u,v,m) = \int_0^T \left(\xi_1 I_1 + \xi_2 I_2 + \chi u^2 + y v^2 + z m^2\right) dt. \tag{5.8}$$

The coefficients ξ_1, ξ_2, χ, y and z are the coefficients associated with the cost over a finite period of time T. $\xi_1 I_1$ and $\xi_2 I_2$ indicate the cost associated with minimising the infection in the first and second community respectively. χ, y and z are relative cost weights for the respective control measures. The main goal is to minimise the number of those infected in both communities at the same time minimising the cost of controls. In this respect, we seek an optimal control u^*, v^* and m^* such that

$$\mathcal{J}(u^*,v^*,m^*) = \min_{u,v,m}\{\mathcal{J}(u,v,m)|u,v,m \in \mathcal{U}\}, \tag{5.9}$$

where

$$\mathcal{U} := \{(u,v,m)|u,v,m : [0,T] \to [0,1], \text{ for all } u,v,m\}.$$

The Hamiltonian is given by,

$$\begin{aligned}
H = {} & \xi_1 I_1 + \xi_2 I_2 + \chi u^2 + y v^2 + z m^2 + \lambda_{S_1}\left[\pi_1 + a_2 S_2 + \omega R_1 - (1-u)\beta_1 \frac{B_1}{K+B_1} S_1\right. \\
& \left. -(1-m)\alpha_1 I_1 S_1 - (a_1+\mu_1) S_1 - v S_1\right] + \lambda_{I_1}\left[(1-u)\beta_1 \frac{B_1}{K+B_1} S_1 + (1-m)\alpha_1 I_1 S_1\right. \\
& \left. + b_2 I_2 - Q_1 I_1 - r I_1\right] + \lambda_{R_1}\left[v S_1 + \gamma_1 I_1 + r I_1 - (\mu_1+\omega) R_1\right] + \lambda_{B_1}\left[\sigma_1 I_1 - Q_2 B_1\right] \\
& + \lambda_{S_2}\left[\pi_2 + a_1 S_1 + \omega R_2 - (1-u)\beta_2 \frac{B_2}{K+B_2} S_2 - (1-m)\alpha_2 I_2 S_2 - (a_2+\mu_2) S_2 - v S_2\right] \\
& + \lambda_{I_2}\left[(1-u)\beta_2 \frac{B_2}{K+B_2} S_2 + (1-m)\alpha_2 I_2 S_2 + b_1 I_1 - Q_3 I_2 - r I_2\right] \\
& + \lambda_{R_2}\left[v S_2 + \gamma_2 I_2 + -(\mu_2+\omega) R_2\right] + \lambda_{R_2}\left[\sigma_2 I_2 - Q_4 B_2\right].
\end{aligned} \tag{5.10}$$

Theorem 5.2.3 (Lenhart & Workman, (2007) [85]). *Let u^*, v^* and m^* be the optimal controls for the system (5.1), x^* be the state space at equilibrium and $\lambda(t)$ positive semi-definite piecewise differentiable functions for all t. If we suppose that for all $0 \leq t \leq T$,*

$$0 = H_u(t, x^*, u^*, v^*, m^*, \lambda(t)) = H_v(t, x^*, u^*, v^*, m^*, \lambda(t)) = H_m(t, x^*, u^*, v^*, m^*, \lambda(t)),$$

then

$$H(t, x^*, u^*(t), v^*(t), m^*(t), \lambda(t)) \leq H(t, x^*, u(t), v(t), m(t), \lambda(t)) \tag{5.11}$$

To prove Theorem 5.2.3, for the model system (5.1), it is enough to find the optimal controls u^*, v^*, m^* that minimise the Hamiltonian as indicated below.

To find the differential equations with respect to the associated adjoint functions, we differentiate the Hamiltonian with respect to each of the state variables

$$\begin{aligned}
\frac{d\lambda_{S_1}}{dt} &= \left[(1-u)\beta_1\frac{B_1}{K+B_1} + (1-m)\alpha_1 I_1\right] S_1(\lambda_{S_1} - \lambda_{I_1}) + (a_1+\mu_1+v)\lambda_{S_1} - v\lambda_{R_1} - a_1\lambda_{S_2},\\
\frac{d\lambda_{I_1}}{dt} &= (1-m)\alpha_1 S_1(\lambda_{S_1} - \lambda_{I_1}) - \xi_1 + (Q_1+r)\lambda_{I_1} - (\gamma_1+r)\lambda_{R_1} - \sigma_1\lambda_{B_1} - b_1\lambda_{I_2},\\
\frac{d\lambda_{R_1}}{dt} &= (\mu_1+\omega)\lambda_{R_1} - \omega\lambda_{S_1},\\
\frac{d\lambda_{B_1}}{dt} &= \frac{(1-u)\beta_1 S_1 K}{(K+B_1)^2}(\lambda_{S_1} - \lambda_{I_1}) + Q_2\lambda_{B_1},\\
\frac{d\lambda_{S_2}}{dt} &= \left[(1-u)\beta_1\frac{B_2}{K+B_2} + (1-m)\alpha_2 I_2\right] S_2(\lambda_{S_2} - \lambda_{I_2}) + v(\lambda_{S_2} - \lambda_{R_2}) + a_2(\lambda_{S_2} - \lambda_{S_1}) + \mu_2\lambda_{S_2},\\
\frac{d\lambda_{I_2}}{dt} &= (1-m)\alpha_2 S_2(\lambda_{S_2} - \lambda_{I_2}) - \xi_2 + (Q_3+r)\lambda_{I_2} - (\gamma_2+r)\lambda_{R_2} - \sigma_2\lambda_{B_2} - b_2\lambda_{I_1},\\
\frac{d\lambda_{R_2}}{dt} &= (\mu_2+\omega)\lambda_{R_2} - \omega\lambda_{S_2},\\
\frac{d\lambda_{B_1}}{dt} &= \frac{(1-u)\beta_2 S_2 K}{(K+B_2)^2}(\lambda_{S_2} - \lambda_{I_2}) + Q_4\lambda_{B_2},
\end{aligned}$$

with transversality condition

$$\lambda_{S_1}(T) = \lambda_{I_1}(T) = \lambda_{R_1}(T) = \lambda_{B_1}(T) = \lambda_{S_2}(T) = \lambda_{I_2}(T) = \lambda_{R_2}(T) = \lambda_{B_2}(T) = 0. \quad (5.12)$$

We note that the for the given transversality condition (5.12)

$$\begin{aligned}
\frac{d\lambda_{S_1}}{dt} &= -\frac{\partial H}{dS_1},\\
&\vdots\\
\frac{d\lambda_{B_2}}{dt} &= -\frac{\partial H}{dB_1}.
\end{aligned}$$

The optimal controls are characterised by the following expressions

$$\begin{aligned}
u^*(t) &= \max\left(0, \min\left(\hat{u}(t), 1\right)\right),\\
v^*(t) &= \max\left(0, \min\left(\hat{v}(t), 1\right)\right), \quad \text{and}\\
m^*(t) &= \max\left(0, \min\left(\hat{m}(t), 1\right)\right).
\end{aligned}$$

The standard control arguments on the controls [86], the optimal controls are such that

$$u^* = \begin{cases} 0 & \text{if } \hat{u} \leq 0, \\ \hat{u} & \text{if } 0 < \hat{u} < 1, \\ 1 & \text{if } \hat{u} \geq 1. \end{cases}$$

The upper bound of u^* would indicate that drinkable water is least likely to be responsible for the oral faecal route of transmitting the infection, most especially if water is chlorinated.

$$v^* = \begin{cases} 0 & \text{if } \hat{v} \leq 0, \\ \hat{u} & \text{if } 0 < \hat{v} < 1, \\ 1 & \text{if } \hat{v} \geq 1. \end{cases}$$

The value $v^* = 1$, would be attributed to a perfectly effective vaccine. Quite often cholera vaccines have low protective efficacy and have adverse effects associated. In one study by the Public Health Agency of Canada [87], the efficacy of the cholera and diarrhoeal vaccine was observed to range between 64% to 85% against *Vibrio cholerae* 01 El Tor.

$$m^* = \begin{cases} 0 & \text{if } \hat{m} \leq 0, \\ \hat{m} & \text{if } 0 < \hat{m} < 1, \\ 1 & \text{if } \hat{m} \geq 1. \end{cases}$$

Similarly, $m^* = 1$, would signify no transmission of the pathogen through consumption of foods, and that all foodstuffs are well prepared and hygienically stored, free from contamination. Unfortunately, this is not usually the case in communities where cholera is endemic.

Differentiating $\mathcal{H}$ with respect to each of the admissible controls, we obtain

$$\begin{aligned} \frac{\partial H}{\partial u} &= 2\chi u + (\lambda_{S_2} - \lambda_{I_2})\,\beta_2 \frac{B_2}{K + B_2} + (\lambda_{S_1} - \lambda_{I_1})\,\beta_1 \frac{B_1 S_1}{K + B_1}, \\ \frac{\partial H}{\partial v} &= 2yv + (\lambda_{R_1} - \lambda_{S_1})\,S_1 + (\lambda_{R_2} - \lambda_{S_2})\,S_2, \\ \frac{\partial H}{\partial m} &= 2zm + (\lambda_{S_1} - \lambda_{I_1})\,\alpha_1 I_1 S_1 + (\lambda_{S_2} - \lambda_{I_2})\,\alpha_2 I_2 S_2. \end{aligned} \tag{5.13}$$

The control characterisations, $\hat{u}$, $\hat{v}$, and $\hat{m}$ of the optimal controls u^*, v^* and m^* are obtained from $\frac{\partial H}{\partial u} = \frac{\partial H}{\partial v} = \frac{\partial H}{\partial m} = 0$

$$\hat{u} = \frac{(\lambda_{I_2} - \lambda_{S_2})\,\beta_2 \frac{B_2}{K+B_2} + (\lambda_{I_1} - \lambda_{S_1})\,\beta_1 \frac{B_1 S_1}{K+B_1}}{2\chi},$$
$$\hat{v} = \frac{(\lambda_{S_1} - \lambda_{R_1})\,S_1 + (\lambda_{S_2} - \lambda_{R_2})\,S_2}{2y},$$
$$\hat{m} = \frac{(\lambda_{I_1} - \lambda_{S_1})\,\alpha_1 I_1 S_1 + (\lambda_{I_2} - \lambda_{S_2})\,\alpha_2 I_2 S_2}{2z}.$$

5.3 Numerical Results

To numerically solve the optimal control problem, we modify code7.m developed by Lenhart and Workman [85]. This optimal control problem is classified as a quadratic programming problem, since the controls are in quadratic form. The state space variables are solved forward in time and the adjoints associated with the state variables solved backward in time. The model system of equations is numerically integrated using the ODE integration routine (ode45) a fourth order Runge-Kutta Method in Matlab. The parameter values used are estimated from published literature and some intuitively selected. For example; the estimated prices per dose of Dukarol and Shanchol are \$4.7 − \$9.4 and \$1.85 respectively [31]. We note however that there are other costs that may be involved related to administration, advertising, transportation and remuneration for the health workers. Hence the value R100 attributed to each square vaccination rate. The unit of the parameters is per day except for those indicated otherwise. The estimated costs associated with the controls per person are given in Table 5.1. The rest of the parameters used for the metapopulation model are given in Table 4.1.

Coefficient	Cost value
ξ_1	R 200 Per percentage reduction in I_1
ξ_2	R 120 Per percentage reduction in I_2
X	R 200 per (level of water related treatment)^2
Y	R 100 per (vaccination rate)^2
Z	R 200 per (hand hygiene related infection reductions)^2

Table 5.1: Costs associated with permissible controls

The algorithm for simulating the system using the "forward-backward sweep method" is adopted from [85]. We outline the steps followed during the simulation for convenience of

the reader;

Step 1. The time interval over which the system is to be integrated is subdivided into N equal subintervals. The initial guesses of piecewise-constant controls $u_0(t), v_0(t)$ and $m_0(t)$ on the interval $t \in [t_i, t_{i+1}]$, for $i = 0, 1, \cdots, N$ are assumed.

Step 2. Using the assumed controls u_0, v_0, m_0 and the initial conditions $\vec{x}(0) = (S_{10}, I_{10}, R_{10}, B_{10}, S_{20}, I_{20}, R_{20}, B_{20})$ of the model, the system is numerically integrated forward in time $[0, T]$ according to its system of differential equations in the optimality system.

Step 3. using the assumed controls $u_0(t), v_0(t)$ and $m_0(t)$ and values of $\vec{x}$, the costate system $\vec{\lambda}(t)$ in accordance with its system of differential equations with the transversality condition, is integrated backward in time $[T, 0]$.

Step 4. The controls vector $\vec{u}$ is updated by entering the new state vector $\vec{x}$ and the costate values $\vec{\lambda}$ in the optimal characterisations.

Step 5. Convergence of the iterations is then checked by ascertaining whether successive iterations are negligibly close for some specified level of tolerance. Once this is achieved, then optimal control is said to have been achieved, the iteration is stopped and the output values recorded as solutions. Otherwise, the algorithm is set back to Step 2.

5.3.1 Isolated communities in presence of controls

The communities are assumed to be isolated if there is no movement across adjacent communities. However, we allow for recruitment from other areas. In the simulation, we use the parameters indicated in Table 4.1 and set all the parameters, describing movement to zero. The trajectories of the infected population in both communities is given in Figure 5.2.

When all the controls are implemented, our results suggest that, the time taken for the disease to be contained, maybe approximately half of the time required to contain the disease without controls, i.e by self limitation. Although the infection is less devastating in the first community, it stays relatively longer in the community compared to the second community (compare the solid lines in Figures 5.2(a) and 5.2(a)). It is plausible that due to a high transmission in the second community, the disease depletes the susceptible pool at a much faster rate and at about 100 days, there are virtually no more susceptible people to infect. In

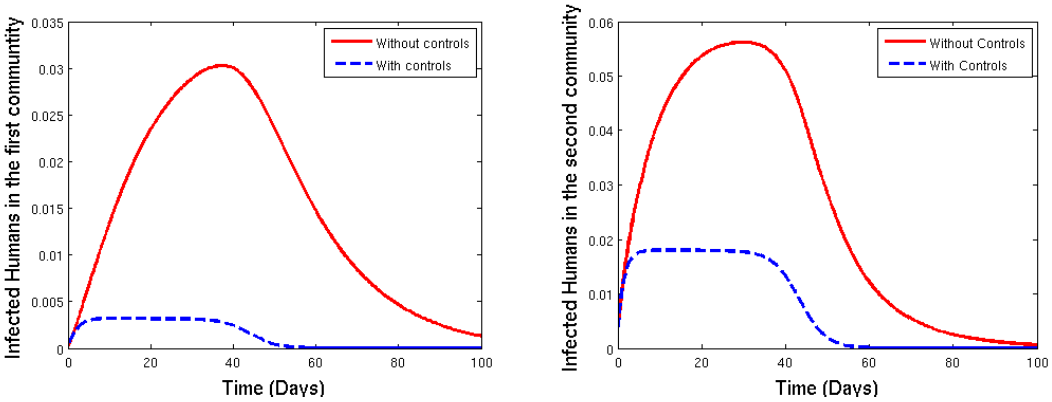

(a) (b)

Figure 5.2: The infectious, I_1 in presence of controls (dashed line) and in absence of controls (solid line)

the model with controls however, the disease is contained at approximately the same time in both communities. Taking a closer look at dashed curves in Figures 5.2(a) and 5.2(a), it can be observed that the disease is contained slightly earlier in the first community than in the second community for the same level of effort. This scenario is a typical comparison of infections with high and low incidence. The trajectories of the state space variables for the model with control, the adjoint and the control values converge around relatively the same time. The iteration process terminates when these different variables converge sufficiently.

5.4 Connected communities in presence of controls

When the communities are connected, the parameters describing movement are all non-zero.

Movement of susceptible and infected people is associated not only with increases severity but also a long duration of the infection in the two communities, see Figures 5.2 and 5.3. In presence of controls however, there is no observed significant difference in the disease severity and duration.

The profiles of control related to clean water supply, vaccination and improved hygiene are indicated in figures 5.4(a), 5.4(b) and 5.5 respectively. It can be be observed that the control process ought to be optimal at the beginning of the epidemic. It is at this point that the infection is explosive in nature and should be contained at a faster rate.

The susceptible group in both communities is initially characterised by depletion followed

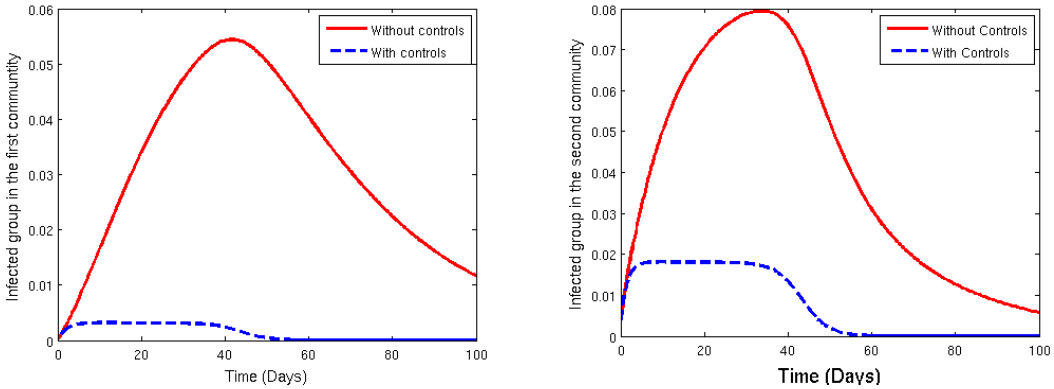

(a) Infected group in the first community (b) Infected group in the first community

Figure 5.3: Infected groups in the two communities with and without controls

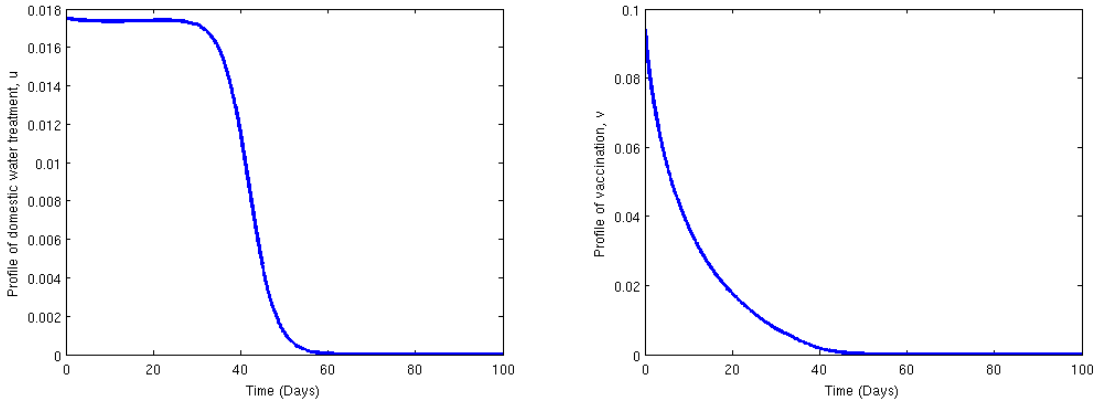

(a) (b)

Figure 5.4: Profiles of controls related to domestic water treatment and vaccination

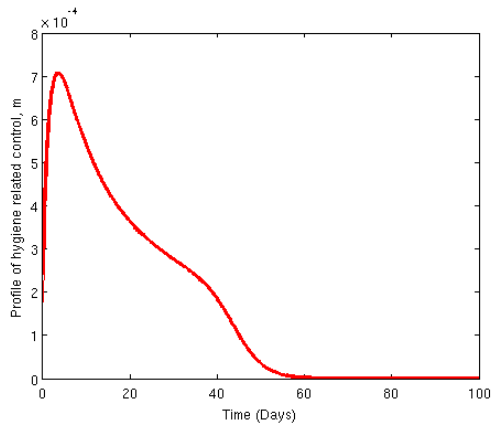

Figure 5.5: Profile of hygiene related control

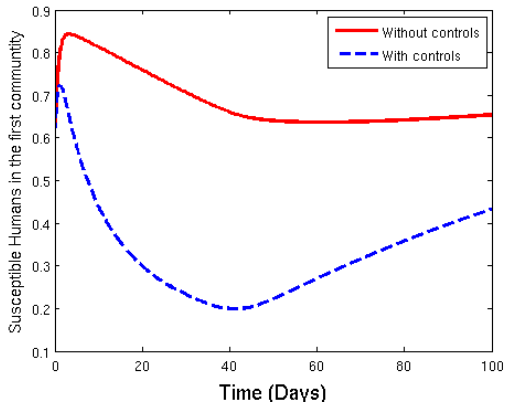

(a) Susceptible group in the first community

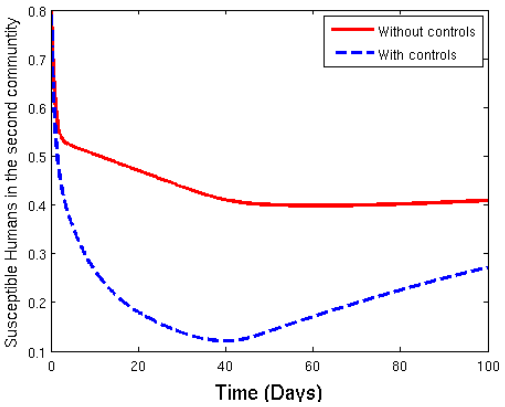

(b) Susceptible group in the second community

Figure 5.6: Susceptible populations in the two communities

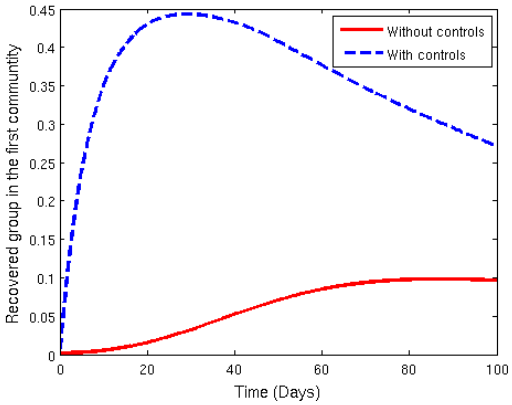

(a) Recovered group in the first community

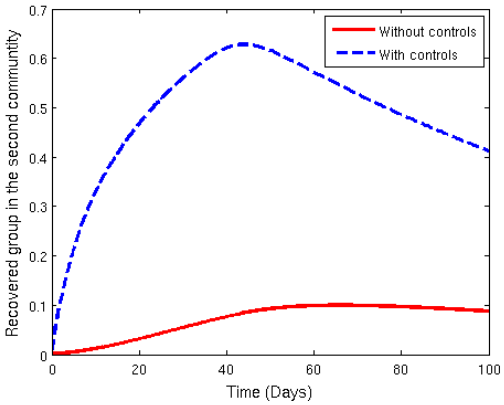

(b) Recovered group in the second community

Figure 5.7: Proportion of recovered individuals in the two communities, with and without controls

by an increase, Figure 5.6. We note that the rapid depletion of the susceptible population is due vaccination, which was assumed to be exponential in the model. As a result the recovered group is replenished and reduces when the control is halted, Figure 5.7. By the end of the entire control period, the community is comprised of the susceptible group. Once the infection has been contained, it is assumed that the small group of people who could still be carrying the disease, may pose a low threat of re-introducing it.

Although the general trajectory of the susceptible groups in the two communities is similar, there is a striking difference that ought to be highlighted. Whereas there is an observed initial increase in the susceptible group in the first community, that in the second community only decreases. This trend is attributed to movement which is inclined toward the first community owing to the better living conditions assumed in the model parameter estimation.

5.5 Conclusion

In this Chapter, a metapopulation model for cholera transmission characterised by exchange of individuals between communities has been analysed. The community specific disease thresholds have been given and their importance determining the existence and stability of equilibria of the model highlighted. The conditions for annihilating the infection based on specific controls while keeping other parameters constant have been indicated. Our numerical results indicate that in presence of controls, in case of an outbreak the disease maybe 8 times less devastating compared to the case without controls. In addition, the duration of the infection in the community is less likely to be more than half the time it would remain prevalent in absence of controls.

The model presented in this chapter is not short of shortfalls. We acknowledge the fact that controls across communities may not be uniform as assumed in the models. Controls efforts are often influenced by demographics of the community (including ageing which is associated with immune dysfunction), the behaviour of individuals involved in the disease transmission dynamics as well as the social economic. In addition, politics which greatly affects the minority groups as well as social inequality which impacts the vulnerable groups, urbanization associated with overcrowding, inadequate infrastructure and economic stochasticity among others. All these affect the bureaucracy associated with implementation of controls, putting up a sustainable solutions and can be source of heterogeneity. The model also assumes a negligible time difference between infection and when one becomes infectious as well as apparition of symptoms. Although such simplifying assumptions may be presumed

feasible, their investigation is necessary to ascertain the effect on the epidemic size and duration.

Chapter 6

Control of *V. cholerae* with bacteriophage

6.1 Introduction

Recent developments in studies to contain cholera infection have focused on prevention of the infection, through “anti-infection strategies". Such strategies range from improvement in sanitation to avoid contamination to sensitisation of the general public to ensure proper hand hygiene, preparation and storage of food stuffs. In regions with no sanitary flash toilets, emphasis is on proper usage of pit latrines. We note however that, in cases where flash toilets are used, not all may be connected to a municipal centrally managed sewer or properly secured sceptic tanks. The run off during rainy seasons, may wash the waste faecal material to the aquatic reservoirs and riverine catchment areas. It may be these same reservoirs (water catchment areas) that could be the prime source of water for some impoverished communities.

Various control measures including improvements in sanitation, chemical treatment of water and vaccination have been previously studied [20, 83, 88] among others. However, the implementation of some of these measures has proved ineffective, in some cases not economically viable and application of chemicals often raises a public outcry over environmental and ecological concerns. Vaccination for example, although believed to confer some immunity to cholera infection, it is not entirely used as a preventive measure and no longer mandatory even for travellers to cholera endemic areas.

An innovative measure of biological control has been studied recently which may be useful and ecologically friendly. If biological control can effectively lead to reduction in the

concentration of *V. cholerae* in the aquatic reservoir, then it would contribute significantly to reducing the likelihood of consuming as infectious dose of the pathogen. Use of specific bacteriophage for *V. cholerae* is ideal in the following ways. Firstly, the use of antibiotics may result into antibiotic resistant vibrios [89]. Secondly, biological control is eco-friendly since the use of chemicals may be lethal to other aquatic inhabitants. Thirdly, specific bacteriophage can be used to attack specific bacteria.

Although the mechanism underlying the rapid proliferation of vibrios during ocean warming is not clearly known, it has been observed that outbreaks are correlated with high temperatures especially those recorded in El Niño Southern Oscillation (ENSO) and Monsoon climate [90]. In the study conducted by Long et al [90], some marine bacteria for example Bacteriodetes, Alphaproteobacteria, and Gammaproteobacteria can impede the growth of *Vibrio cholerae*. These are referred to as antagonistic bacteria. They are however, less active at high temperatures and easily out-competed by the *vibrios*. The association of high proliferation of *Vibrio cholerae* at high temperatures and low activity of antagonistic bacteria related to production of anti-bacterial agents by the *vibrios*.

In recent observations, existence of bacteriophage in aquatic environments has been antagonistic with existence of *V. cholerae* and consequently the incidence of cholera [37]. Once in the aquatic environment vibrios remain viable and the cells can maintain proper metabolic activity although they maybe non-culturable [91]. Nelson *et al.* [91] reported that the multiplication of vibrios is antagonistic to the concentration of lytic bacteriophage in the aquatic environment. In addition, vibrios once shed from stool in the aquatic environment, they quickly decay from a more hyperinfective to a less hyperinfective but more persevering state. It is in the non-hyperinfective state that the vibrios may be active but non-culturable. In this state, the vibrios are well adapted to survival in the environment. Containing vibrios in such a state by biological control may require using of effective and efficient bacteriophage or else other remedies ought to be employed.

The potential biocontrol strategy for controlling virulent *V. cholerae* may entail using lytic bacteriophage specific for *V. cholerae*. The use of the bacteriophage as therapy would involve direct inoculation of the bacteriophage into the environment [92]. The strong assumption under this control measure comes with the fact that the environmental hosts for pathogenic bacteria such as water, soil, food and other organisms do not have complex systems to select against the foreign agents (bacteriophage) as opposed to the human body [92]. The rationale of using biocontrol is that it would reduce the concentration of pathogenic bacteria in the ecological niche thereby reducing the likelihood of infection as well as the severity and per-

sistence of the bacterial epidemic. If the bacteriophage directly preys on the pathogen, then presence of phage will reduce the density of the pathogen in aquatic environment. Consequently, this reduces the likelihood of consuming the amount of vibrios equivalent to the infectious dose in contaminated water. Although organic nutrients may exist in the aquatic reservoir depending on whether it is oligotrophic, mesotrophic or eutrophic, we assume that the phage may feed on the vibrios in preference to the organic nutrients. Bacteriophage specific for *Vibrio cholerae* were isolated in fresh water samples in Kenya [93] around lake Victoria all of the *Myoviridae* family. The isolated bacteriophage were suggested to be lytic to *Vibrio cholerae* basing on the tiny, round and clear plaques they (phages) produced. This is an important promise for biological control of the *V. cholerae*.

Two models have been presented previously accounting for the use of a bacteriophage in the control of cholera [37, 38]. A summary of the model by Jensen *et al.* [38] was given in Chapter 2. Although it has been indicated that lytic bacteria may also kill vibrios in infected individuals [38], we do not consider such a scenario in this modelling work. We instead concentrate on the potential reduction of vibrios in the aquatic environment. If the density of the vibrios is reduced, it is the concentration of those remaining in the aquatic environment that can aggravate the spread of the epidemic. In essence, reduction of the concentration of virulent vibrios in the aquatic environment reduces the likelihood of consuming an infectious dose if contaminated water is consumed. Das and Mukherjee [37] considered a four equations model for cholera transmission in the presence of *V. cholerae* as well as the bacteriophage that acts as a predator for the vibrios. The population of the lytic phage was considered be solely dependent on the vibrios for survival and no alternative food sources. Replenishment of the *V. cholerae* was considered to follow Malthusian growth and with additional shedding from the infected human population. The assumption of Malthusian growth may only be valid at lower concentration of the pathogen when the nutrients are in abundance and there is no intra specific competition. The term describing predation interaction was based on mass action or the typical Holling type I response functional. Such a response function has some shortfalls and may not be realistic as will be indicated in the model development.

6.2 Model development

We construct a mathematical model for the dynamics of bacteriophage and *V. cholerae* population. We assume that the organisms are not uniformly distributed in the aquatic environment. This is due to uneven distribution of nutrients, water currents and the interaction with preying phage. The interaction of the phage and bacteria results in movements of both

organisms which we ought not ignore. This necessitate analysis of the dynamics of the two interacting populations assuming a spatially heterogeneous environment.

Although the study by Capasso and Paveri-Fontana [41] indicates that vibrios can not sustain their concentration in the aquatic environment, some recent studies indicate the sustainability possibility. In the study by Vital *et al.* [54], *V. cholerae* subtype O1 Ogawa El tor was shown to grow extensively in different kinds of fresh water. In the study a low density innoculum of $(5 \times 10^3 \text{cells ml}^{-1})$ was observed to multiply upto a density of $(1.55 \times 10^6 \text{cells ml}^{-1})$. We note that this extensive growth was observed in river, lake as well as effluent waste water from a treatment plant.

Faruque *et al.* [94] suggested that, in the aquatic reservoir, the bacteriophage and the bacteria (pathogen) reproduce and interact. In the modelling work involving the human population, the vibrios and the bacteriophage, Jensen et al. [38], proposed that vibrios grow logistically in the aquatic environment, whereas Das and Mukherjee [37] considered Malthusian growth. in both the aforementioned models, the interaction of the phage and vibrios is assumed to modulate concentration of vibrios and consequently the severity of cholera.

6.3 Biological control model

With regard to biocontrol as a model of time-and space continuous systems of two interacting species, the general model has been proposed in [95, 96, 97] among others. This is given by the following general coupled pair of reaction-diffusion equations,

$$\begin{aligned} \frac{\partial V(x,t)}{\partial t} &= D_1 \nabla^2 V + \phi(V,B), \\ \frac{\partial B(x,t)}{\partial t} &= D_2 \nabla^2 B + \psi(V,B). \end{aligned} \tag{6.1}$$

x is the co-ordinate that measures the position in a linear habitat, t stands for time [98]. We note also that the system (6.1) can be analysed in a 1D, 2D and 3D space, but the higher the space dimension the more intractable the analysis is.

Therefore, the equations give the evolution of the two co-existing sub-populations in time and space. The terms $V(x,t)$ and $B(x,t)$ are the densities of the population of vibrios and bacteriophage species respectively. D_1 and D_2 are diffusion coefficients of the pathogen and bacteriophage. These diffusion coefficients are taken to be constant. However, we acknowledge the expected irregularities in real life cases where these diffusion coefficients may vary [98] due to vibrio and phage population densities, alternative food resources available and

the excretion of anti bacterial agents by the vibrios. One of the major challenges of a reaction-diffusion biocontrol system is determining the suitable functions for $\phi(V,B)$ and $\psi(V,B)$ which best describe the interaction yet solvable. $\phi(V,B)$ is a reaction term that describes the population growth dynamics of the vibrios as well as their interaction with bacteriophage. $\psi(V,B)$ is a reaction term that describes the dynamics of the growth of the population of the bacteriophage. The term accounts for the development of bacteriophage which is influenced by their consumption of the vibrios. It is under the assumption that; consumption vibrio contributes positively to the growth of the bacteriophage population at some specific rate. It also describes the natural mortality of the bacteriophage. Some of the functional responses use in such predator-prey systems include; Holling types I, II and III [99, 100] which are respectively given by

$$\phi(V,B) = AVB, \quad \phi(V,B) = A\frac{VB}{H+V} \quad \text{and} \quad \phi(V,B) = A\frac{V^2B}{H^2+V^2}.$$

In the last two expressions, H is the half-saturation of the density of the prey, and A is the predation rate [52, 95]. In a model for biological control of cholera by Das and Mukherjee [37], the growth rate of the pathogen was assumed to be Malthusian in absence of predation. We note also that Jensen *et al* [38] considered the pathogen growth to be logistic. In both models in [37, 38] the optimal choice for the response function for predation was a Holling type I. This type of functional response is based on two assumptions namely; (1) predation by Bacteriophage increases linearly with vibrio density and (2) the time it takes the phage to handle vibrios is negligible and therefore, there is no interference between the phage's searching for the vibrios and feeding. In our view, this may be an oversimplification of the rather complex interaction in the aquatic environment.

We assume that the population of pathogenic vibrios grows logistically in absence of predatory bacteriophage species. We also account for the population decrease of pathogenic vibrios resulting from predation at a constant rate μ. This constant represents the maximum amount of resource that can be obtained from consuming a prey per unit time. For the population of the phage, given other food sources the phage population is expected to increase following a key assumption that, the bacteriophage have more preference of vibrio as a food source to other available sources in the aquatic habitat. We note that in areas where cholera is endemic, there may be constant shedding of the pathogen into the aquatic environment. We let the pathogen be shed into the aquatic reservoir at a rate Λ. We note that once the vibrios are shed into the aquatic environment through diarrhoea, they multiply rapidly contaminating the water source. We assume that this rapid multiplication of the vibrios follows logistic growth. In an ideal predatory biological control process, we would consider the phage to be

entirely dependent on the pathogen as the food source. This may not be the case since the phage may still live on an alternative food source. We assume that the phage's population increases mainly as a result of predation.

$$\phi(V,B) = \Lambda + r_v V\left(1 - \frac{V}{K_v}\right) - \mu\frac{VB}{V+M}, \tag{6.2a}$$

$$\psi(V,B) = -\delta B + \frac{\mu\xi VB}{V+M}, \tag{6.2b}$$

where μ is also referred to as the catchability coefficient, conversion efficiency or predation coefficient [95], ξ is a parameter that gives the predation benefits ($\mu > \xi$), δ the natural mortality rate of the predators, K_v the carrying capacities of the vibrio population.

The resultant system of partial differential equations is given by

$$\frac{\partial V(x,t)}{\partial t} = D_1\frac{\partial^2 V}{\partial x^2} + \Lambda + r_v V\left(1 - \frac{V}{K_v}\right) - \mu\frac{VB}{V+M}, \tag{6.3a}$$

$$\frac{\partial B(x,t)}{\partial t} = D_2\frac{\partial^2 B}{\partial x^2} - \delta B + \frac{\mu\xi VB}{V+M}. \tag{6.3b}$$

The initial and boundary conditions are such that

$$V = B = 0 \quad \text{on } \partial\Omega\times(0,\infty), \tag{6.4}$$

$$V(x,0) = V_0(x), \;\; B(x,0) = B_0(x), \; x \in \Omega. \tag{6.5}$$

where $\partial\Omega$ is the boundary of the domain Ω.

Note that the system of equations is coupled only by the non-linearities in the functions ϕ and ψ. The two important conditions on ψ and ϕ are such that; for all

$$V, B \geq 0, \;\; \psi(0,B) \geq 0 \;\text{ and }\; \phi(V,0) \geq 0. \tag{6.6}$$

6.4 Model analysis

Before embarking on the combined interaction between two organisms, we study the dynamics of a single species present in the aquatic environment. We propose that growth of population of *V. cholerae* follows logistic growth. The term V^2 describes the limitation in the population size. Considering the single population equation of vibrios, enables us to understand the qualitative behaviour of solutions of the considered reaction-diffusion equation. Suppose the vibrio population grows at a rate r_v, and K_v the carrying capacity of the vibrios in the aquatic environment. If we let the vibrios to move at a rate D_v, then the equation

describing this movement is given by

$$\frac{\partial V(x,t)}{\partial t} = D_v \nabla^2 V + \Lambda + r_v V \left(1 - \frac{V}{K_v}\right). \tag{6.7}$$

The various parameters in the equation are defined as follows; D_v is the diffusivity (L^2T^{-1}), α is the growth rate of the pathogen (T^{-1}), K the carrying capacity (measured as population) and Λ the recruitment rate into the pathogen population (measured as population per unit time). It is often important to reduce the PDE to dimensionless form. See [101, 96] for some examples. Our non-dimensionalisation process requires scaling the different variables as indicated indicated below;

$$\begin{cases} \tau &= r_v t \quad \text{: Scaling time to the pathogen growth rate} \\ z &= x\sqrt{\frac{r_v}{D_v}} \quad \text{: Scalling the distance to diffusion length} \\ \tilde{V} &= \frac{V}{K} \quad \text{: Scalling the population to carrying capacity} \end{cases} \tag{6.8}$$

Using the scaled terms, we have

$$\frac{\partial \tau}{\partial t} = r_v, \quad \frac{\partial z}{\partial x} = \sqrt{\frac{r_v}{D_v}}$$

Then the components of the PDE (6.7) transformed to the rescaled variables are given as

$$\begin{cases} \frac{\partial V}{\partial t} &= \alpha K \frac{\partial \tilde{V}}{\partial \tau}, \\ \frac{\partial V}{\partial x} &= \sqrt{\frac{\alpha}{D}} \frac{\partial \tilde{V}}{\partial z}, . \\ \frac{\partial^2 V}{\partial x^2} &= \frac{\alpha K}{D} \frac{\partial^2 \tilde{V}}{\partial z^2} \end{cases} \tag{6.9}$$

Substituting the necessary terms in (6.9) into equation (6.7) (and dropping the tildes), we obtain the non-dimensional form as

$$\frac{\partial V}{\partial \tau} = \frac{\partial^2 V}{\partial z^2} + \nu + V(1 - V), \tag{6.10}$$

where $\nu = \Lambda / r_v K_v$. Assuming no diffusion occurs (i.e $D_v = 0$) and applying principles of dynamical systems to the resulting ODE, at equilibrium the ODE has only steady state points given by

$$V = \frac{1 \pm \sqrt{1 + 4\nu}}{2}. \tag{6.11}$$

Note that if $\nu = 0$, the equation (6.10) reduces to the typical Fisher-equation with two equilibrium points $V = 0$ and $V = 1$. In the case of equation (6.10) however, there is only the non-trivial equilibrium point (6.11) which is unstable. This stability condition can be

investigated by assuming that the PDE (6.10) admits a travelling wave solution, followed by transforming the PDE into a second order non-linear ODE. The resultant ODE can be reduced to a system of first order ODEs and stability of resultant equilibrium point investigated using eigenvalues from the Jacobian evaluated at the equilibrium point in which case all the eigenvalues are non-negative for all values of Q.

We look for solutions of the form

$$V(x,t) = U(x-ct) = U(s), \;\; s := x - ct.$$

Note that $\frac{ds}{dx} = 1$ and $\frac{ds}{dt} = -c$. Therefore, the components of the partial differential equation (6.10) can be transformed as follow;

$$\frac{\partial V}{\partial x} = \frac{dU}{ds}\cdot\frac{ds}{dx} = \frac{dU}{dx},$$
$$\frac{\partial^2 V}{\partial x^2} = \frac{\partial}{\partial x}\left(\frac{dU}{dx}\right) = \frac{d^2U}{ds^2}\cdot\frac{ds}{dz} = \frac{d^2U}{ds^2},$$

for the partial derivative with respect to space and

$$\frac{\partial V}{\partial t} = \frac{dU}{ds}\cdot\frac{ds}{dt} = -c\frac{dU}{ds},$$

for the partial derivative with respect to time. The resulting second order ODE is given by

$$\frac{d^2U}{ds^2} + c\frac{dU}{ds} + \nu + U\left(1-U\right). \tag{6.12}$$

If we let $W := U'$, the equation (6.12) can be decomposed into a system of first order ODEs such that

$$\begin{cases} U' = W, \\ W' = -\left[cW + \nu + U\left(1-U\right)\right]. \end{cases} \tag{6.13}$$

The steady states of the system are given as $W = 0$, and $U = \frac{1\pm\sqrt{1+4\nu}}{2}$. Since the dynamical system monitors evolution of populations, then the only feasible paired solution is $\left(0, \frac{1+\sqrt{1+4\nu}}{2}\right)$. It is important to note that in absence of additional replenishment of the population (i.e $\nu = 0$), the steady states for the system (6.13) will be the trivial equilibrium and the carrying capacity. These are the typical equilibria for the Fisher equation [98].

The steady state $\left(0, \frac{1+\sqrt{1+4v}}{2}\right)$

Suppose the system is perturbed to start at a new point in the neighbourhood of the equilibrium point

$$(W^*, U^*) := \left(0, \frac{1+\sqrt{1+4v}}{2}\right).$$

We linearise the system (6.13) and evaluate the Jacobian at the steady state (W^*, U^*) to obtain

$$Df(W^*, U^*) = \begin{pmatrix} 0 & 1 \\ -1+2U^* & -c \end{pmatrix}.$$

The resultant eigenvalues are given by

$$\begin{aligned} \lambda_\pm &= \frac{-c \pm \sqrt{c^2 - 4(1-2U^*)}}{2}, \\ &= \frac{-c \pm \sqrt{c^2 + 4\sqrt{1+4v}}}{2}. \end{aligned}$$

Thus, the steady state (W^*, U^*) whenever it exists is unstable. This is not surprising since for the Fisher equation, the non trivial equilibrium is unstable as well.

6.4.1 Non-dimensionalisation of the full systems of equation

To non-dimensionalise the system of equations (6.3), we rescale the values as follows using expressions similar to [101] such that

$$\begin{aligned} &\tau = rt, \;\; z = x\sqrt{\frac{r}{D_1}} \;\; \alpha = \frac{D_2}{D_1}, \;\; \tilde{V} = \frac{V}{K_v}, \;\; Q = \frac{M}{K_v}, \\ &\tilde{B} = B\left(\frac{\mu}{rK_v}\right), \;\; \gamma = \frac{\mu\xi}{r}, \;\; c = \frac{\delta}{r}, \;\; v = \frac{\Lambda}{rK_v}. \end{aligned} \tag{6.14}$$

From the rescaled terms, we have

$$\frac{d\tau}{dt} = r, \quad \frac{dz}{dx} = \sqrt{\frac{r}{D_1}}.$$

The components of the system of partial differential equations are then give as

$$\frac{\partial v}{\partial t} = k\frac{\partial \tilde{V}}{\partial \tau} \cdot \frac{d\tau}{dt} = rk\frac{\partial \tilde{V}}{\partial \tau}$$

The second partial derivative is given by

$$\begin{aligned}\frac{\partial^2 V}{\partial x^2} &= \frac{\partial}{\partial x}\left(k\sqrt{\frac{r}{D_1}}\frac{\partial \tilde{V}}{\partial z}\right)\\ &= k\sqrt{\frac{e}{D_1}}\frac{\partial^2 \tilde{V}}{\partial z^2}\cdot\frac{dz}{dx}\\ &= \frac{rK}{D_1}\frac{\partial^2 \tilde{V}}{\partial z^2}\end{aligned}$$

Following the same principle, the partial derivatives for the second partial differential equation are given by

$$\begin{cases}\frac{\partial B}{\partial t} &= \frac{r^2 K}{\mu}\frac{\partial \tilde{B}}{\partial \tau}, \text{ and}\\ \frac{\partial^2 B}{\partial x^2} &= \frac{r^2 K}{\mu D_1}\frac{\partial^2 \tilde{B}}{\partial z^2}.\end{cases} \tag{6.15}$$

We now substitute the rescaled terms from equation (6.14) and the partial derivative components (6.15) into the system of equations (6.3), replace τ with t, z with x and also drop the tildes, to obtain

$$\begin{aligned}\frac{\partial V}{\partial t} &= \frac{\partial^2 V}{\partial x^2} + v + V(1-V) - \frac{BV}{V+Q},\\ \frac{\partial B}{\partial t} &= \alpha\frac{\partial^2 B}{\partial x^2} - cB + \frac{\gamma BV}{V+Q}.\end{aligned} \tag{6.16}$$

Similar to the system of equations (6.3), the initial and boundary conditions for the non-dimensionalised system are such that

$$V = B = 0 \quad \text{on } \partial\Omega\times(0,\infty), \tag{6.17}$$

$$V(x,0) = V_0, \;\; B(x,0) = B_0, \text{ for } \; 0 < x < 1. \tag{6.18}$$

From equation (6.16), if the maximum obtainable resources from the prey consumption are a unit, then the bacteriophage density is produced by converting the *Vibrio cholerae* to phage biomass at a conversion factor γ.

6.4.2 Well-posedness of the model

We consider well-posedness of the model (6.3), in the sense observed by the French mathematician Jacques Salomon Hadamard (1868-1963). According to Hadamard [102], a model describing a physical phenomenon is said to be well posed if the solution; exists, is unique and continuously depends on the initial data. In this case, if one or more of the conditions is violated, then the problem is said to be ill-posed [103]. This further implies that if the prob-

lem is well posed, then the behaviour of the solution remains relatively unchanged when there is a small perturbation in the initial conditions.

Definition 6.4.1 (Invariant region [101]). *The invariant region of a system of partial differential equations (6.3), is a closed subset $\mathbb{D}$ of the phase-space $\mathbb{R}^2$ such that for any initial population $(V_0(x), B_0(x))$ that lies in $\mathbb{D}$ for all $x \in \Omega$, then the solution $(V(x,t), B(x,t))$ lies in $\mathbb{D}$ for all x and for all $t > 0$ for which the solution exists.*

6.4.3 Non-negativity of the solution

When any of the species grows to the corresponding carrying capacity, then it implies that the other has been completely out competed.

Lemma 6.4.1. *Let us consider $V_0, B_0 \in L^\infty(\Omega)$ and that*

$$\psi(x,t,V,B), \phi(x,t,V,B) : \Omega \times [0,\infty) \times \mathbb{R} \times \mathbb{R} \to \mathbb{R}$$

are measurable, then the response functions ψ and ϕ are Liptschz continuous.

Proof. Let V,$\hat{V}$,B and $\hat{B} \in \mathbb{D}$ be such that for all $x \in \Omega$ and $t \in [0,t)$,

$$0 < |V|, |\hat{V}|, |A|, |\hat{B}| < \rho,$$

then we want to show that

$$|\psi(x,t,V,B) - \psi(x,t,\hat{V},\hat{B})| + |\phi(x,t,V,B) - \phi(x,t,\hat{V},\hat{B})| \leq C(\rho)\left(|V-\hat{V}| + |B-\hat{B}|\right)$$

Given our functional responses ψ and ϕ, each of the species population is bounded by the corresponding carrying capacity. Therefore, for all x and $t > 0$, we have that $0 \leq V(x,t) < K_v$ and $0 \leq B(x,t) < K_b$ □

6.4.4 Linear analysis of a spatially homogeneous model

It can be observed that the model (6.16) in absence of diffusion reduces to a system of first order coupled ordinary differential equations;

$$\begin{aligned} \frac{dV}{dt} &= v + V(1-V) - \frac{BV}{V+Q}, \\ \frac{dB}{dt} &= -cB + \frac{\gamma BV}{V+Q}. \end{aligned} \tag{6.19}$$

The system of equations (6.19) can be analysed in presence or absence of constant replenishment of the vibrio concentration in the aquatic environment from infected individuals. In presence of constant vibrio shedding in the environment (i.e, $v \neq 0$), the system (6.19) has two equilibrium points.

1. The equilibrium point $\mathbb{E}^0_{bc}$ given by

$$\mathbb{E}^0_{bc} = \left(\frac{1+\sqrt{1+4v}}{2}, 0 \right). \tag{6.20}$$

Note that for the case when there is no shedding of the pathogen into the aquatic environment, $v = 0$, the equilibrium point $\mathbb{E}^0_{bc}$ reduces to $(1, 0)$ and the system would have a trivial equilibrium point $(0, 0)$ as indicated in [104]. Therefore, not considering the shedding of the pathogen into the aquatic environment leads to underestimation of the pathogen concentration.

Stability of the steady state $\mathbb{E}^0_{bc}$

To determined the local stability of the $\mathbb{E}^0_{bc}$, we linearise the system of equations (6.19) at the equilibrium point. The Jacobian of system (6.19) is given by

$$\mathcal{J}(E) = \begin{pmatrix} 1 - 2V - \frac{BQ}{(Q+V)^2} & -\frac{V}{V+Q} \\ \frac{\gamma BQ}{(V+Q)^2} & -c + \frac{\gamma V}{V+Q} \end{pmatrix}. \tag{6.21}$$

At the equilibrium point $\mathbb{E}^0_{bc}$, the Jacobian is given by

$$\mathcal{J}(\mathbb{E}^0_{bc}) = \begin{pmatrix} 1 - 2V^* & -\frac{QV^*}{V^*+Q} \\ 0 & -c + \frac{\gamma V^*}{V^*+Q} \end{pmatrix}. \tag{6.22}$$

The eigenvalues corresponding the Jacobian (6.22) are

$$\lambda_1 = 1 - 2V^* \quad \text{and} \quad \lambda_2 = -c + \frac{\gamma V^*}{V^* + Q}.$$

We note that the following conditions hold for the vibrio concentration;

$$0 \leq \frac{V}{K_v} \leq 1 \text{ and } 0 \leq \frac{V}{M+Q} < 1. \tag{6.23}$$

Considering the lower limits of (6.23) (a case when the concentration of the pathogen is very low), we obtain

$$\lambda_1 = 1 < 0 \text{ and } \lambda_2 = -c < 0.$$

Therefore, the equilibrium point $\mathbb{E}^0_{bc}$, is a saddle point whose stable manifold is in the V-direction and the unstable manifold is locally in the B-direction.

On the contrary, if we apply the upper bound of (6.23), we obtain

$$\lambda_1 = -1 < 0 \text{ and } \lambda_2 = -c + \gamma > 0, \ c < \gamma.$$

This implies that the equilibrium point $\mathbb{E}^0_{bc}$, is still a saddle point whose stable manifold is in the B-direction and the unstable manifold is locally in the V-direction if $c < \gamma$. Otherwise, the equilibrium point will be a stable point.

2. The equilibrium point $\mathbb{E}^1_{bc} = (V^{**}, B^{**})$ where

$$V^{**} = \frac{cQ}{\gamma - c}, \text{ where } \gamma > c,$$
$$B^{**} = \frac{\gamma}{c}\left[v + \frac{cQ}{\gamma - c}\left(1 - \frac{cQ}{\gamma - c}\right)\right].$$

Stability of the steady state $\mathbb{E}^1_{bc}$.

To show local stability of the equilibrium $\mathbb{E}^1_{bc}$, we linearise the non-diffusive system (6.19) at the equilibrium point to obtain the Jacobian

$$\mathcal{J}(\mathbb{E}^1_{bc}) = \begin{pmatrix} 1 - 2V^{**} - \frac{B^{**}Q}{(Q+V^{**})^2} & -\frac{V^{**}}{V^{**}+Q} \\ \frac{\gamma B^{**}Q}{(V^{**}+Q)^2} & -c + \frac{\gamma V^{**}}{V^{**}+Q} \end{pmatrix}. \tag{6.24}$$

To determine stability of $\mathbb{E}^1_{bc}$, it is enough to determine the signs of the eigenvalues of $\mathcal{J}(\mathbb{E}^1_{bc})$. We determine the sign of determinant and that of the trace. The determinant of the Jacobian is given by

$$\det \mathcal{J}(\mathbb{E}^1_{bc}) = \left(1 - 2V^{**} - \frac{B^{**}Q}{(Q+V^{**})^2}\right)\left(-c + \frac{\gamma V^{**}}{V^{**}+Q}\right) + \frac{\gamma Q B^{**} V^{**}}{(V^{**}+Q)^3}.$$

We note that, at the steady state, when $B^{**} \neq 0$, then $-c + \frac{\gamma V^{**}}{V^{**}+Q} = 0$. Therefore,

$$\det \mathcal{J}(\mathbb{E}^1_{bc}) = \frac{\gamma Q B^{**} V^{**}}{(V^{**}+Q)^3} > 0.$$

Since $\det \mathcal{J}(\mathbb{E}^1_{bc}) > 0$, the resulting roots are either both positive or both negative.

The trace of the Jacobian $\mathcal{J}(\mathbb{E}^1_{bc})$ is given by

$$\begin{aligned} tr(\mathcal{J}(\mathbb{E}^1_{bc})) &= 1 - 2V^{**} - \frac{B^{**}Q}{(Q+V^{**})^2} + \left(-c + \frac{\gamma V^{**}}{V^{**}+Q}\right), \\ &= 1 - 2V^{**} - \frac{B^{**}Q}{(Q+V^{**})^2}. \end{aligned} \tag{6.25}$$

Assuming at the endemic equilibrium $\mathbb{E}^1_{bc}$, $V/K_v \approx 1$, then

$$tr(\mathcal{J}(\mathbb{E}^1_{bc})) = -\left(1 + \frac{B^{**}Q}{(Q+V^{**})^2}\right).$$

Given that $\det \mathbb{J} > 0$ and $tr(\mathcal{J}(\mathbb{E}^1_{bc})) < 0$ then the eigenvalues of the Jacobian $\mathcal{J}$ are all negative. Hence, the fixed point $\mathbb{E}^1_{bc}$ is stable.

Before embarking on the numerical results of the heterogeneous model, we give the numerical results of the homogeneous non-dimensionalised model.

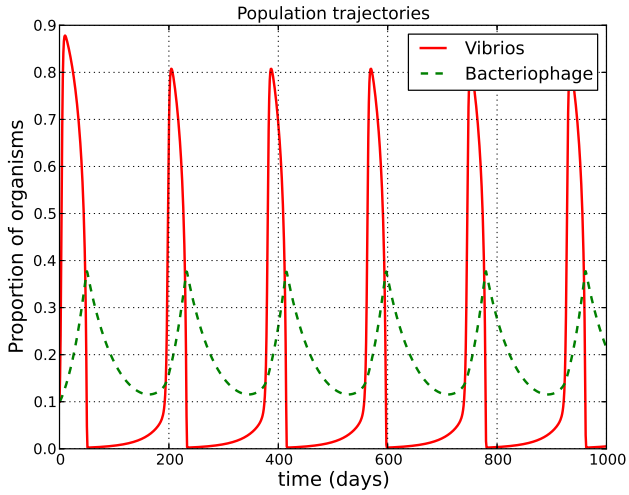

Figure 6.1: Interaction of *V. cholerae* and bacteriophage obtained for parameter values; $\gamma = 0.0488$, $c = 0.0182$, $\nu = 0.015$, $Q = 0.05$, $V_0 = 0.1$, $B_0 = 0.05$

The population of vibrios is predicted to grow explosively due to anticipated availability of resources. Although the carrying capacity is approximately 1, the vibrio concentration may hardly reach the carrying capacity as presence of predatory bacteriophage regulates their population, Figure 6.1. Predation from bacteriophage reduces the vibrios until they reach negligible concentrations. On the other hand, the bacteriophage concentration in the aquatic environment increases until there is not enough vibrios as their food supply. The bacteriophage concentration gradually decreases due do lack of resources and only increases again when there is enough vibrios to prey on. The trend of a typical predator-prey relation is observed throughout. The interaction between vibrios and bacteriophage is antagonistic (see Figure 6.2) in nature. This kind of relation was predicted in the models by Jensen *et al.* [38] and Das and Mukherjee [37].

Figure 6.2: Phase portrait of *V. cholerae* and bacteriophage obtained for parameter values: $\gamma = 0.0488$, $c = 0.0182$, $\nu = 0.015$, $Q = 0.05$, $V_0 = 0.1$, $B_0 = 0.05$

We note here also that the model is highly sensitive to changes in parameters most especially; ν which is related to shedding of vibrios from the human population. With increased shedding of vibrios, the vibrio population would increase uncontrolled and this increases the likelihood of consuming an infectious dose of vibrios from a contaminated environment. At the same time, the parameter related to the predation rate ought to be high, together with lower depletion of the bacteriophage population if the vibrio population is to be easily contained. For the selected set of parameter values, the phase portrait, Figure 6.2 remains as unchanged even when the simulation is run over a longer period of time. This kind of scenario predicts a stable limit cycle in the model for the selected set of parameters.

6.5 Numerical simulations of the heterogeneous model

To solve the system with diffusion numerically, we ought to discretise the system of equations. The discretisation can be done using finite element method or finite difference discretisation schemes, Crank Nicholson scheme among others. We note that in the dynamics of the model system, only solutions in the positive quadrant $V \geq 0$, $B \geq 0$ are biologically feasible since the model monitors organisms. Although a variety of discretisation schemes exist, we use the Crank-Nicholson scheme for our system of equations. The major motivation for using the Crank Nicholson scheme is that, it is unconditionally stable. This discretisation is implicit in time and the diffusion term is given as the average of finite difference of the corresponding component at the current time and one time step ahead. With the Crank-

Nicholson method, we transform the components of the PDE for the vibrio population as follows

$$\frac{\partial V}{\partial t} = \frac{V_i^{j+1} - V_i^j}{\Delta t},$$
$$\frac{\partial^2 V}{\partial x^2} = \frac{1}{2(\Delta x)^2}\left[\left(V_{i+1}^{j+1} - 2V_j^{j+1} + V_{j-1}^{j+1}\right) + \left(V_{i+1}^j - 2V_i^j + V_{i-1}^j\right)\right].$$

The term Δx is the width of the grid, i.e the distance between any two adjacent spatial discretisation points. Δt is the distance between any two consecutive temporal discretisation points.

The other terms can be approximated as follow;

$$\begin{cases} V &= \frac{1}{2}\left(V_i^{j+1} + V_i^j\right), \\ B &= \frac{1}{2}\left(B_i^{j+1} + B_i^j\right). \end{cases}$$

The subscript i represents the space component and the superscript j time. Similar definitions are used for the bacteriophage populations. The Crank-Nicholson scheme is sought here since it is unconditionally stable.

$$\frac{V_i^{j+1} - V_i^j}{\Delta t} = \frac{1}{2(\Delta x)^2}\left[V_{i+1}^{j+1} - 2V_i^{j+1} + V_{i-1}^{j+1} + V_{i+1}^j - 2V_i^j + V_{i-1}^j\right] + \nu + V_i^j\left(1 - V_i^j\right) - \frac{V_i^j B_i^j}{V_i^j + Q}.$$

If we let $R_1 = \frac{\Delta t}{2(\Delta x)^2}$ and we transfer all terms forward in time to the left side of the expression, we obtain

$$\begin{aligned} -R_1 V_{i-1}^{j+1} + (1 + 2R_1)V_i^{j+1} - R_1 V_{i+1}^{j+1} &= R_1 V_{i-1}^j + \nu\Delta t \\ &+ \left[(1 - 2R_1) + \left((1 - V_i^j) - \frac{B_i^j}{V_i^j + Q}\right)\Delta t\right] V_i^j + R_1 V_{i+1}^j. \end{aligned} \quad (6.26)$$

Applying the boundary conditions, we note that

$$\frac{\partial V(0,t)}{\partial x} = \frac{\partial V(1,t)}{\partial x} = 0,$$

imply that, at the left boundary

$$\frac{V_i - V_{i-1}}{\Delta x} = 0 \quad \Longrightarrow \quad V_{i-1} = V_i,$$

and

$$\frac{V_{i+1} - V_i}{\Delta x} = 0 \quad \Longrightarrow \quad V_{i+1} = V_i,$$

on the right boundary. Applying the boundary conditions and recursively the points on the stencil, the resulting system of equations can be written as

$$A_V V_i^{j+1} = bV_i^j + f_{V_{\text{vec}}}, \text{ for } i = 1, 2, \cdots, n. \tag{6.27}$$

where A_V and b_V are tridiagonal matrices and $f_{B_{\text{vec}}}$ is a approximating the coupling terms for the dynamics of vibrio population. The left side of the equation (6.27) is given as

$$A_V V_i^{j+1} = \begin{pmatrix} (1+R_1) & -R_1 & 0 & 0 & \cdots & 0 & 0 \\ -R_1 & (1+2R_1) & -R_1 & 0 & \cdots & 0 & 0 \\ 0 & -R_1 & (2R_1+1) & -R_1 & \cdots & 0 & 0 \\ \vdots & \vdots & \vdots & \vdots & \vdots & \vdots & \vdots \\ 0 & 0 & 0 & 0 & \cdots & -R_1 & 0 \\ 0 & 0 & 0 & 0 & \cdots & (2R_1+1) & -R_1 \\ 0 & 0 & 0 & 0 & \cdots & -R_1 & (R_1+1) \end{pmatrix} \begin{pmatrix} V_0^{j+1} \\ V_1^{j+1} \\ V_2^{j+1} \\ \vdots \\ V_{n-2}^{j+1} \\ V_{n-1}^{j+1} \\ V_n^{j+1} \end{pmatrix}.$$

The terms on the right side of the equation(6.27) are given as

$$bV_i^j = \begin{pmatrix} (1-R_1) & R_1 & 0 & 0 & \cdots & 0 & 0 \\ -R_1 & (1-2R_1) & R_1 & 0 & \cdots & 0 & 0 \\ 0 & R_1 & (1-2R_1) & -R_1 & \cdots & 0 & 0 \\ \vdots & \vdots & \vdots & \vdots & \vdots & \vdots & \vdots \\ 0 & 0 & 0 & 0 & \cdots & R_1 & 0 \\ 0 & 0 & 0 & 0 & \cdots & (1-2R_1) & -R_1 \\ 0 & 0 & 0 & 0 & \cdots & R_1 & (1-R_1) \end{pmatrix} \begin{pmatrix} V_0^j \\ V_1^j \\ V_2^j \\ \vdots \\ V_{n-2}^j \\ V_{n-1}^j \\ V_n^j \end{pmatrix}.$$

and

$$f_{V_{\text{vec}}} = \begin{pmatrix} (\Delta t) V_0^j \left((1 - V_0^j) - \frac{B_0^j}{V_0^j + Q} \right) \\ (\Delta t) V_1^j \left((1 - V_1^j) - \frac{B_1^j}{V_1^j + Q} \right) \\ \vdots \\ (\Delta t) V_{n-1}^j \left((1 - V_{n-1}^j) - \frac{B_{n-1}^j}{V_{n-1}^j + Q} \right) \\ (\Delta t) V_n^j \left((1 - V_n^j) - \frac{B_n^j}{V_n^j + Q} \right) \end{pmatrix}.$$

We now apply the Crack-Nicholson scheme to the equation describing the evolution of the

bacteriophage to obtain

$$\frac{B_i^{j+1}-B_i^j}{\Delta t}=\frac{\alpha}{2(\Delta x)^2}\left[B_{i+1}^{j+1}-2B_i^{j+1}+B_{i-1}^{j+1}+B_{i+1}^j-2B_i^j+B_{i-1}^j\right]-cB_i^j+\frac{\gamma B_i^j V_i^j}{V_i^j+Q}. \tag{6.28}$$

We let $R_2=\frac{\alpha(\Delta t)}{2(\Delta x)^2}$ and transfer the terms with superscript $(j+1)$ to the left side of the equation obtaining

$$-R_2B_{i-1}^{j+1}+(1+R_2)B_i^{j+1}-R_2B_{i+1}^{j+1}=R_2B_{i-1}^j+(1-2R_2)B_i^j-c(\Delta t)B_i^j+\frac{(\Delta)t\gamma B_i^j V_i^j}{V_i^j+Q}+R_2B_{i+1}^j.$$

We now apply boundary conditions such that

$$\frac{\partial B(0,t)}{\partial x}=\frac{\partial B(1,t)}{\partial x}=0,$$

which implies that, at the left boundary

$$\frac{B_i-B_{i-1}}{\Delta x}=0 \quad\Longrightarrow\quad B_{i-1}=B_i,$$

and

$$\frac{B_{i+1}-B_i}{\Delta x}=0 \quad\Longrightarrow\quad B_{i+1}=B_i,$$

on the right boundary. Applying the boundary conditions and recursively the points on the stencil, the equation (6.26) results into a system of equations given as

$$A_BB_i^{j+1}=bB_i^j+g_{B_{\text{vec}}},\ \text{ for }\ i=1,2,\cdots,n. \tag{6.29}$$

where A_B and b_B are tridiagonal matrices and $g_{B_{\text{vec}}}$ is a approximating the coupling terms. The left side of equation (6.29) is given by

$$A_BB_i^{j+1}=\begin{pmatrix}(1+R_2)&-R_2&0&0&\cdots&0&0\\-R_2&(1+2R_2)&-R_2&0&\cdots&0&0\\0&-R_2&(2R_2+1)&-R_2&\cdots&0&0\\\vdots&\vdots&\vdots&\vdots&\vdots&\vdots&\vdots\\0&0&0&0&\cdots&-R_2&0\\0&0&0&0&\cdots&(2R_2+1)&-R_2\\0&0&0&0&\cdots&-R_2&(R_2+1)\end{pmatrix}\begin{pmatrix}B_0^{j+1}\\B_1^{j+1}\\B_2^{j+1}\\\vdots\\B_{n-2}^{j+1}\\B_{n-1}^{j+1}\\B_n^{j+1}\end{pmatrix}.$$

And the terms on the right side given by

$$bB_i^j = \begin{pmatrix} (1-R_2) & R_2 & 0 & 0 & \cdots & 0 & 0 \\ R_2 & (1-2R_2) & R_2 & 0 & \cdots & 0 & 0 \\ 0 & R_2 & (1-2R_2) & R_2 & \cdots & 0 & 0 \\ \vdots & \vdots & \vdots & \vdots & \vdots & \vdots & \vdots \\ 0 & 0 & 0 & 0 & \cdots & R_2 & 0 \\ 0 & 0 & 0 & 0 & \cdots & (1-2R2) & R_2 \\ 0 & 0 & 0 & 0 & \cdots & R_2 & (1-R_1) \end{pmatrix} \begin{pmatrix} B_0^j \\ B_1^j \\ B_2^j \\ \vdots \\ B_{n-2}^j \\ B_{n-1}^j \\ B_n^j \end{pmatrix}.$$

and

$$g_{B_{\text{vec}}} = \begin{pmatrix} (\Delta t)B_0^j\left(-c + \frac{\gamma V_0^j}{V_0^j+Q}\right) \\ (\Delta t)B_1^j\left(-c + \frac{\gamma V_1^j}{V_1^j+Q}\right) \\ \vdots \\ (\Delta t)B_{n-1}^j\left(-c + \frac{\gamma V_{n-1}^j}{V_{n-1}^j+Q}\right) \\ (\Delta t)B_n^j\left(-c + \frac{\gamma V_n^j}{V_n^j+Q}\right) \end{pmatrix}.$$

6.5.1 Numerical simulations

The numerical simulation of the model is carried out using python-scipy. For a given set of initial conditions we simulate the systems of equations (6.27) and (6.29) and obtain steady state solutions of the simulation. The spatial dimension is set on a range of $0-1$ where the limits indicate the hostile boundaries of the aquatic reservoir. The spatial dimension is subdivided into 100 partitions. The temporal dimension is set from $0-100$ with approximately 1000 partitions. We set the initial proportions of the bacteriophage and vibrios in a ratio of $1:2$. The simulation is done using a linear systems solver in *python-scipy* as indicated below.

```
V_new = numpy.linalg.solve(A_V, b_V.dot(V) + f_vec(V,B))
B_new = numpy.linalg.solve(A_B, b_B.dot(B) + g_vec(V,B))
```

The output of the simulation is put in a 100×1000 multidimensional space-time array. The outputs are similar at each position but differ from one time step to another.

Case with persistent oscillations

The simulation is run and steady state proportions are obtained. The initial conditions for all the simulations are in concentrations of bacteriophage:Vibrios as 0.05 : 0.1. Figure 6.3 shows the initial concentration set for the two organisms.

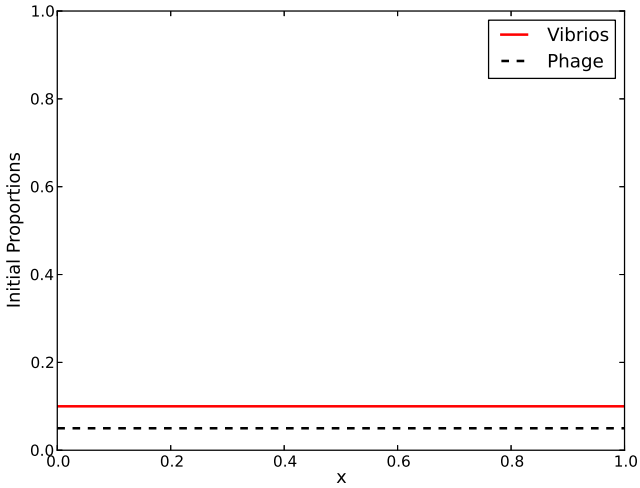

Figure 6.3: Initial conditions vibrio and bacteriophage proportions

In the model simulations, we observe essential features of the oscillatory behaviour of a predator-prey system, see Figures 6.4(a) and 6.4(b). The change in the populations of the vibrios is antagonistic to that of bacteriophage. The cycles of the antagonistic fluctuation in the population for the two organisms are at regular intervals of approximately 180 time points. This is approximated to about 6 months. A similar time scenario is observed in the case when homogeneity is assumed, Figure 6.1.

Since the data output is a multidimensional dataset, it is plausible to visualise such data using heat plots. In the heat plots, clusters of rows with similar proportions are displayed on the plot with similar colours with high values being dark and lower values represented with brighter colours. In the obtained heat map, the lowest proportion of the vibrios and bacteriophage is set to dark blue in accordance with the default gradient of colours for the heat map, see Figure 6.6(a). The bright yellow/brown colour with differing intensity correspond to the highest values. The intensity of the colour map gradually reduces to a dark blue colour which corresponds to the lowest value of the vibrio proportion. The colour bands follow the oscillatory behaviour exhibited in the model output. The time difference between the colour bands an estimate of about 180 days. This would be synonymous with the biannual occurrence the infection. Similarly, in the heat plot for bacteriophage proportion, Figure 6.6(b),

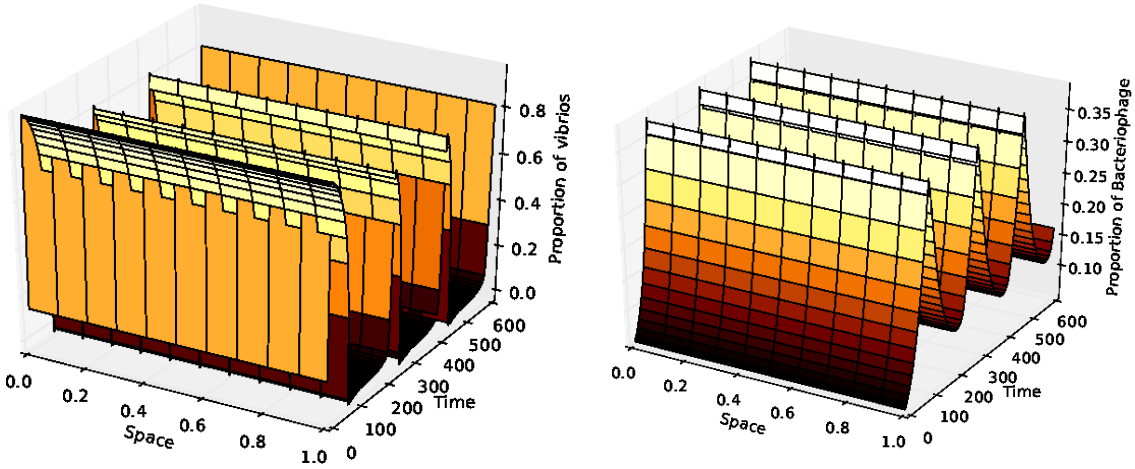

Figure 6.4: 3D display of *V. cholerae* and bacteriophage proportions in a heterogeneous environment. Parameter values used are $\gamma = 0.0488$, $c = 0.0182$, $\nu = 0.015$, $Q = 0.05$, $V_0 = 0.1$, $B_0 = 0.05$, $\alpha = 1.8$

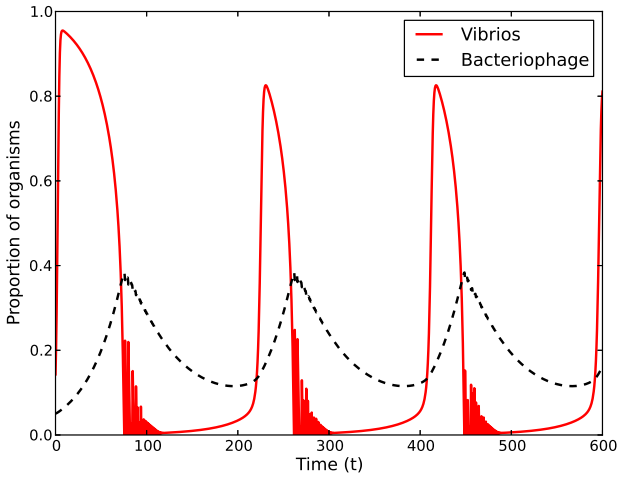

Figure 6.5: Temporal evolution of vibrio and bacteriophage proportions. The parameter values used are: $\gamma = 0.0488$, $c = 0.0182$, $\nu = 0.015$, $Q = 0.05$, $V_0 = 0.1$, $B_0 = 0.05$, $\alpha = 1.8$

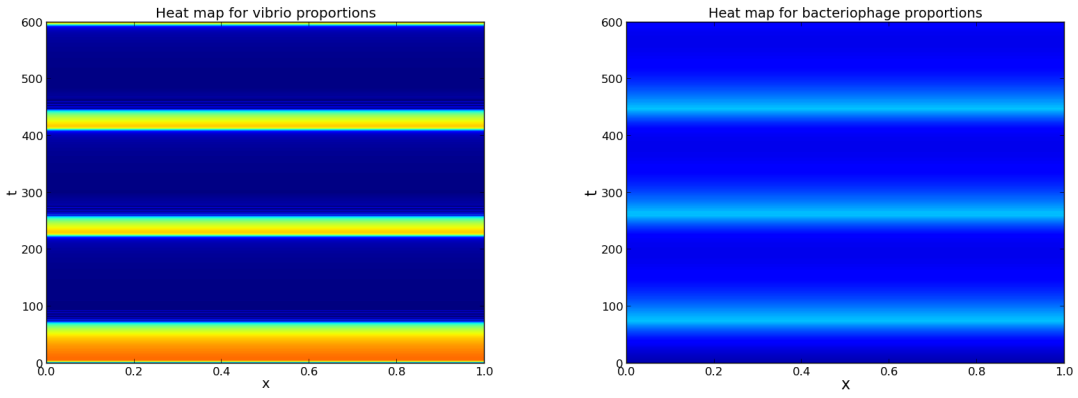

Figure 6.6: Heat plots of proportions vibrios and bacteriophage proportions

the lowest values of the bacteriophage proportion as displayed with a dark blue colour. The colour intensity gradually reduces to light blue which represents the highest value of the bacteriophage proportion.

With respect to biological control of the infection, this scenario would not be effective. The infection would keep recurring due to increased likelihood of consuming an infectious dose of the pathogen at high concentrations of the vibrios in the environment. This may occur at regular intervals of about 6 months periods as observed in the Figures 6.1 and 6.5.

Case with potential control of the vibrios

The numerical results in this subsection as obtained modify some parameter values as will be indicated in the figure captions contrary the figures in the previous subsection. The change in the parameter value the intuitive view that is if the vibrio concentration is to be contained by using the bacteriophage, the following cases ought to be in place:

- The bacteriophage should be more effective and efficient in clearing the vibrios hence a high predation rate.
- The bacteriophage should have a high survival time in the aquatic environment to increase the predatory rate per bacteriophage in clearing the pathogens.
- Efforts should be in place to reduce the replenishment of vibrio concentrations into the aquatic environment from external sources.

In our obtained results with the conditions above implemented, we observe that, although initially the proportional of vibrios is two folds higher than that of the bacteriophage, predatory interaction considerably depletes the concentration of vibrios. The resulting proportions indicate a high concentration of bacteriophage in the environment and a negligible concentration of the vibrios, see Figures 6.8 and 6.9 .

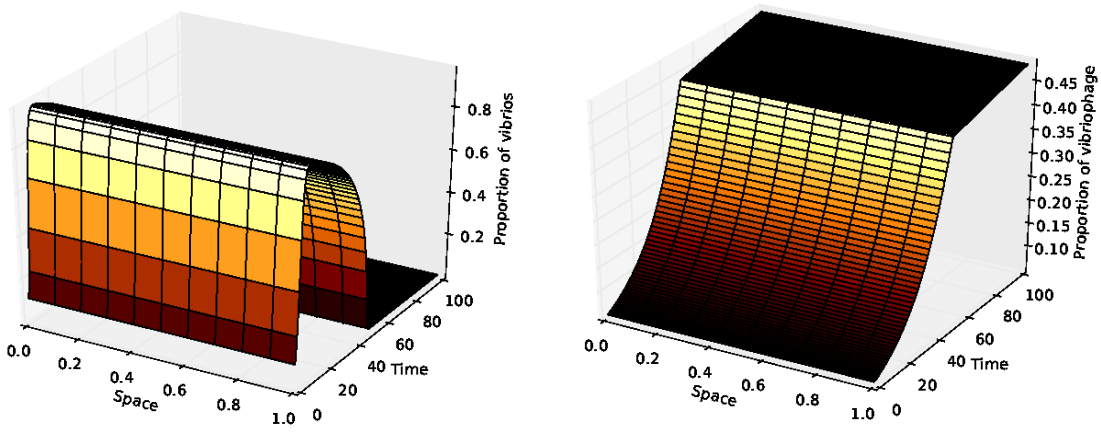

Figure 6.7: Space-time display of vibrio and phage proportions in space and time for parameter values: $\gamma = 0.05$, $c = 0.018$, $\nu = 0.03$, $Q = 0.05$, $V_0 = 0.1$, $B_0 = 0.05$, $\alpha = 1.8$

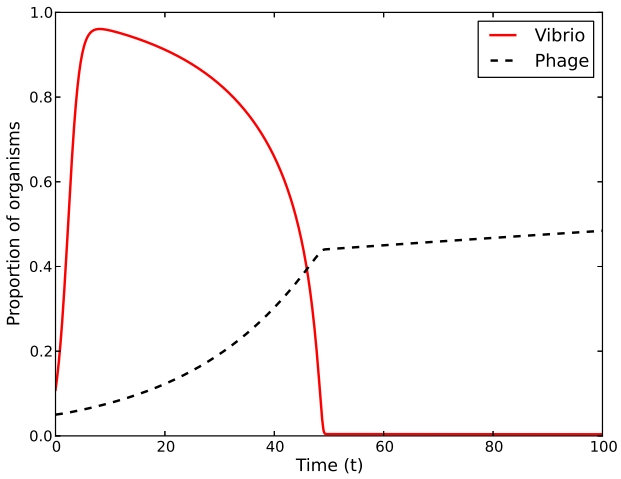

Figure 6.8: Evolution of vibrio and bacteriophage proportions with time: $\gamma = 0.05$, $c = 0.018$, $\nu = 0.03$, $Q = 0.05$, $V_0 = 0.1$, $B_0 = 0.05$, $\alpha = 1.8$

Similar to the previous subsection, the multidimensional dataset can be visualised using heat plots. In the heat plot for the vibrios, the lowest proportion of the vibrios to dark blue in accordance with the default gradient of colours for the heat map, see Figure 6.9(a). The

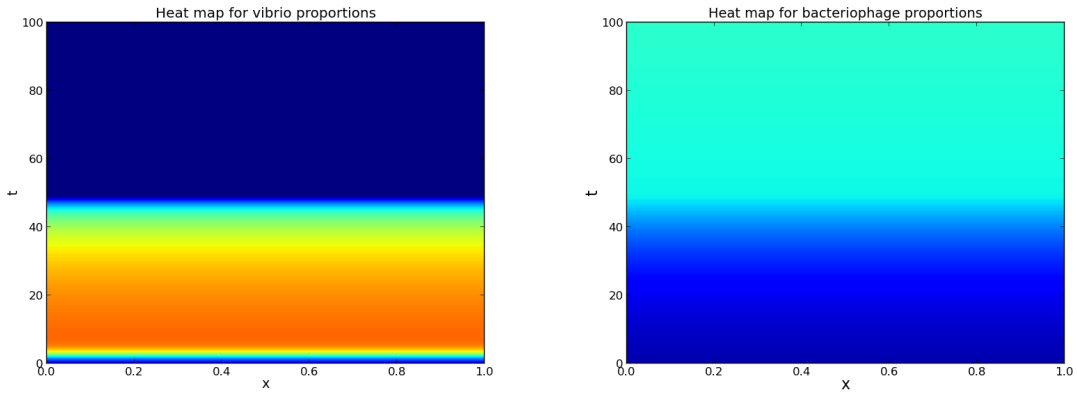

Figure 6.9: Heat plots of proportions vibrios and bacteriophage proportions: $\gamma = 0.05$, $c = 0.018$, $\nu = 0.03$, $Q = 0.05$, $V_0 = 0.1$, $B_0 = 0.05$, $\alpha = 1.8$

bright yellow/brown colour with differing intensity correspond to the highest values. The intensity of the colour map reduces to a dark blue colour which corresponds to the lowest value of the vibrio proportion. The sharp change of the colour bands indicates an explosive increase or drop on the vibrio concentrations in presence of the bacteriophage. A rapid increase in vibrio population was previously observed in the study be Vital *et al.* [54], on *V. cholerae* subtype O1 Ogawa El tor.

In the heat plot for bacteriophage proportion, Figure 6.9(b), the lowest values of the bacteriophage proportion are also displayed with a dark blue colour. The highest values are displayed with a hight blue colour. The colour intensity gradually reduces dark blue to light blue which indicating a gentle increase in bacteriophage concentrations.

6.6 Conclusion

In this chapter, two scenarios of the interaction between vibrios and bacteriophage have been considered. Firstly, the typical oscillatory predator-prey system which depicts the antagonistic interaction between the vibrios and the bacteriophage. Such an interaction does not result into containment of infection. Secondly, a case with a more effective bacteriophage that results in containing the vibrio concentration. The steady state proportions indicate a negligible concentration of vibrios in the aquatic reservoir. If this is successfully achieved, it considerably reduces the likelihood of consuming an infectious dose of vibrios even if contaminated water is consumed.

However, the numerical results still indicated a persistent high concentration of the bacterio-

phage even when the *V. cholerae* concentration is negligible. This is an unforeseen behaviour since in the model, the bacteriophage entirely depends on the vibrios and have no alternative food source. In addition the numerical results in Figure 6.8 show noise at the transition points. Unfortunately, we have not yet been able to establish the real cause of such noise although we believe, they could be due multiple oscillations in the discretised system at the corresponding points.

Chapter 7

Conclusion and discussion

In this thesis, we used mathematical models to study the transmission dynamics of cholera with the main view of understanding possible ways through which the disease can be contained or an outbreak prevented. Four key aspects were considered, i.e the importance of hygiene, meta-population dynamics with movement between communities, optimal control and biological control of the infection using a vibrio specific bacteriophage. Our study of cholera with focus on hygiene related contact function, metapoulation spread of cholera with no cross community infection, and optimal control of the infection in a metapopulation setting with no cross community infection but exchange of individuals between communities is the first of the kind. In addition, although biological control *vibrio cholerae* density using a bacteriophage is not a new concept, modelling of such an interaction with parabolic reaction-diffusion equations has not been attempted prior to this work (to best of our knowledge).

In Chapter 3, the model describing the transmission dynamics of cholera was presented. The model incorporated two transmission routes namely; (1) contact with the contaminated aquatic environment where the contact probability follows a maximum saturation function which is dependent on the concentration of the pathogen in the environment, and (2) person to person contact which is assumed to be influenced by the level of hygiene. The model has a disease free equilibrium which is globally stable and an endemic equilibrium which is unique. Extensive selection of model parameters was done, sensitivity analysis performed using the Latin hypercube sampling scheme and numerical simulations were also done.

In the metapopulation model, heterogeneity was considered where two communities having similar cholera transmission dynamics were analysed. The community specific disease thresholds were obtain for two cases namely; (1) when the communities were assumed to be

isolated with no movement between them and (2) when the communities were connected by back and forth movement of both immunologically naive as well as the infected individuals. Vital dynamics of the model were analysed including the invariant region/region of biological significance. The model equilibria were obtained including the disease free equilibrium and the community specific equilibria (boundary equilibria). The disease free equilibrium was showed to be globally asymptotically stable when the community specific disease thresholds in non-isolated communities were each less than unity. Both the community specific endemic equilibria exist whenever the community specific disease thresholds are greater than unity, the equilibria are unique and locally asymptotically stable.

The considered communities were classified with the assumption of difference in living condition. Our numerical results indicate that, in isolated communities the disease was likely to stay longer in the community with poor facilities compared to one with better living conditions. If the communities are connected, with only movement of those susceptible, there is a likelihood of the disease greatly affecting the community with better living conditions. This has been attributed to the high susceptible pool that would increase the likelihood of new infections. If the communities are connected by a migratory network there is likely synchronous fluctuation of the population of both the infected and immunologically naive individuals. However, the severity of the infection is more inclined to the community that gets more susceptible and infected immigrants.

Optimal control of cholera in a metapopulation setting with exchange of individuals between communities and no cross community transmission was considered. Our observations indicate that, an epidemic in community in presence of controls can be contained in approximately half the time it would take through self-limitation.

In the model for biological control of cholera using a vibrio specific bacteriophage, two scenarios were observed. First, a scenario where the disease is likely to remain persistent due to the recurring high concentrations of the pathogen. This a case when the bacteriophage is assumed to be less effective in clearing the *V. cholerae*. Secondly, a scenario with a more effective predatory bacteriophage, with high survival rate and reduced shedding of the vibrios in the aquatic environment. This would result in faster containment of the *V. cholerae* concentration. If the vibrio concentration is reduced, this reduces the likelihood of infection with cholera if contaminated water is consumed. A reduced concentration of the pathogen in the aquatic environment reduces the likelihood of consuming the concentration of the pathogen equivalent to the infectious dose.

7.1 Limitations and future work

One of the major challenges we faced during this study was the fact that we were unable to obtain data most especially data for the $2000-2002$ cholera outbreak that devastated most provinces in South Africa. This was the case despite the numerous communications made to personnel potentially having the data. Availability of a complete trusted dataset on a cholera epidemic would have aided in estimating community specific disease parameter and testing possible control scenarios for future reference in case of an outbreak.

The models we used do not put into account the time delay between the time infection and when the infected person becomes infectious. This is time delay was predicted in [41]. It may be plausible to investigate the effect of delay on the transmission dynamics of the disease. In addition the infection rate may not necessarily be constant throughout the epidemic period. We acknowledge the fact that considering time dependent parameter may give more insights into the disease dynamics. The metapopulation models do not put into account the possibility of cross community infection and access to a common contaminated water source for adjacent communities. This aspect may have a significant effect on the transmission dynamics and severity of the disease.

In the models used in Chapters 4 and 5, the infected population is not classified into those symptomatic and asymptomatic individual. In addition, stochasticity that may be attributed to the environmental conditions could influence the infection pattern related to both the primary and secondary routes. The noise resulting from such stochastic consideration may give a more realistic picture of the fluctuating non constant disease transmission rates.

The dynamics of the vibrios and the lytic bacteriophage occur in a completely heterogeneous environment with varying levels of salinity, temperature, nutrient supply and changing water currents. However, coupling a complete model with the human population (using ODEs) as well as the heterogeneous dynamics of the vibrios and the bacteriophage (using reaction-diffusion system of equations) may be a challenging task. However, if implemented it would give a more comprehensive view of the potential importance of the bacteriophage in the control of cholera.

Bibliography

[1] Global cholera cases and deaths reported to the World Health Organization, 1970 to 2004. Available from worldwater.org/wp-content/uploads/sites/22/2013/07/Table14.pdf, Last Accessed on July 11, 2014.

[2] J. Berman. WHO: Waterborne disease is world's leading killer. VOANews. U.S.Government,Last updated on October 29, 2009 12:28 PM: Available from http://www.who.int/topics/cholera/impact/en/index.html, 2011.

[3] WHO. Water sanitation health: Water-related diseases. Available from http://www.who.int/water_sanitation_health/diseases/en/, Accessed on August 20, 2012.

[4] R-G Zhang, D. L. Scott, M. L. Westbrook, S. Nance, B. D. Spangler, G. G. Shipley, and E. M. Westbrook. The three-dimensional crystal structure of cholera toxin. *J. Mol. Biol.*, 251:563–573, 1995.

[5] Health Plant. Your diseases and treatment: Cholera details. Available from http://healthplant.wordpress.com/2010/01/29/cholera-details/, Visited in: July, 2014.

[6] Orphanet. Cholera. Available from http://www.orpha.net/consor/cgi-bin/OC_Exp.php?Lng=GB&Expert=173, Visited on: September, 2014.

[7] C. Seas and E. Gotuzzo. Cholera: Overview of epidemiologic, therapeutic, and preventive issues learned from recent epidemics. *Int. J Infect Dis*, 1:37–46, 1996.

[8] S. M. Blower and H. Dowlatabadi. Sensitivity and uncertainty analysis of complex models of disease transmission: An HIV model as an example. *Int. Stat. Rev.*, 62:229–243, 1994.

[9] M. Pascual, M. J. Bouma, and A. P. Dobson. Cholera and climate: revisiting the quantitative evidence. *Microbes Infect.*, 4:237–245, 2002.

[10] K.T. Goh, S. LAM, and M. K. Ling. Epidemiological characteristics of an institutional outbreak of cholera. *T. Roy. Soc. Trop. Med. H.*, 81:230–232, 1987.

[11] M. Embrey, P. Hunter, J. Sellwood, P. Wyn-Jones, S. L. Percival, and R. Chalmers. *Microbiology of waterborne diseases: Microbiological aspects and risks*. Elsevier academic press, 2004.

[12] CDC. Laboratory methods for the diagnosis of vibrio cholerae: Laboratory identification of *Vibrio Cholerae*. Available from http://www.cdc.gov/cholera/pdf/laboratory-methods-for-the-diagnosis-of-vibrio-cholerae-chapter-6.pdf, Accessed on August 11, 2014.

[13] K. Lee. The global dimension of cholera. *Global Change & Human Health*, 2:6–17, 2001.

[14] M. E. Asplund. *Ecological aspects of marine Vibrio bacteria: Exploring relationships to other organisms and a changing environment*. PhD thesis, University of Gothenburg, 2013.

[15] V.T.P Sedas. Influence of environmental factors on the presence of vibrio cholerae in the marine environment: a climate link. *J. Infect. Developing Countries*, 1:224–241, 2007.

[16] Jr J. Glenn Morris. Cholera: modern pandemic disease of ancient lineage. *Emerging Infectious Diseases*, 17:2099–2104, 2011.

[17] R. R. Colwell. Global climate and infectious disease: the cholera paradigm. *Science*, 274:2025–2031, 1996.

[18] S. M. Butler and A. Camilli. Going against the grain: chemotaxis and infection in *Vibrio cholerae*. *Nat. Rev. Microbiol.*, 3:611–620, 2005.

[19] A. R. Tuite, J. Tien, M. Eisenberg, D.J.D Earn, J. Ma, and D. N. Fisman. Cholera epidemic in Haiti, 2010: Using a transmission to explain spatial spread of disease and identity optimal control interventions. *Ann Intern Med.*, pages 1–24, 2011.

[20] R. L. M. Neilan, E. Schaefer, H. Gaff, K. R. Fister, and S. Lenhart. Modelling optimal intervention strategies for cholera. *Bull. Math. Bio.*, 72:2007–2018, 2010.

[21] M. Carrel, M. Emch, P. K. Streatfield, and M. Yunus. Spatio-temporal clustering of cholera: The impact of flood control in matlab, bangladesh, 1983âĂŞ2003. *Health & Place*, 15:771–782, 1996.

[22] FAO. *Lectures Presented at the Fifth FAO/SIDA workshop on aquatic pollution in relation to protection of living resources*. Swedish funds-in-trust, TF-RAS 34 (SWE) Suppl. 1, 1977.

[23] WHO. Prevention and control of cholera outbreaks: Who policy and recommendations: Vaccines. Available from http://www.who.int/cholera/technical/prevention/control/en/index5.html, Accessed on September 17, 2013.

[24] Medical Dictionary. Cholera. Available from http://medical-dictionary.thefreedictionary.com/cholera, Visited in: August, 2013.

[25] J. Clemens, S shin, D. Sur, G. B. Nair, and J. Holmgren. New-generation vaccines against cholera. *Nat Rev Gastroenterol Hepatol*, 8:701–710, 2011.

[26] M. M. Levine. Immunogenicity and efficacy of oral vaccines in developing countries: lessons from a live cholera vaccine. *BMC Biology*, 8:doi:10.1186/1741–7007–8–129, 2010.

[27] Z. Mukandavire, D. L. Smith, and Jr J. Glenn Morris. Cholera in Haiti: Reproductive numbers and vaccination coverage estimates. *Scientific Reports*, 3:DOI: 10.1038/srep00997, 2013.

[28] M. Isaäcson, K. R. Clarke, G. H. Ellcombe, W. A. Smit, P. Smit, H. J. Koornhof, L. S. Smith, and L. J. Kreil. The recent cholera outbreak in the South African gold mining industry: A preliminary report. *S. A. Medical Journal*, 48:2557–2560, 1974.

[29] WHO. Cholera vaccines: WHO position paper. *Wkly Epidemiol Rec.*, 85:117–128, 2010.

[30] I. M. Longin Jr, A. Nizam, M. Ali, M. Yunus, N. Shenvi, and J. D. Clemens. Controlling endemic cholera with oral vaccines. *PLoS Medicine*, 4:1776–1783, doi:10.1371/journal.pmed.0040336.g001, 2007.

[31] WHO. Use of oral cholera vaccine in humanitarian emergencies. Available from http://www.who.int/cholera/vaccines/OCV_in_humanitarian_emergencies_15Jan2014.pdf, 2014.

[32] WHO. WHO/Paul-Ehrlich-Institut Informal Consultation on Scientific and Regulatory Considerations on the Stability Evaluation of Vaccines under Controlled Temperature Chain (ctc). Available from http://who.int/biologicals/vaccines/CTC_Final_Mtg_Report_Langen.pdf, 2013.

[33] K. A. Date, A. Vicari, T. B. Hyde, E. Mintz, M. C. Danovaro-Holliday, A. Henry, J. W. Tappero, T. H. Roels, J. Abrams, B. T. Burkholder, C. Ruiz-Matus, J. Andrus, and V. Dietz. Considerations for oral cholera vaccine use during outbreak after earthquake in Haiti, 2010-2011. *Emerg. Infect. Dis.*, 17:2105–2112, 2011.

[34] Z. Mukandavire, S. Liao, J. Wang, H. Gaffd, D. L. Smith, and Jr. J. G. Morris. Estimating the reproductive numbers for the 2008-2009 cholera outbreaks in Zimbabwe. *PNAS*, 108:8767–8772, 2011.

[35] F. Rao. The impact of climate on the disease dynamics of cholera. *Eur. J. Clin. Microbiol. Infect. Dis.*, 15:29–31, 2009.

[36] C. T Codeço. Endemic and epidemic dynamics of cholera: the role of the aquatic reservoir. *BMC Infect. Dis.*, 1:1, 2001.

[37] P. Das and D. Mukherjee. Qualitative analysis of a cholera bactriophage model. *ISRN*, Volume 2012:doi:10.5402/2012/621939, 2012.

[38] M. Jensen, S. M. Faruque, J. J Mekalanos, and B. Levin. Modelling the role of bacteriophage in the control of cholera outbreaks. *PNAS*, 103:46–52, 2006.

[39] J.B.H Njagarah and F. Nyabadza. A metapopulation model for cholera transmission dynamics between communities linked by migration. *Appl.Math.Comput.*, 241:317–331, 2014.

[40] J. P. Tian and J. Wang. Global stability for cholera epidemic models. *Math. Biosci.*, 232:31–41, 2011.

[41] V. Capasso and S. L. Paveri-Fontana. A mathematical model for the 1973 cholera epidemic in the European mediterranean region. *Revue dépidémiologie et de santé Publiqué*, 27:121, 1979.

[42] D. M Hartley, J.G Morris, and D. L. Smith. Hyperinfectivity: a critical element in the ability of *V. cholerae* to cause epidemics? *Plos Medicine*, 3:0063, 2006.

[43] M Bentivoglio and P. Pacini. Filippo pacini: A determined obeserver. *Brain Res. Bull.*, 38:161–165, 1995.

[44] J. Wang and S. Liao. A generalized cholera model and epidemic-endemic analysis. *J. Biol. Sci.*, 6:568–589, 2012.

[45] E. Bertuzzo, S. Azaele, A. Maritan, M. Gatto, I Rodrigues-Iturbe, and A Rinaldo. On the space time evolution of a cholera epidemic. *Water Resour. Res.*, 44:doi:10:1029/2007WR006211, 2008.

[46] J-P Raufman. Cholera. *Am. J. Med.*, 104:386–394, 1998.

[47] E. K. Kipp, A. Huq, and R. R Colwell. Effects of global climate on infectious disease: the cholera model. *Clin Microbiol. Rev.*, 15:757–770, 2002.

[48] M. A. de Guimaraens and C.T Codeço. Experiments with mathematical models to simulate hepatitis A population dynamics under different levels of endemicity. *Cad, Saúde Pública, Rio de Janeiro.*, 21:1531–1539, 2005.

[49] G. Birkhoff and G-C Rota. *Ordinary differential equations*. John Wiley & Sons, Inc., Canada, third edition, 1978.

[50] Z. Mukandavire, A. Tripathi, C. Chiyaka, G. Musuka, F. Nyabadza, and H. G. Mwambi. Modelling and analysis of the intrinsic dynamics of cholera. *Differ Equ Dyn Syst*, 19:253–265, 2011.

[51] P. van den Driessche and J. Watmough. Reproduction numbers and sub-threshold endemic equilibria for compartmental models of disease transmission. *Math. Biosci.*, 180:29–48, 2002.

[52] J. D. Murray. *Mathematical Biology: I. An introduction*, volume 17. Springer-Verlag Berlin Heidelberg, third edition, 2002.

[53] J. P. LaSalle. The stability of dynamical systems. *Society for Industrial and Applied Mathematics, Philadelphia*, 1976.

[54] M. Vital, H. P. Füchslin, and F. Hammes. Growth of *Vibrio cholerae* 01 Ogawa Eltor in freshwater. *Microbiology*, 153:1993–2001, 2007.

[55] Statistic South Africa. Mid-year population estimates, 2010. Available from www.statssa.gov.za/publications/P0302/P03022010.pdf; Accessed on September 27,2013.

[56] Disease and mortality in Sub-Saharan africa, 2006. World Bank, Washington D.C.

[57] P. M. Munro and R. R. Colwell. Fate of *Vibrio cholerae* 01 in seawater microcosms. *Wat. Res.*, 30:pp. 47–50, 1996.

[58] A. King, E. L. Ionides, M. Pascual, and M. Bouma. Inapparent infections and cholera dynamics. *Nature*, 454:877–880. doi:10.1038/nature07084, 2008.

[59] T. R. Hendrix. The pathophysiology of cholera. *Bull. N. Y. Acad. Med.*, 47:1169–1180, 1971.

[60] J. B. Kaper, J. G. Morris, and D.L. Smith. Cholera. *Clin. Microbiol. Rev.*, 8:48–86, 1995.

[61] M. M. Levine, J. B. Kaper, D. Herrington, G. Losonsky, J. G. Morris, M. L. Clements, R. E. Black, B. Tall, and R. Hall. Volunteer studies of deletion mutants of *Vibrio cholerae* 01 prepared by recombinant techniques. *Infect. Immun.*, 56:161–167, 1988.

[62] E. Bertuzzo, R. Casagrandi, M. Gatto, I. Rodriguez-Iturbe, and A. Rinaldo. On spatially explicit models of cholera epidemics. *J. R. Soc. Interface*, 7:321–333, 2010.

[63] L. Mari, E. Bertuzzo, L. Righetto, R. Casagrandi, M. Gatto, I Rodrigues-Iturbe, and A Rinaldo. Modelling cholera epidemics: the role of waterways, human mobility and sanitation. *J. R. Soc Interface*, page doi:10.1098/rsif.2011.0304, 2011.

[64] J. Sepulveda, H. Gomez-Dantes, and M. Bronfman. Cholera in the Americas: An overview. *Infection*, 20:243–248, 1992.

[65] D. M. Hamby. A review of techniques for parameter sensitivity analysis of environmental models. *Environ. Monit. Assess.*, 32:135–154, 1994.

[66] A. Hoare, D. G. Regan, and D. P. Wilson. Sampling and sensitivity analyses tools (SaSAT) for computational modelling. *Theor Biol Med Model.*, 5:doi:10.1186/1742–4682–5–4, 2008.

[67] R. P. Saches, C. P. Fereira, and R. A. Kraenkel. The role of immunity and seasonality in cholera epidemics. *Bull. Math. Biol.*, 73:2916–2931, 2011.

[68] G. R. Fulford, M. G. Roberts, and J. A. P. Heesterbeek. The metapopulation dynamics of an infectious disease: Tuberculosis in Possums. *Theor Popul Biol*, 61:15–29, 2002.

[69] B. M. Bolker *et al.* Group report: Spatial dynamics of infectious diseases in natural populations. In B. T. Grenfell and A. P. Dobson, editors, *Ecology of Infectious Diseases in Natural Populations*, pages 384–398. Cambridge University Press, Cambridge, UK, 1995.

[70] A. L. Lloyd and R. M. May. Spatial heterogeneity in epidemic models. *J. Theor. Biol.*, 179:1–11, 1996.

[71] A. Liebhold and N. Kamata. Population dynamics of forest-defoliating insects. *Popul. Ecol.*, 42:205–209, 2000.

[72] S. F. Matter. Synchrony, extinction, and dynamics of spatially segregated, heterogeneous populations. *Ecol. Model.*, 141:217–226, 2001.

[73] P. J. Hudson and I. M. Cattadori. The moran effect: a cause of population synchrony. *TREE*, 14:PII: S0169–5347(98)01498–0, 1999.

[74] C. Mugero and AKM Hoque. A review of cholera epidemic in South Africa with focus on KwaZulu Natal province. April 2001.

[75] J. B. H. Njagarah and F. Nyabadza. Modeling the impact of rehabilitation, amelioration and relapse on the prevalence of drug epidemics. *J. Biol. Syst.*, 21:DOI: 10.1142/S0218339013500010, 2013.

[76] F. Nyabadza, J.B.H. Njagarah, and R. J. Smith? Modelling the dynamics of crystal meth ("Tik") abuse in the presence of drug-supply chains in south africa. *Bull. Math. Biol.*, 75:24–48, 2013.

[77] J. B. H. Njagarah and F. Nyabadza. Modelling the role of drug barons on the prevalence of drug epidemics. *Math Biosci Eng.*, 10:843–860, 2013.

[78] C. Castillo-Chavez and B. Song. Dynamical models of Tuberculosis and their application. *Math. Biosci. Eng.*, 1:361–404, 2004.

[79] F. Nyabadza and S. D. Hove-Musekwa. From heroin epidemics to methamphetamine epidemics: Modelling substance abuse in a South African province. *Math. Biosci.*, 225:134–140, 2010.

[80] B. M. Bolker and B. T. Grenfell. Impact of vacccination on the spatial correlation of persistence of measles dynamics. *Proc. Natn. Acad. Sci. USA*, 93:12648–12653, 1996.

[81] Z. Ma, Y Zhou, and J. Wu, editors. *Modelling and dynamics of infectious diseases*. Higher Eductation Press, World Scientific, 2009.

[82] R. E. Rowthorn, R. Laxminarayan, and C. A. Gilligan. Optimal control of epidemics in metapopulations. *J. R. Soc. interface*, 6:1135–1144, 2009.

[83] J. Wang and C. Modnak. Modeling cholera dynamics with controls. *Canadia Applied Mathematics Quarterly*, 19:255–273, 2011.

[84] L. S. Pontryagin, V. G. Boltyanskii, R. V. Gamkrelidze, and E. F. Mishchenko. *The mathematical theory of optimal processes*. John Wiley and Sons, Inc, Newyork. London, 1962.

[85] S. Lenhart and J. T. Workman. *Optimal control applied to biological problems*. Chapman & Hall/CRC, Boca Raton London Newyork, 2007.

[86] K. O. Okosun and O. D. Makinde. Modelling the impact of drug resistance in malaria transmission and its optimal control analysis. *Int. J. Phys. Sci.*, 6:6479–6487, 2011.

[87] PHAC. Canadian Immunization Guide: Cholera and Enterotoxigenic *Escherichia Coli* (etec) Travellers' Diarrhea vaccine. Available from http://www.phac-aspc.gc.ca/publicat/cig-gci/p04-cho-eng.php#a3, Accessed on October 30, 2013.

[88] Z. Mukandavire, F. K. Mutasa, S. D. Hove-Musekwa, S. Dube, and J. M. Tchuenche. *Mathematical Analysis of a cholera models with carriers and assessing the effects of treatment*, chapter 4. In Mathematical Biology Research Trends, Nova Science Publishers, Inc., 2008.

[89] M. Aktaruzzamn M. S. Hossain, A. N. M Fakhruddin, M.J. Uddin, S.H. Rahman, M. A. Z. Chowdhury, and M. K. Alam. Antimicrobia susceptibility of vibrio species isolated from brackish water shrimp culture environment. *Journal of Bangladesh Academy of Sciences*, 36:213–220, 2012.

[90] A. R. Long, D. C. Rowley, E. Zamora, J. Liu, D. H. Bartlett, , and F. Azam. Antagonistic interactions among marine bacteria impede the proliferation of *Vibrio cholerae*. *Appl. Environ. Microbiol.*, 71:8531–8536, 2005.

[91] E. J. Nelson, J. B. Harris, Jr J. Glenn Morris, S. B. Calderwood, and Andrew Camilli. Cholera transmission: the host, pathogen and bacteriophage dynamic. *Nat Rev Microbiol.*, 7:doi:10.1038/nrmicro2204., 2009.

[92] R. K Gupta N Ezard. Phage in time of cholera. *Reflection and Reaction*, 6:257–258, 2006. Available from http://infection.thelancet.com.

[93] A. N. Maina, F. B. Mwaura, J. Oyugi, D. Goulding, A. L. Toribio, and S. Kariuki. Characterization of *Vibrio cholerae* bacteriophages isolated from the environmental waters of the lake Victoria region of Kenya. *Curr. Microbiol.*, 68:64–70, 2014.

[94] S. M. Faruque, M. J. Islam, Q. S. Ahmad, A. S. G. Faruque, D. A. Sack, G. B. Nair, and J. J. Mekalanos. Self-limiting nature of seasonal cholera epidemics: Role of host-mediated amplification of phage. *PNAS*, 102:6119–6124, 2005.

[95] H. Malchow, S. V. Petrovskii, and E. Venturino. *Spatiotemporal patterns in ecology and epidemiology: theory, models and simulations*. Mathematical and Computational Biology series. Chapman & Hall/CRC Taylor and Francis Group, 2007.

[96] J. D. Murray. *Mathematical Biology: II. Spatial models and Biomedical Applications*, volume 18. Springer-Verlag Berlin Heidelberg, third edition, 2003.

[97] N. Shigesada and K. Kawasaki. *Biological Invasions: Theory and Practice*. Oxford University Press, 1997.

[98] R. S. Fisher. The wave of advance of advantageous genes. *A Eug.*, 7:355–369, 1937.

[99] C. S. Holling. The components of predation as revealed by a study of small-mammal predation of the European pine sawfly. *Can. Entomol.*, 91:293–320, 1959.

[100] C. S. Holling. Some characteristics of simple types of predation and parasitism. *Can. Entomol.*, 91:385–398, 1959.

[101] M. R. Garvie and C. Trenchea. Spatiotemporal dynamics of two generic predator-prey models. *Journal of Biological dynamics*, 4:559–570, 2010.

[102] J. Hadamard. Sur les problèmes aux dérivées partielles et leur signification physique. *Princeton Univ. Bull.*, 13:49–52, 1902.

[103] J. Clausen and K. Krabbenhoft. Existence and uniqueness of solutions in nonassociated mohr-coulomb elastoplasticity. *8th. World Congress on Computational Mechanics (WCCM8)*, 2008.

[104] F. Rao. Spatiotemporal dynamics in a reaction-diffusion toxic-phytoplankton-zooplankton model. *J. Stat. Mech.*, 6:P08014, 2013.